Model and System Inversion with Applications in Nonlinear System Identification and Control

Ola Markusson

Automatic Control
Department of Signals, Sensors and Systems
Royal Institute of Technology
Stockholm, Sweden

Submitted to the School of Electrical Engineering, Royal Institute of Technology, in partial fulfillment of the requirements for the degree of Doctor of Philosophy.

TRITA–S3–REG–0201
ISSN 1404–2150
ISBN 91-7283-228-2

To Celina, Oskar
and
Elisabeth

Abstract

Inversion plays an important role in both control and parameter estimation. Control can be viewed as *system* inversion since the objective is to determine the input to a system, given a desired output. In estimation, prediction error and maximum likelihood methods requires *model* inversion. In this thesis, techniques for both these applications are studied.

Iterative learning control (ILC) is a way to obtain the inverse of a system or a model and this method is here placed in the realm of numerical optimization. This clarifies the role played by the design variables and how they relate to, e.g., convergence properties. A model based interpretation of these design variables is given and also a sufficient condition for convergence. This condition shows that the desired performance has to be traded against modeling accuracy. Finally, the possibility of non-causal control is an advantage of ILC. This is given a comprehensive coverage in the case of non-minimum phase systems.

Experiment design based on system inversion is further introduced for *control relevant identification*. It is shown that the experimental conditions should coincide with the desired closed loop operating conditions when identifying control relevant models. To achieve this, it is proposed to do approximate system inversion by means of, e.g., ILC. It is further shown that a desired closed loop response of a nonlinear system, for a given reference signal, can be achieved using a controller based on a linear model. This is possible if the linear model is able to capture the input-output behavior of the nonlinear system for the desired response.

A *feedback inversion technique* useful for model inversion is studied that can easily be implemented in numerical software. Sufficient conditions are derived for the existence of a stable causal inverse. The technique is motivated by maximum likelihood estimation of nonlinear stochastic models where inversion of the model is required. In addition, parameter estimation in nonlinear stochastic models by *spectral matching* is studied. Theoretical results on convergence, parameter covariance and identifiability are presented.

Acknowledgments

The book in your hand can be considered as a travel report. The journey started a couple of years ago and has taken place in the world of control and identification. The manager of the travel agency, Professor Bo Wahlberg, provided me with a ticket which included more than I expected, thank you Bo!

My advisor and guide, Dr Håkan Hjalmarsson has with great skill guided me to many interesting places. We have, for example, visited a place called ILC where I was introduced to some of the local people. Thank you Dr Mikael Norrlöf and Dr Svante Gunnarsson for valuable comments and discussions.

I have not been the only traveler in this part of the world and I have enjoyed meeting many other travelers. For example, when climbing one of the mountains I met Björn Henriksson and together we visited some excellent viewpoints.

I truly appreciate my guides enthusiasm in pointing out interesting places and suggesting numerous examples of what to do and see. Thank you Håkan for not loosing faith in me! I truly admire your expertise and support.

My wife Elisabeth has supported me from the start and I appreciate her love and patience more than words can say. We have introduced two new travelers to the world, Oskar and Celina, and I am so proud to call you my family. Together I hope that we can make many journeys, exploring the world outside control and identification.

Contents

Chapter 1

Introduction

1.1 General overview

Issues on *identification* and *control* of *systems* are studied in this thesis. Loosely speaking a system is here considered as an object where variables interact and produce observable signals (Ljung 1999). We will study mathematical models of such systems.

Models are fitted to a system by an *identification* process fitting a model to the data from the system. This process can roughly be divided into three steps; collecting data, choosing a model structure and fitting the model to the data. When the type of model is chosen, the fitting process can be described as tuning the parameters such that the fit is as good as possible. In other words, when a model structure is chosen, the parameters of that model are to be estimated.

Control of a system can be described as determining the input such that the output follows as closely as possible a desired reference signal, despite disturbances or errors in the model.

Let us denote a system by P, the input signal by u and the output by y. We then have the relationship

$$y = P(u).$$

Observable signals from systems are further denoted outputs and the signals that can be manipulated are called inputs. Inputs that cannot be manipulated are called disturbances and disturbances can be either measurable or not. Systems are commonly categorized as either linear

or nonlinear. A linear system satisfies the superposition principle, which means that for a sum of inputs

$$u = \sum_{i=0}^{\infty} a_i u_i,$$

the output is the corresponding sum of outputs

$$y = \sum_{i=0}^{\infty} a_i P(u_i),$$

where the a_i's are arbitrary constants. If this is not satisfied the system is nonlinear.

A linear model can be described by a transfer function, a state-space realization or an impulse response and the identification of linear models is the topic of many papers and books, see e.g. (Ljung 1999) and (Söderström and Stoica 1989). Commonly used identification methods for linear models are, e.g., prediction error methods, maximum likelihood and spectral based methods, see (Ljung 1999). Even though the control of linear systems is still an area of ongoing research, there are powerful techniques developed for the analysis and synthesis of control laws for linear systems, see e.g., (Skogestad and Postlethwaite 1996) or (Goodwin *et al.* 2001).

However, linear models cannot always describe physical phenomena. Nonlinear models, on the other hand, offer a wider range of models. Control and identification of nonlinear systems have also been studied for quite some time and a brief overview of different approaches are given below.

Roughly, this thesis deals with two aspects of identification, parameter estimation and identification for control. Control of nonlinear systems is also studied in the area of iterative learning control. The connection between these areas is highlighted in the next section.

1.2 One thesis - different topics - similar ideas

Perhaps the topics of this thesis appear to be picked at random when glancing through the contents. There are, however, strong links between the different areas. Nonlinear systems is a common denominator as well

as inversion of such systems. Parameter estimation is another link which is present in some of the chapters. Let us give a brief description and motivation to the choice of topics in this thesis.

It once started with the problem of estimating parameters in a nonlinear stochastic model (Markusson and Bohlin 1997). The problem was solved by the maximum likelihood method based on inversion of the model. This lead to the first of the four parts of this thesis *Feedback Inversion* - of nonlinear stochastic models, presented in Chapter 4.

Despite the method suggested in Chapter 4, determining the inverse of a nonlinear model is not always a trivial thing, assuming that it exists. If, e.g., the nonlinear system is non-minimum phase, a stable inverse is nontrivial to implement. This puts focus on iterative learning control (ILC) where the inverse can be obtained in a recursive manner. The results of this study are presented as *Iterative learning control - a general framework* in Chapter 5.

The purpose of identification may vary, e.g., a model can be used to predict future outputs or to design a controller that, applied to the system, stabilizes or improves the performance of a system. When the specific objective of the identification is for control purposes, the area is sometimes denoted *control relevant identification* or *identification for control*, which is the third part of this thesis presented in Chapter 6. The main objective is to study the cases where a linear controller can be used for the control of a nonlinear system. The controller is to be tailored for a specific reference signal and the controller is obtained by first identifying a linear model. The identification procedure depends on the desired input which is obtained by inverting the system. Hence, the connection to other results in this thesis. The results in this part can thus be interpreted from an experiment design perspective.

Finally, some models are extremely hard to invert, e.g., when there are more inputs than outputs. These models motivated the study of a spectral based method for parameter estimation presented in Chapter 7.

In summary the content of this thesis is to large extent devoted to inversion and parameter estimation in nonlinear models. However, the results go beyond these purposes in some cases.

1.2.1 Example - one system, different problems

Let us consider the system depicted in Figure 1.1, which consists of an inverted pendulum attached to a cart. The cart can be positioned in the y direction.

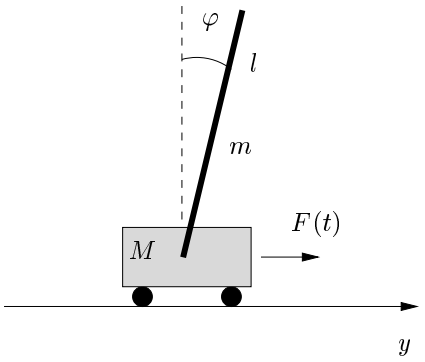

Figure 1.1: Inverted pendulum attached to a cart.

The system can be described by a model as

$$\dot{x}(t) = f(x(t), \theta, F(t), e(t)), \tag{1.1}$$

where t is the time-index, $x(t)$ is the state vector and θ is the parameter vector. The states of the system can be chosen to represent the position of the cart y, its velocity $\dot{y}$, the position of the pendulum φ and its angular velocity $\dot{\varphi}$. The input $F(t)$ is the force which can be applied to the cart and $e(t)$ denotes a non-measured disturbance which acts on the pendulum. The output of the model can be chosen to be, e.g., the position of the cart.

Now, at least two problems can be associated with the inverted pendulum, *parameter estimation* and *control*, both of which are considered in this thesis. Parameter estimation is motivated since it is possible to derive the differential equations in (1.1) from physical principles. However, there are still a number of parameters to be determined, e.g., the masses of the cart and the pendulum, the length of the pendulum and friction coefficients. Control on the other hand is first of all applied to keep the pendulum in an upright position but, in addition, control can also be applied to govern the position of the cart.

If we consider the control problem we first notice that the system is unstable, meaning that if the pendulum is positioned straight up and thereafter displaced slightly then it will not return to its initial position. The pendulum can, however, be controlled by moving the cart in a certain manner such that the pendulum remains in an upright position even if disturbances act on the pendulum. To control the pendulum we can use

a controller given by

$$F(t) = -L_f x(t) + u(t),$$

where L_f is a vector and $u(t)$ is a control signal. If we consider the case where the cart is supposed to move according to a desired trajectory $y_d(t)$ it is possible to calculate $u(t)$ such that this is achieved. In other words we want to invert the system for a desired output the corresponding input is to be calculated. Either an accurate enough model is available for the calculation of the inverse directly, or if this is not the case, an iterative method can be used where

$$u_{k+1}(t) = u_k(t) + L\varepsilon_k(t), \tag{1.2}$$

where L is an operator and $\varepsilon_k(t) = y_d(t) - y_k(t)$ is the error between the desired and the actual position of the cart. In (1.2) the index k denotes an iteration index. This approach is called Iterative Learning Control (ILC). Upon convergence of this algorithm the error is zero and the method can then be interpreted as a way of inverting the system.

Another approach to the control problem could be to first specify the behavior of the system for a specific reference signal. The problem is then to obtain a controller such that a specific reference signal results in a desired output. If a linear model is capable of capturing the input-output relationship of the system, then a linear controller can be used. Now, the output is given but the input to the system remains unknown since the controller is unknown. A question is then how an experiment (i.e., input signal) can be designed such that the result of the experiment can be used to identify a linear model. Hence, the inverse of the system is desired and, if applied as above, the ILC method can be used. Thus, in the case of the pendulum we can specify a desired closed loop response to a given reference signal and apply experiments tailored by the ILC algorithm to get the input signal. The output and the corresponding input signal is further used for identification of a linear model which is finally used for feedback control design.

Parameter estimation was the other problem listed above. Here we assume that a model is derived from physical principles, although certain parameters must be determined from experimental data. One approach is the Maximum Likelihood (ML) method where a likelihood function $L(\theta)$ is optimized w.r.t. θ to obtain the parameter estimates. In this example it can be assumed that a disturbance $e(t)$ is acting on the pendulum. The disturbance is not measured but it can be obtained by inversion. If the

probability density function (PDF) of $e(t)$ is known then it can be used to calculate the likelihood function. Hence, by applying

$$e(t) = P^{-1}(y^t, \theta, F^t), \tag{1.3}$$

we can obtain $e(t)$. In (1.3) the exponent t denotes that values of y up to time-instant t are considered. The likelihood function $L(\theta)$ can now be obtained from $e(t)$ and by optimization of $L(\theta)$ w.r.t. the parameter vector θ a parameter estimate can be found.

In conclusion, different problems can be associated with a single system. In this thesis, techniques to solve these problems are studied.

1.2.2 Identifying nonlinear systems - background

In the literature it is common to differentiate between the levels of a priori knowledge about a system, see e.g., (Bohlin 1991) or (Sjöberg *et al.* 1995):

> *White-box models.* The case when a model is entirely known from physical insight and prior knowledge.
>
> *Grey-box models.* The case when some physical insight is formulated as hypotheses to be tested and there are unknown parameters to be estimated.
>
> *Black-box models.* The case when no physical insight is available or used. The model structures are on the other hand chosen from families of models known to be flexible and useful.

Identification of nonlinear systems has attracted significant interest, see e.g., (Wiener 1958), and is still an active research area. Representation of nonlinear models can be made in many ways and well known descriptions are Volterra and Wiener series (Billings 1980). These series expansions are built on kernels that have to be determined and in (Hung and Stark 1977, Schetzen 1980) methods for kernel determination are discussed. In (Sjöberg *et al.* 1995, Juditsky *et al.* 1995) an overview and a mathematical background to the identification of nonlinear black-box models are given. Examples of nonlinear black-box models are regressor based models, neural networks and wavelet networks. For example, in (Leontaritis and Billings 1985*a*, Leontaritis and Billings 1985*b*) nonlinear discrete-time models are referred to as nonlinear autoregressive moving average models (NARMAX). The above mentioned nonlinear models are

intended to cover a broad class of models, and are therefore quite complicated. To achieve somewhat simpler model descriptions linear systems and static (zero-memory) nonlinear systems can be combined. Different types of combinations are possible, but the Wiener and the Hammerstein models are perhaps the most well known. A Wiener system consists of a dynamic linear system followed by a static nonlinearity, while a Hammerstein model is the opposite with a static nonlinearity followed by a dynamic linear system. These models have been found useful in many situations and different methods have been derived for the identification. Methods based on extended Kalman filtering and recursive prediction error methods are, e.g., derived and evaluated in (Nordsjö 1998). In (Chen 1995) modeling and identification of parallel nonlinear systems are considered using input and output measurements. The spectral density functions of input-output relationships are examined in (Bendat 1990) claiming that frequency domain formulas are easier to interpret than associated time-domain correlation formulas.

In (Tong 1990) nonlinear time-series models are considered. Different model structures are presented including methods to estimate the parameters. Often physical knowledge about a process includes nonlinearities. This is pointed out in (Bohlin 1991) where grey-box identification is thoroughly described. The identification is built on the assumption that probabilistic ideas can be applied, especially ideas of Bayes and hypothesis testing. Maximum likelihood (ML) estimation is considered and estimation based on inversion and ML are described along with other methods. An example of grey-box identification is given in (Bohlin 1994), where a steel rinsing process is studied.

When considering parameter estimation we will focus on the case where the model structure is given, e.g. based on a priori physical knowledge of the system.

1.2.3 Control of nonlinear systems - background

A number of techniques exist for the control and analysis of nonlinear systems. Depending, e.g., on the type of model and the confidence of that model, different methods can be applied. Examples of existing methods for the control of a nonlinear system are, to name a few, linearization, gain scheduling, exact feedback linearization, sliding mode control. Theory for the analysis of nonlinear control is given in e.g, (Isidori 1995) and (Khalil 1996). In (Vidyasagar 1993) analysis of nonlinear systems, including systems with or without feedback is presented.

The application of linear controllers designed using linear approximations of the nonlinear system should perhaps not be underestimated. This is due to that feedback is forgiving in terms of incomplete system knowledge. In fact, uncertain system knowledge is one of the motivations for applying feedback in the first place.

1.3 Contributions and outline

As previously noted, this thesis consists of four main parts where each part is treated in a separate chapter. However, in the next two chapters, introductions to nonlinear systems and parameter estimation are given.

Chapter 2
A general introduction to linear and nonlinear systems is given in Chapter 2 where also a background to inversion of linear and nonlinear models is provided.

Special attention is given to:

- The representation of nonlinear systems, where the state-space representation is reviewed.
- The concept of minimum and non-minimum phase for linear and nonlinear systems.
- Inversion of linear and nonlinear systems where special attention is given to the inversion of linear non-minimum phase systems.

Chapter 3
A general background to parameter estimation is given in Chapter 3, both in the time and the frequency domain. Special attention is given to the ML criterion, where it is emphasized that the inverse relationship can be used to calculate the likelihood function.

Chapter 4

Prediction error and maximum likelihood estimation of stochastic models require inversion of the model. This is a step which may require substantial efforts, either in terms of manual calculations or through the use of software capable of symbolic computations. In Chapter 4 it is shown that model inversion can be easily implemented in numerical software such as, e.g., Matlab/Simulink and Matrix$_X$/Systembuild, by means of a feedback connection based on the model. It is further shown how the gradients, used for the optimization of the cost function, can be generated by a linear time-varying feedback system associated with the nonlinear model. In addition, sufficient conditions for the existence of a stable causal inverse, as well as sufficient conditions for the initial transient to decay, are derived. These conditions are given in terms of properties for a linear time-varying model associated with the nonlinear model.

The main contributions can be summarized as:

- An easily implementable method for inversion of nonlinear models using e.g., Matlab and Matrix$_X$ is presented.
- Sufficient conditions for the existence of a stable causal inverse as well as sufficient conditions for the initial transient to decay are derived.
- It is shown how the gradients, used for the optimization of the cost function, can be generated by a linear time-varying feedback system.

The work in Chapter 4 has resulted in two conference papers and a journal article. The general idea is presented in

> O. Markusson and H. Hjalmarsson, "Parameter Estimation in Partitioned Nonlinear Stochastic Models", In Proc. 9th European Signal Processing Conference (EUSIPCO), Rhodes, Greece, vol 2, pp 1021-1024 (1998).

and the criteria for existence and convergence are further discussed in

> O. Markusson and H. Hjalmarsson, "Inversion of nonlinear stochastic models for parameter estimation", In Proc. 39th IEEE Conference on Decision and Control, (CDC), Sydney, Australia, pp 1591-1596 (2000).

The result of Chapter 4 is also accepted for publication in

> O. Markusson and H. Hjalmarsson, "Inversion of Nonlinear Stochastic Models for the purpose of parameter estimation" International Journal of Control. To appear.

Chapter 5

The study of iterative learning control (ILC) in this thesis can be partly motivated by the need of model inversion in ML estimation, especially in the case of nonlinear non-minimum phase models. However, the results in Chapter 5 can also be applied to control, which is the main objective in this chapter.

In Chapter 5 we place ILC in the realm of numerical optimization. This clarifies the role played by the design variables and how they are related to e.g., the convergence properties. We give a model based interpretation of these design variables and also a sufficient condition for convergence of ILC. The condition is similar in spirit to the sufficient and necessary condition previously derived for linear systems. This condition shows that the desired performance has to be traded against modeling accuracy. Finally, the possibility of non-causal control, one of the main benefits of ILC, is highlighted. This is extremely useful when controlling non-minimum phase systems.

The main contributions can be summarized as:

- The role of the design variables of ILC is clarified.
- A sufficient condition for the convergence of ILC for nonlinear systems is given.
- It is shown how ILC can be used to invert nonlinear non-minimum phase systems.

The results are presented in

> O. Markusson, H. Hjalmarsson and M. Norrlöf, "Iterative learning control of nonlinear non-minimum phase systems and its application to system and model inversion" , In Proc. 40th IEEE Conference on Decision and Control (CDC), Orlando, USA, (2001).

Here the idea of using a linear non-minimum phase model to obtain the inverse of a nonlinear non-minimum phase system is presented. A general

approach that phrase ILC in the framework of optimization is submitted as

> O. Markusson, H. Hjalmarsson and M. Norrlöf, "A General Framework for Iterative Learning Control", IFAC World Congress on Automatic Control, Barcelona, Spain, (2002),

where also a convergence criterion is given in the context of a feedback system.

Chapter 6

Control of nonlinear systems, by means of linear time-invariant model based control design, is considered in Chapter 6. It is shown that if a linear model can capture the input-output behavior of a nonlinear system, for a specific pair of input-output signals, then it can be used to derive a suitable feedback controller. Thus, the controller is tailored for this specific operating condition. A method for identification is designed for this purpose, where inversion plays an important role. If for inversion, e.g. the ILC algorithm is considered, we get an experiment design method. Inversion is thus essential and both the results of Chapters 4 and 5 are utilized.

The main contributions of this chapter are the following

- It is shown that, for a given reference signal, the closed loop response of a nonlinear system can be achieved using a controller designed from a linear approximation. This holds if the linear approximation can capture the input-output behavior of the nonlinear system for that specific pair of input-output signals.
- It is further shown how a system in a feedback framework can be used to obtain an approximation of its own inverse.

The result of Chapter 6 is presented in

> B. Henriksson, O. Markusson and H. Hjalmarsson, "Control Relevant Identification of Nonlinear Systems using Linear Models", In Proc. American Control Conference (ACC), Arlington, USA , pp 1178-1183 (2001).

Chapter 7

Parameter estimation in nonlinear stochastic models by spectral matching is considered in Chapter 7. Models with a measured output and known inputs and unknown disturbance inputs are considered. Simulated data is used to estimate the spectrum of the nonlinear model and two different cost functions are suggested for the matching of the spectrum. Theoretical results on convergence and parameter covariance are presented, and an identifiability condition for a class of nonlinear models is given. The motivation for studying this type of identification is models where inversion is hard and conventional ML as described in Chapter 3 is cumbersome to implement. An extension to the matching idea is also made using higher order statistics.

The main contributions can be summarized as

- A spectral based parameter estimation method for nonlinear models is presented.
- An identifiability criterion is derived for a class of nonlinear systems.
- Theoretical results on convergence and accuracy are presented.

The result of Chapter 7 is presented in three different conference papers. The general idea and results on convergence and and accuracy are presented in

> O. Markusson and H. Hjalmarsson, "Spectral Based Parameter Estimation in Nonlinear Stochastic Models", In Proc. IFAC Symposium on System Identification (SYSID), Santa Barbara, USA (2000).

An extension to higher order statistics are presented in

> O. Markusson and H. Hjalmarsson, "Higher Order Cumulant based Parameter Estimation in Nonlinear Time Series Models", In Proc. American Control Conference (ACC), Arlington, USA , pp 4888-4889 (2001).

The results on identifiability and exogenous inputs are presented in

> O. Markusson and H. Hjalmarsson, "Spectral matching for parameter estimation in nonlinear input-output models", European Control Conference (ECC), Porto, Portugal, pp 3665-3670 (2001).

1.4 Notation

θ	parameter vector
$y(t)$	the output signal of a system at time instant t
y^t	a vector of previous values $(y(t), y(t-1), ..., y(0))$
$e(t)$	noise input to a system at time instant t
e^t	a vector of previous values $(e(t), e(t-1), ..., e(0))$
$w(t)$	output of an inverse model
$\delta(t-s)$	Kronecker's delta: zero unless $t = s$, $\delta(0) = 1$
E	expected value
$r(\tau)$	covariance function $r(\tau) = E\{y(t)y(t-\tau)\}$
$\phi(\omega)$	spectrum, the Fourier transform of $r(\tau)$
$V(\theta)$	cost function of θ
$var(x)$	variance of x
$p_e(\cdot)$	probability density function, also abbreviated PDF
$\log(\cdot)$	the natural logarithm ($y = \log x \Leftrightarrow x = e^y$)
$L(\theta; y)$	Likelihood function of θ given y.
P	A general nonlinear system
W	denotes the inverse relationship
$P(e^t, \theta)$	A general nonlinear system parameterized by θ.
$N(e^t, \theta)$	A nonlinear system parameterized by θ.
$\mathcal{M}$	set of models
$\mathcal{X}$	experimental conditions
$\mathcal{S}$	system

1.5 Abbreviations

ACF	autocorrelation function
ARMA	auto regressive moving average
BIBO	bounded input bounded output
BT	Blackman-Tukey
CRLB	Cramér Rao lower bound
EF	exponentially forgetting
FIR	finite impulse response
HOS	higher order statistics
IIR	infinite impulse response
ILC	iterative learning control
LTI	linear time invariant
LTIE	linear time invariant equivalent

LTV	linear time varying
MIMO	multiple-input multiple-output
ML	maximum likelihood
PDF	probability density function
PEM	prediction error method
QSD	quadratic spectral difference
ROC	region of convergence
SISO	single-input single-output
SML	spectral maximum likelihood

Chapter 2

Introduction to model inversion

This chapter gives a background to inversion of nonlinear models. First the representation and inversion of linear systems will be considered. Stability of the inverse and its connection to minimum and non-minimum phase systems will also be reviewed. Nonlinear systems will be considered in a similar manner and difficulties with stable inversion will be highlighted. This chapter ends with a short summary on related work.

2.1 Linear systems

Studying inversion of linear systems serves as a good introduction to inversion on nonlinear systems. In Chapter 5 it will also be shown how linear models can be used to invert the dynamics of a nonlinear system in an iterative fashion. Special attention is given in this section to stable inversion of non-minimum phase systems. Where not noted otherwise single-input single-output (SISO) systems will be considered below.

Let us first note that a system is causal if, for every choice of t_0, the output sequence value at $t = t_0$ depends only on the input sequence values for $t \leq t_0$.

2.1.1 Input output descriptions of linear systems

A minimal realization of a discrete-time linear time invariant (LTI) system can be completely characterized in the time domain by its impulse response $g(n)$. The output $y(n)$, resulting from the input $x(n)$ is specified by the convolution

$$y(n) = u(n) * g(n) = \sum_{k=-\infty}^{\infty} u(k)g(n-k).$$

The discrete time is denoted by n to emphasize that we are considering discrete time sequences. Later the index t will also be used to index discrete time instances. The Fourier transform (Oppenheim and Schafer 1989) relates the frequency response to the impulse response. The z-transform is a generalization of the Fourier transform given by

$$\mathcal{Z}\{x(n)\} = \sum_{n=-\infty}^{\infty} u(n)z^{-n} = U(z).$$

As shown in, e.g., (Oppenheim and Schafer 1989) the z-transform of the output of an LTI system, $Y(z)$, is related to the z-transform of the input, $U(z)$, by the z-transform of the impulse response, $G(z)$, as

$$Y(z) = G(z)U(z).$$

Here $G(z)$ is referred to as the system function or the transfer function. Let us now consider the class of systems whose input and output satisfy a linear difference equation with constant coefficients of the form

$$\sum_{k=0}^{N} a_k y(n-k) = \sum_{k=0}^{M} b_k u(n-k).$$

By applying the z-transform, using the linearity property[1] and the time-shift property[2] (Oppenheim and Schafer 1989), we get

$$\sum_{k=0}^{N} a_k z^{-k} Y(z) = \sum_{k=0}^{M} b_k z^{-k} U(z),$$

and the transfer function equals

$$G(z) = \frac{Y(z)}{U(z)} = \frac{\sum_{k=0}^{M} b_k z^{-k}}{\sum_{k=0}^{N} a_k z^{-k}}.$$

The input-output behavior of an LTI system is completely defined by its transfer function together with its region of convergence (ROC). The ROC is a ring centered at the origin and the ROC will be bounded by some of the poles although not containing any. If the system is stable then the ROC includes the unit circle. Also, if the system is causal the ROC must be outside the pole with the largest magnitude. Hence, for a system to be both stable and causal all the poles need to be inside the unit circle.

Consider the *stable*, finite dimensional, linear system

$$y(t) = G(q)u(t),$$

where q denotes the time-shift operator. The z-transform of G is

$$G(z) = \frac{A(z)C(z)}{B(z)D(z)} = \frac{\left(\sum_{i=0}^{n_A} a_i z^{-i}\right)\left(\sum_{i=-n_C}^{0} c_i z^{-i}\right)}{\left(\sum_{i=0}^{n_B} b_i z^{-i}\right)\left(\sum_{i=-n_D}^{0} d_i z^{-i}\right)}, \qquad (2.1)$$

and it is assumed that $a_0 = b_0 = c_0 = d_0 = 1$. In (2.1) all the roots of $z^{n_A}A(z)$ and $z^{n_B}B(z)$ are considered to be inside the unit circle of the z-plane and correspondingly the roots of $C(z)$ and $D(z)$ are considered to be outside the unit circle. We say that, $A(z)$ and $C(z)$ contain the causal

[1] The linearity property states that

$$ax_1(n) + bx_2(n) \overset{\mathcal{Z}}{\longleftrightarrow} aX_1(z) + bX_2(z).$$

[2] The time-shift property states that, for an integer n_0,

$$x(n - n_0) \overset{\mathcal{Z}}{\longleftrightarrow} z^{-n_0} X(z).$$

(minimum phase) and the anti-causal (maximum phase) zeros of the system. Likewise $B(z)$ and $D(z)$ contain the causal and the anti-causal poles of the system. The notion of the causal and the anti-causal poles derives from that, since the system is stable, $\frac{1}{B(z)}$ has to be expanded in powers of z^{-1} when deriving the impulse response which gives rise to a causal part. With $D(z)$ having zeros outside the unit circle, $\frac{1}{D(z)}$ has to be expanded in powers of z giving rise to an anti-causal part of the impulse response. The corresponding notion for the zeros stems from similar considerations when inverting the system in a stable manner. This will be discussed in more detail in the next section.

2.1.2 Inversion

The transfer function $G(z)$ has a corresponding inverse system denoted $G^{-1}(z)$ such that if it is cascaded with $G(z)$ the overall effective system is

$$T(z) = G(z)G^{-1}(z) = 1,$$

thus, this implies that

$$G^{-1}(z) = \frac{1}{G(z)}. \tag{2.2}$$

Below we will consider stable linear systems, meaning that the ROC includes the unit circle. Using the description in (2.1) it follows that the causal (and anti-causal) zeros of $G(z)$ becomes the causal (and anti-causal) poles of $G^{-1}(z)$. Hence, if the zeros of $G(z)$ are strictly outside the unit circle non-causal filtering must be used. Most software uses causal filtering and then the following procedure is useful.

Consider first the z-transform of the output sequence, computed as

$$Y(z) = G_{-}(z)U(z),$$

where $G_{-}(z)$ only has maximum phase zeros. By reversing the sequence $y(n)$ we get $\bar{y}(n) = y(-n)$, which has the z-transform

$$\bar{Y}(z) = Y(z^{-1}) = G_{-}(z^{-1})U(z^{-1}),$$

where the time-reversion corresponds to reflecting the poles (and zeros) of $G_{-}(z)$ in the unit circle. This gives

$$U(z^{-1}) = G_{-}^{-1}(z^{-1})Y(z^{-1}),$$

where the poles (and zeros) of $G^{-1}(z^{-1})$ are reflected versions of the poles (and zeros) of $G_-^{-1}(z)$. Hence, $G^{-1}(z^{-1})$ will have only causal poles if $G(z)$ has only anti-causal zeros. Let us study an example to illustrate how this is used.

Example 2.1. *Consider the linear system*

$$y(t) = G_-(q)u(t),$$

where $G(z)$ is a maximum phase system given by

$$G_-(z) = \frac{z+b}{z},$$

where $|b| > 1$. Hence, the zero is outside the unit circle. The question is now how $u(t)$ can be obtained from $y(t)$ in a stable fashion. The question is valid since the inverse

$$G_-^{-1}(z) = \frac{z}{z+b}$$

has a pole outside the unit circle and if the filtering is done causally, i.e.

$$u(t) = -bu(t-1) + y(t)$$

this is an unstable system. However, non-causal filtering gives a stable inverse as will be shown next. By reflecting the zeros (and poles) of $G_-(z)$ we get

$$G_-(z^{-1}) = \frac{z^{-1}+b}{z^{-1}}$$

and correspondingly

$$G_-^{-1}(z^{-1}) = \frac{z^{-1}}{z^{-1}+b}.$$

The reflected zeros (and poles) can be accompanied by a time-reversion of the signals, and in the time-domain we have

$$\bar{u}(t) = -\frac{1}{b}\bar{u}(t-1) + \frac{1}{b}\bar{y}(t)$$

where $\bar{u}$ and $\bar{y}$ denotes time-reversed sequences, e.g., $\bar{u}(t) = u(-t)$ which is stable. Thus by first reversing the sequence $y(t)$ we get $\bar{y}(t) = y(-t)$, filtering gives

$$\bar{u}(t) = G_-^{-1}(q^{-1})\bar{y}(t), \tag{2.3}$$

and the resulting sequence $u(t)$ is obtained as $u(t) = \bar{u}(-t)$.

Let us now formulate the above example as an algorithm. Under the assumption that $G_-(z)$ is a maximum phase system the inverse is obtained as follows.

i) Construct a time-reversed sequence $\bar{y}(t) = y(-t)$

ii) Construct a stable inverse as $G_-^{-1}(z^{-1})$

iii) Compute $\bar{u}(t)$ by causal filtering as

$$\bar{u}(t) = G_-^{-1}(q^{-1})\bar{y}(t)$$

where q^{-1} is the backward shift operator.

iv) Finally the input sequence is $u(t) = \bar{u}(-t)$.

For systems where the zeros are both inside and outside the unit circle the transfer function can be partitioned as

$$G(z) = G_+(z)G_-(z) \tag{2.4}$$

where $G_+(z)$ includes the minimum phase zeros and $G_-(z)$ includes the maximum phase zeros. In this case the stable inverse of $G_+(z)$ will be causal, while the stable inverse of $G_-(z)$ is non-causal. Thus the algorithm above can be used for the filtering through $G_-(z)$, see (Shalvi and Weinstein 1994) and (Forssell and Hjalmarsson 1999) for further details and examples. The stable inversion of linear models will be further utilized in Chapter 5.

Remark: Not all systems have inverses. For example, an ideal low pass filter does not have an inverse (Oppenheim and Schafer 1989) since there is no way to recover the frequency components above the cutoff frequency that are set to zero by the ideal low pass filter. Thus, a condition for a system to be invertible is that there is a one-to-one correspondence between the input and the output.

2.1.3 State-space description of linear systems

Let us for completeness also consider an LTI system described by a state-space formulation. Consider an nth order SISO state-space model

$$\begin{aligned} x(t+1) &= Fx(t) + Ge(t) \\ y(t) &= Hx(t) + De(t), \end{aligned} \tag{2.5}$$

where $x(t) \in \mathbb{R}^n$ is the state vector, while $e(t) \in \mathbb{R}$ and $y(t) \in \mathbb{R}$ are the input and output signals, respectively. The matrices have the following dimensions $F \in \mathbb{R}^{n\times n}$, $G, H \in \mathbb{R}^n$ and D is a scalar ($D \in \mathbb{R}$), since we will here only consider SISO systems. The transfer function of (2.5) is given by

$$G(z) = H(zI - F)^{-1}G + D. \tag{2.6}$$

The zeros of the transfer function (2.6) are given as the roots of

$$H(zI - F)^{-1}G + D = 0,$$

and the poles are given by

$$\det(zI - F) = 0.$$

The inversion of continuous time linear systems on state space form is the topic of (Hirschorn 1979*b*). The ideas behind the inversion will be applied to discrete time systems below. The causal inverse of a state space description (2.5) is given by

$$\begin{aligned} x(t+1) &= (F - GD^{-1}H)x(t) + GD^{-1}y(t) \\ e(t) &= -D^{-1}Hx(t) + D^{-1}y(t), \end{aligned} \tag{2.7}$$

provided D is nonzero. If $D = 0$ then (2.7) cannot be applied. The inverse is then found by considering time shifts of $y(t)$ ($y(t+1), y(t+2), ...$) until the coefficient in front of the input $e(t)$ is nonzero. To illustrate this we consider

$$y(t+1) = Hx(t+1) = H[Fx(t) + Ge(t)] = HFx(t) + HGe(t),$$

and if $HG = 0$ we continue with

$$y(t+2) = HF^2x(t) + HFGe(t),$$

etc. until $HF^pG \neq 0$. Thus if one of HG, HFG, HF^2G, ..., $HF^{n-1}G$, is nonzero, the system is invertible. The relative order r is defined to be the smallest positive integer r such that $HF^{r-1}G \neq 0$. Hence, by definition we have $HF^{r-1}G \neq 0$, hence,

$$y(t+r) = HF^rx(t) + HF^{r-1}Ge(t).$$

The input $e(t)$ can then be obtained by

$$e(t) = (HF^{r-1}G)^{-1}\left(y(t+r) - HF^rx(t)\right). \tag{2.8}$$

As seen in (2.8) we need the states $x(t)$, which are computed by solving

$$\begin{aligned} x(t+1) &= Fx(t) + Ge(t) \\ &= (F - G(HF^{r-1}G)^{-1}HF^r)x(t) + G(HF^{r-1}G)^{-1}y(t+r). \end{aligned}$$

Hence, the model is acting as a kind of state observer, estimating the unknown states. To apply both causal and anti-causal filtering of a system on state-space form the system has to be partitioned into a minimum phase and maximum phase system first.

Remark: Strictly speaking the time-shift using the relative degree above is a non-causal operation. We will, however, not emphasize this fact since we mainly consider non-causal filtering as filtering when a whole sequence of data is reversed as in Example 2.1.

Related work for multiple-input multiple-output (MIMO) systems the invertibility criteria are given in (Hirschorn 1979*a*) for continuous time systems.

2.2 Nonlinear systems

A nonlinear system can be described in a number of ways. We will consider nonlinear single-input single-output (SISO) systems described on state-space form as

$$\begin{aligned} x(t+1) &= f(x(t), e(t)) \\ y(t) &= h(x(t), e(t)), \end{aligned} \tag{2.9}$$

where $x(t) \in \mathbb{R}^n$ denotes a state vector, $e(t) \in \mathbb{R}$ denotes the input and $y(t) \in \mathbb{R}$ the output. The dependence of a parameter vector is omitted to simplify the notation. In the following sections inversion of nonlinear state-space systems will be considered. This implies that there is a one-to-one mapping between the input and the output.

First, let us give the definitions of relative degree and the state space description on normal form. This is necessary to later define the concept of minimum phase in the nonlinear case, and in extension the concept of non-minimum phase. As in the linear case these concepts are related to the stability of the inverse.

Given a nonlinear discrete-time SISO system as in (2.9), the relative degree r is given by the number of time-shifts that has to be applied to the output such that it explicitly depends on the input (Califano *et*

al. 1998). By applying a state transformation, where $z = T(x)$, the description (2.9) can be written on normal form as

$$\begin{aligned} z_1(t+1) &= z_2(t) \\ &\vdots \\ z_{r-1}(t+1) &= z_r(t) \\ z_r(t+1) &= \varphi(z(t), \eta(t), e(t)) \\ z_{r+1}(t+1) &= \psi_1(z(t), \eta(t), e(t)) \\ &\vdots \\ z_n(t+1) &= \psi_{n-r}(z(t), \eta(t), e(t)). \end{aligned} \tag{2.10}$$

The output is given by

$$y(t) = z_1(t),$$

and the vectors $z(t)$ and $\eta(t)$ are defined as $z(t) = (z_1(t), \ldots, z_r(t))^T$ and $\eta(t) = (z_{r+1}(t), \ldots, z_n(t))^T$ such that we can write

$$\eta(t+1) = \Psi(z(t), \eta(t), e(t)). \tag{2.11}$$

The dynamics of (2.11) is commonly denoted *internal dynamics* or *zero dynamics*. If the system is linear and written on normal form then the eigenvalues of the zero dynamics will be the same as the zeros of the linear system. Hence, the concepts of minimum, non-minimum and also maximum phase are related to the zero dynamics.
Remark: According to (Califano *et al.* 1998) the normal form in (2.10) can be directly related to the continuous time form given in e.g., (Isidori 1995) if it satisfies

$$\frac{d\eta(t+1)}{de(t)} = 0.$$

Let us now consider continuous time systems written on normal form, which is similar to (2.10) with time shifts of the left hand side replaced by time-derivatives with a similar subsystem denoted as the zero dynamics, (Isidori 1995). A continuous time system is denoted minimum phase if the zero dynamics is asymptotically stable (Khalil 1996). A system with unstable zero dynamics is, thus, not minimum phase and therefore denoted non-minimum phase. A similar definition is given in (Chen and

Paden 1996) where system is considered to be non-minimum phase if there exists a stable feedback that can hold the system output identically zero, while the zero dynamics become unstable.

In the discrete time case, the definition of a minimum phase system is similar to the continuous time case (Monaco and Normand-Cyrot 1987) or (Chen and Khalil 1995).

Definition 2.1. *The system in (2.9) is minimum phase if the zero dynamics is asymptotically stable.*

Consider the linearization at the origin of the zero dynamics

$$A = \frac{d}{d\eta}\Psi(0,0,0), \tag{2.12}$$

where the eigenvalues of A reflect the locations of the zeros of the linearized system. Thus, the zero dynamics is asymptotically stable, at least in a local sense, if all eigenvalues of A are strictly inside the unit circle. In (Vidyasagar 1993) more details are given on asymptotic stability of nonlinear systems based on linearization.

The system in (2.9) is non-minimum phase if it is not minimum phase, which means that, at least one of the eigenvalues of A are outside the unit circle.

Remark: The concept of maximum phase is sometimes used to denote the case in which all the eigenvalues of A in (2.12) are outside the unit circle.

2.2.1 Inversion of nonlinear systems

In the linear case it was possible to separate the parts with stable and unstable zero dynamics, i.e., zeros inside and outside the unit circle, to obtain a stable inverse, c.f. Section 2.1. In the nonlinear case this is not a trivial task if at all possible. Instead we will first consider a minimum phase system and later also show an example for a maximum phase system. In Chapter 5 we will return to nonlinear non-minimum phase systems to present and analyze an iterative method that can be used to obtain a stable inverse.

Inversion of nonlinear minimum phase systems

The inverse of the system on normal form in (2.10) is found by solving

$$y(t+r) = \varphi(z(t), \eta(t), e(t))$$

for $e(t)$ as

$$e(t) = \varphi^{-1}(z(t), \eta(t)), \tag{2.13}$$

provided that the inverse of φ exists. The states of (2.13) are given by

$$\begin{aligned} z_1(t) &= y(t) \\ &\vdots \\ z_r(t) &= y(t+r) \\ \eta_1(t) &= \psi_1(z(t-1), \eta(t-1), e(t-1)) \\ &\vdots \\ \eta_{n-r}(t) &= \psi_{n-r}(z(t-1), \eta(t-1), e(t-1)). \end{aligned} \tag{2.14}$$

The causal inverse of (2.10) will be stable if the zero dynamics is asymptotically stable. In the case of non-minimum and maximum phase systems, the inverse as applied in (2.13) and (2.14), will not be stable if applied causally. There are however methods that can be used in these cases. In the maximum phase case, time reversion can give a stable inverse as exemplified below. In the case of a non-minimum phase system we show in Chapter 5 that the method of iterative learning control (ILC) can be applied. The ILC algorithm is based on a linear approximation and non-causal filtering is used to iteratively find the inverse.
Remark: In the case the system is given on the form

$$\begin{aligned} x(t+1) &= f(x(t)) + g(x(t))e(t) \\ y(t) &= h(x(t)) \end{aligned}$$

where $x(t) \in \mathbb{R}^n$ and $e(t), y(t) \in \mathbb{R}$ the normal form is can be written as

$$\begin{aligned} z_1(t+1) &= z_2(t) \\ &\vdots \\ z_{r-1}(t+1) &= z_r(t) \\ z_r(t+1) &= \alpha(z(t), \eta(t)) + \beta(z(t), \eta(t))e(t) \\ z_{r+1}(t+1) &= \varphi_1(z(t), \eta(t), e(t)) \\ &\vdots \\ z_r(t+1) &= \varphi_{n-r}(z(t), \eta(t), e(t)). \end{aligned} \tag{2.15}$$

This results in the inverse

$$e(t) = \left(z_r(t+1) - \alpha(z(t), \eta(t))\right) / \beta(z(t), \eta(t)),$$

where

$$\begin{aligned} z_1(t) &= y(t) \\ &\vdots \\ z_r(t) &= y(t+r) \\ \eta(t) &= \Psi(z(t), \eta(t-1), e(t-1)). \end{aligned}$$

Let us now consider a simple example of the inversion technique just described.

Example 2.2. *Consider the system*

$$\begin{aligned} x_1(t+1) &= \theta_1 x_2(t) \\ x_2(t+1) &= \theta_2 x_2(t) + \theta_3 x_1(t) e(t) \\ y(t) &= x_1(t), \end{aligned}$$

where $x_i(t), (i = 1, 2)$ *are the states,* $e(t)$ *is the input,* $y(t)$ *is the output and* $(\theta_i, i = 1, 2, 3)$ *are parameters. We can calculate* $e(t)$ *from the output by considering time-shifted values of* $y(t)$

$$\begin{aligned} y(t+1) &= x_1(t+1) = \theta_1 x_2(t) \\ y(t+2) &= \theta_1 x_2(t+1) = \theta_1\theta_2 x_2(t) + \theta_1\theta_3 x_1(t) e(t) \\ &= \theta_2 y(t+1) + \theta_1\theta_3 y(t) e(t). \end{aligned} \tag{2.16}$$

Now, we can calculate $e(t)$ *from (2.16) as*

$$e(t) = \frac{1}{\theta_1\theta_3 y(t)} \left(y(t+2) - \theta_2 y(t+1)\right). \tag{2.17}$$

Notice that we need $y(t+2)$ *to compute* $e(t)$ *and, hence, strictly speaking the filter is non-causal. However, in the following we will rather consider the case when the whole data set is reversed as non-causal. This will not be a problem for off-line identification purposes.*

Inversion of nonlinear maximum phase systems

As mentioned above, the stability of the zero dynamics is essential for the stability of the inverse system. In the linear case we showed an example where the zeros of a non-minimum phase system were transformed by reversing the time series. Similar ideas can be applied in the nonlinear case, which we will exemplify without further analysis. We consider the following example where the system is given on normal form as

$$\begin{aligned} z_1(t+1) &= z_2(t) \\ z_2(t+1) &= 0.5z_1(t) + z_2(t)\eta(t) + z_2(t)e(t) \\ \eta(t+1) &= -0.5\eta(t) + e(t) \\ y(t) &= z_1(t) \end{aligned} \tag{2.18}$$

where $e(t)$ is the input and $y(t)$ denotes the output. Given the output, the input is computed by solving (2.18) as

$$e(t) = (z_2(t+1) - z_2(t)\eta(t))/z_2(t).$$

This gives

$$\begin{aligned} \eta(t+1) &= -0.5\eta(t) + e(t) \\ &= -0.5\eta(t) + (z_2(t+1) - z_2(t)\eta(t))/z_2(t) \\ &= -1.5\eta(t) + z_2(t+1)/z_2(t) \end{aligned}$$

which is unstable since the coefficient in front of $\eta(t)$ has an absolute value greater than one. However, by reversing the time-series, the state $\eta(t)$ can be written as

$$\eta(t) = -[\eta(t+1) - (z_2(t+1) - 0.5z_2(t))/z_2(t)]/1.5, \tag{2.19}$$

which corresponds to a stable system. Then the input can be computed as

$$e(t) = (z_2(t+1) - 0.5z_2(t) - z_2(t)\eta(t))/z_2(t)$$

where $\eta(t)$ is computed by (2.19).

2.3 Some related work

Inversion of linear and nonlinear systems is used both in the area of identification and control. Here we will give examples on some of the work presented in these areas. We will also review the definitions of right and left invertibility.

2.3.1 Inversion for system identification

In (Tong 1990) the connection between invertibility and stationarity is noted. In (Chen and Billings 1989) the concept of model-invertibility (also called m-invertibility) is developed in the context of nonlinear autoregressive moving average (NARMA) models

$$y(t) = f(y(t-1), ...y(t-n_y), e(t-1), ..., e(t-n_e)) + e(t),$$

where $f(\cdot)$ is some nonlinear function. Since the noise term $e(t)$ is added to f the inverse is

$$\varepsilon(t) = y(t) - f(y(t-1), ...y(t-n_y), \varepsilon(t-1), ..., \varepsilon(t-n_e)),$$

and the model is claimed to be invertible if

$$E\{(e(t) - \varepsilon(t))^2\} \to 0 \text{ as } t \to \infty. \tag{2.20}$$

As pointed out in (Chen and Billings 1989), when the actual system generating $y(t)$ is more complex than the model, then the condition (2.20) might be unrealistic. Therefore, m-invertibility is introduced and provided that the $y(t)$ and ε and their initial conditions stay within certain boundaries, then the m-invertibility condition is

$$E\{(\varepsilon^{[1}(t) - \varepsilon^{[2}(t))^2\} \to 0 \text{ as } t \to \infty, \tag{2.21}$$

where $[1, [2$ denotes different initial conditions.

2.3.2 Inversion for control purposes

Given a desired output signal, the computation of a suitable control signal (input) may be achieved using an inverse. As an example in linear control theory, the internal model control (IMC) method, (Morari and Zafiriou 1989*a*), is based on the inversion of at least some parts of the model that can be inverted causally. The inversion of nonlinear continuous time control systems has been considered in, e.g., (Hirschorn 1979*b*, Hirschorn 1979*a*) and in (Isidori 1995).

2.3.3 Right and left invertibility

Right and left invertibility are two different concepts of invertibility that appear in the literature, see e.g., (Fliess 1986, Kotta 1990) or (Perdon

et al. 1992). Loosely speaking, *left invertibility* is about uniquely finding the input, given the output and *right invertibility* is about finding one input sequence (not necessarily unique) such that the output is equal to a desired reference signal.

To give a formal definition we consider a continuous time state-space model

$$\dot{x}(t) = f(x(t), \theta) + e(t)g(x(t), \theta)$$
$$y(t) = h(x(t), \theta),$$

where f, g, h denote nonlinear functions, x denotes the state vector, $e(t)$ is the input and $y(t)$ is the output. In the following $\mathcal{Z}^+$, will denote the set of non-negative integers. The state space is denoted X and the output space is denoted by Y. In the case where a reference function r is used it also equals the desired output.

Definition 2.2. *A system is said to be* left invertible at time k, *if, for every* $l \in \mathcal{Z}^+$, *there exists an integer* $\sigma \in \mathcal{Z}^+$ *such that the input is uniquely determined over the interval* $[k-l, k]$ *by the knowledge of the initial state* $x(k-l)$ *and of the output* y *over the interval* $[k-l, k+\sigma]$.

Definition 2.3. *A system is said to be* right invertible at time k, *if, for every* $l \in Z^+$, $x_0 \in X$ *and the reference function* $r(\cdot) \in Y$ *is defined over the interval* $[k, k+l+1]$, *there exists an integer* $\sigma \in \mathcal{Z}^+$ *and an input* u *defined over the interval* $[k-\sigma, k+l]$ *such that for the initial state* $x(k-\sigma) = x_0$ *the output* $y(j) = r(j)$ *for all* $j \in [k, k+l+1]$.

As will be clear in the following chapters we have to consider cases where we can uniquely find the input given the output when the inversion is used for identification purposes. Left inverses and invertibility are therefore important for identification. However, it can be noted that, in cases with a one-to-one relationship, a right inverse might act as a left inverse. Finally, right invertibility is the adequate concept for control by inversion. For nonlinear systems different implementations of the inverse have been used, see e.g., (Devasia *et al.* 1996) for output tracking of nonlinear systems. In (Kotta 1990) and (Kotta 1995) the right inverse of discrete-time nonlinear systems is considered.

Chapter 3

Introduction to parameter estimation.

Parameter estimation is reviewed in this chapter. A background to the prediction error method (PEM) and the maximum likelihood (ML) method is given, and relations to frequency domain methods are highlighted.

3.1 Prediction error methods

Recall the example of the inverted pendulum in Chapter 1 where the parameters could be considered as unknown a priori. By calibrating these parameters to obtain, in some sense, the best possible model we get the parameter estimates. There are different procedures for parameter estimation and we will first consider the prediction error method followed by the maximum likelihood method.

Let us start by restating some of the results in (Ljung 1999), e.g, what can be interpreted as "the best possible" model. First we consider models $\mathcal{M}(\theta)$ parameterized by the parameter vector $\theta \in D_M \subset \mathbb{R}^d$. A general description of nonlinear state-space discrete-time SISO model is

$$\begin{aligned} x(t+1) &= f(x(t), u(t), e(t), \theta) \\ y(t) &= h(x(t), u(t), v(t), \theta) \end{aligned} \tag{3.1}$$

where $x(t) \in \mathbb{R}^n$ is a state vector, $u(t) \in \mathbb{R}$ is a known input signal while $y(t) \in \mathbb{R}$ denotes the measured output. The functions f and h represent

general nonlinear functions and the disturbance signals $e(t) \in \mathbb{R}$ and $v(t) \in \mathbb{R}$ are independent random variables. A predictor of the output $y(t)$ in (3.1) is given by

$$\hat{y}(t|\theta) = g(t, Z^{t-1}, \theta), \tag{3.2}$$

where $g(\cdot)$ is based on the model. In (3.2), Z^{t-1} denotes the data set

$$Z^{t-1} = [y(1), u(1), y(2), u(2), \ldots, y(t-1), u(t-1)],$$

where $u(t)$ and $y(t)$ denotes the measured inputs and outputs of the system. Parameter estimation can be seen as the task of using measured data Z^N to find a suitable value, which we will denote $\hat{\theta}$, of θ.

As stated in (Ljung 1999), parameter estimation can be represented by the mapping

$$Z^N \to \hat{\theta} \in D_M,$$

where it is also shown that the prediction error

$$\varepsilon(t, \theta) = y(t) - \hat{y}(t|\theta),$$

is an appropriate performance measure. To measure the size of the prediction error a cost function

$$V_N(\theta) = \frac{1}{N} \sum_{t=1}^{N} l(\varepsilon(t, \theta)), \tag{3.3}$$

is introduced. In (3.3), $l(\varepsilon(t, \theta))$ is a scalar function of $\varepsilon(t, \theta)$ (l is typically a positive function). A standard choice of l is the quadratic function

$$l(\varepsilon(t, \theta)) = \frac{1}{2}\varepsilon^2(t, \theta), \tag{3.4}$$

since it is convenient both for computation and analysis. The parameter estimates are given by

$$\hat{\theta} = \arg \min_{\theta \in D_M} V_N(\theta).$$

3.2 The maximum likelihood method

The maximum likelihood (ML) method is a general method for parameter estimation for which the statistical properties are good and it can

be applied in many situations (Åström 1980). The analysis of convergence and consistency for the ML method, when applied to identification of dynamical systems, has been covered in, e.g., (Ljung 1999) and (Hjalmarsson 1993). The main idea is to consider the observed output $y(t)$ as a random variable with some probability density function (PDF) $p_y(y, \theta)$. Thus the PDF depends on an unknown parameter vector θ. For the estimation of θ from observations of $y(t)$, the method aims at choosing a value of θ that maximizes the likelihood function

$$L(\theta; y^N) = p_y(y^N; \theta).$$

Here we consider N observations of $y(t)$ and denote all observations

$$y^N = (y(N), y(N-1), ..., y(1))^T.$$

To further analyze the ML method, we first assume that the model has the following structure

$$y(t) = g(t, Z^{t-1}, \theta) + e(t), \tag{3.5}$$

where $e(t)$ is a white disturbance signal. The optimal predictor for the model is

$$\hat{y}(t|\theta) = g(t, Z^{t-1}, \theta), \tag{3.6}$$

and the prediction error is

$$\varepsilon(t, \theta) = y(t) - \hat{y}(t|\theta) \tag{3.7}$$

where $\varepsilon(t, \theta)$, under the model assumption, are independent for different values of t and have the PDF $p_e(x, t, \theta)$. The likelihood function is given by

$$\begin{aligned} L(\theta; y^N) &= \prod_{t=1}^{N} p_e(y(t) - g(t, Z^{t-1}, \theta), t, \theta) \\ &= \prod_{t=1}^{N} p_e(\varepsilon(t, \theta), t, \theta). \end{aligned} \tag{3.8}$$

Maximizing $L(\theta; y^N)$ in (3.8) is the same as minimizing $-\log L(\theta; y^N)$, since the natural logarithm function is a monotonic increasing function. Thus, we can use the cost function

$$-\frac{1}{N} \log L(\theta; y^N) = -\frac{1}{N} \sum_{t=1}^{N} \log p_e(\varepsilon(t, \theta), t, \theta).$$

With

$$l(\varepsilon(t,\theta),t,\theta) = -\log p_e(\varepsilon(t,\theta),t,\theta)$$

we obtain

$$\hat{\theta} = \arg\min_{\theta} \frac{1}{N}\sum_{t=1}^{N} l(\varepsilon(t,\theta),\theta,t).$$

Hence, the ML method can be seen as a special case of PEM. In the case of Gaussian distributed prediction errors with the PDF

$$p_e(x,t,\theta) = \frac{1}{\sqrt{2\pi\sigma^2}} e^{-\frac{x^2}{2\sigma^2}}, \tag{3.9}$$

where σ^2 is the noise variance, we get

$$-\log p_e(\varepsilon(t,\theta),t,\theta) = const + \frac{1}{2}\log\sigma^2 + \frac{\varepsilon(t,\theta)^2}{2\sigma^2}.$$

Hence, if the variance σ^2 is given, either a priori or by separate optimization, then the ML criterion is the same as the quadratic criterion in PEM.

3.2.1 Inversion based ML estimation

The computation of the likelihood in (3.8) is based on the case where the model is linear in the disturbance as exemplified in (3.5). If the model is nonlinear in the disturbance, i.e., the model includes a nonlinear function of the disturbance, then the likelihood is given by an inverse of the model (Bohlin 1991).

Let us introduce the following notation for the model

$$y^N = P_N(e^N,\theta), \tag{3.10}$$

where e^N is defined similarly to y^N

$$e^N = (e(N), e(N-1), ..., e(1))^T.$$

Recall that the principle of the ML method is based on treating the observed variable, $y(t)$, as a random variable with a PDF, denoted $p_y(y,\theta)$. This PDF depends on the model and the PDF, $p_e(e,\theta)$, of the input. The probability of $y(t)$ thus depends on the parameter vector θ. To estimate

θ from the observations of $y(t)$, the method chooses a θ, which maximizes the likelihood, similar to what was done in (3.8).

The PDF $p_y(y^N;\theta)$ can be derived using the inverse of the model which will be shown below. Let us first define the model residuals $w(t,\theta)$ by

$$y^N = P_N(w^N(\theta),\theta). \tag{3.11}$$

Assuming that y^N has been generated by (3.10) for some $\theta = \theta_0$, note that the model residuals $w(t,\theta)$ will be equal to the true input $e(t)$ only if $\theta = \theta_0$ and the model uses the same initial states as the true system. We denote the relationship between the sequences $w^N(\theta)$ and y^N by $W_N(y^N,\theta)$, thus

$$w^N(\theta) = W_N(y^N,\theta). \tag{3.12}$$

As shown in (Jazwinski 1970), $p_y(\cdot)$ can be computed as

$$p_y(y^N;\theta) = p_e(W_N(y^N,\theta);\theta)\left\|\frac{dW_N(y^N,\theta)}{dy^N}\right\|, \tag{3.13}$$

where $p_e(\cdot)$ is the PDF of the white disturbance input $e(t)$ and $\|\cdot\|$ denotes the absolute value of the determinant. In Appendix A the derivation of (3.13) is restated.

Remark: It is further on assumed that the output y at time instant t depends on the stochastic input e at time instant t. This assumption is of pure bookkeeping nature since time-shifts in the stochastic disturbance has no practical effect. If, e.g., there is a delay of r samples between an input $\bar{e}(t)$ and $y(t)$, then the system description must, when used as described here, be compensated for the time delay. Thus, instead of using $\bar{e}(t)$, the input $e(t+r) = \bar{e}(t)$ should be used such that there is no delay between $y(t)$ and $e(t)$, otherwise the determinant will be zero. Note that the time-shift r is identical to the relative degree in Section 2.2.

The inverse is considered to be causal if the output of the inverse depends only on previous inputs up to that time-instant. Correspondingly, if the output depends on the input from that time-instant and future inputs, the inverse is anti-causal. In both these cases the matrix $\frac{dW_N(y^N,\theta)}{dy^N}$ is triangular and the determinant is the product of all the diagonal elements. Thus, we get

$$L(\theta;y^N) = \prod_{i=1}^{N} p_e(W_N(y^N,\theta),\theta)\left|\frac{\partial W(y^N,\theta)}{\partial y(i)}\right|, \tag{3.14}$$

where $|\cdot|$ denotes the absolute value.

Maximizing the likelihood is the same as minimizing the negative logarithm of $L(\theta; y^N)$. Assuming that p_e is a Gaussian PDF, the logarithm of the likelihood in (3.14) becomes,

$$-\log L(\theta; y^N) = \frac{1}{2\sigma^2}\sum_{i=1}^{N} w^2(i) - \sum_{i=1}^{N}\log\left|\frac{\partial W(y^M,\theta)}{\partial y(i)}\right| + N\log\sigma + \frac{N}{2}\log 2\pi. \tag{3.15}$$

Without loss of generality we can assume that $\sigma^2 = 1$ since if this does not hold, we can include a corresponding gain in the model P. Correspondingly, if the variance is unknown, the gain can be included in the parameter vector θ and thus be identified. Thus, since $\log(1) = 0$ and the last term of (3.15) is a constant the minimization of (3.15) is equivalent to minimizing

$$V(\theta) = \sum_{i=1}^{N}\left(\frac{1}{2}w^2(i) - \log\left|\frac{\partial W_N(y^N,\theta)}{\partial y(i)}\right|\right). \tag{3.16}$$

Finally, the ML estimate of θ is obtained as

$$\hat{\theta} = \arg\min_{\theta} V(\theta).$$

The log$|\cdot|$ term in (3.16).

The log term in (3.16) might appear unfamiliar at first. This is probably due to that it vanishes for models of the type

$$y(t) = f(y^{t-1}, e^{t-1}, \theta) + e(t), \tag{3.17}$$

where $f(\cdot)$ can be either linear or nonlinear. Since $e(t)$ appears explicitly in the right hand side of (3.17), the inverse is easily computed as

$$w(t,\theta) = y(t) - f(y^{t-1}, w^{t-1}, \theta), \tag{3.18}$$

and $\frac{\partial w(t,\theta)}{\partial y(t)} = 1$ in this case. Assuming that the relationship (3.18) is causal, the $\log|\cdot|$ term vanishes and the loss function reduces to

$$V(\theta) = \sum_{i=1}^{N}\frac{1}{2}w^2(i,\theta). \tag{3.19}$$

Additive disturbances as in (3.17) is commonly assumed in the literature, see e.g., (Tong 1990), which motivates the cost function (3.19). Further details on ML estimation are given in e.g. (Ljung 1999).

Non-causal systems

Recall that the step to derive (3.14) required causality or anti-causality. However, in the linear case this requirement can be relaxed. Consider the stable linear system in (2.1) which can be described by a matrix formulation as

$$y^N = D^{-1}B^{-1}ACe^N \tag{3.20}$$

where A, B, C and D are Toeplitz matrices with elements being the impulse responses of $A(z), B(z)$ etc. Thus the elements are given by

$$A_{ij} = \begin{cases} a_{i-j} & 0 \le i-j \le n_A \\ 0 & \text{otherwise} \end{cases}$$
$$B_{ij} = \begin{cases} b_{i-j} & 0 \le i-j \le n_B \\ 0 & \text{otherwise} \end{cases}$$
$$C_{ij} = \begin{cases} c_{i-j} & -n_C \le i-j \le 0 \\ 0 & \text{otherwise} \end{cases}$$
$$D_{ij} = \begin{cases} d_{i-j} & -n_D \le i-j \le 0 \\ 0 & \text{otherwise} \end{cases} .$$

Hence, A and B are lower triangular matrices and C and D are upper triangular matrices. All matrices will have ones in the diagonal due to the assumption $a_0 = b_0 = c_0 = d_0 = 1$, and zero initial conditions are assumed. The inverse relationship of (3.20) is given by

$$e^N = C^{-1}A^{-1}BDy^N, \tag{3.21}$$

thus

$$\frac{dW_N(y^N, \theta)}{dy^N} = C^{-1}A^{-1}BD.$$

Since the diagonal elements of all matrices are equal to one

$$\det\left(\frac{dW_N(y^N, \theta)}{dy^N}\right) = 1.$$

In conclusion, the $\log|\cdot|$ term is equal to zero, under the conditions above, even if the system is non-causal in the linear case. The stability, and the practical implementation of the inverse in the non-causal case, will be covered in Section 2.1.2. However, first the calculation of the log term will be considered.

Calculation of the log $|\cdot|$ term in (3.16).

Recall the system

$$y^N = P_N(e^N)$$

and the inverse $W_N(\cdot)$ which satisfies

$$P_N\left(W_N(y^N)\right) = y^N,$$

where we have dropped the θ-argument to simplify the notation and assuming zero initial conditions. Taking the derivative w.r.t. y^N gives

$$\frac{d}{dy^N}\left(P_N\left(W_N(y^N)\right)\right) = \frac{dP_N}{de^N}\frac{dW_N(y^N)}{dy^N} = I_N.$$

Hence,

$$\frac{dP_N}{de^N} = \left(\frac{dW_N(y^N)}{dy^N}\right)^{-1},$$

provided the inverse exists. Thus, $\frac{dP_N}{de^N}$ is a matrix with the ijth element

$$\left[\frac{dP_N}{de^N}\right]_{ij} = \frac{\partial P_{N,i}(e^N)}{\partial e(j)}.$$

Since $\det(A^{-1}) = (\det(A))^{-1}$ we can use

$$\det\left(\frac{dW_N(y^N)}{dy^N}\right) = \left(\det\frac{dP_N}{de^N}\right)^{-1}.$$

Let us now assume a state-space description of P, i.e.

$$\begin{aligned} x(t+1) &= f(x(t), e(t)) \\ y(t) &= h(x(t), e(t)), \end{aligned}$$

where $x(t)$ is a state vector, $e(t)$ is the input and $y(t)$ is the output. Then $\frac{\partial P(e^t)}{\partial e(t)} = \frac{\partial y(t)}{\partial e(t)}$ is given by

$$\frac{\partial y(t)}{\partial e(t)} = \left.\frac{\partial h}{\partial x}\right|_{\substack{x=x(t)\\e=e(t)}} \frac{\partial x(t)}{\partial e(t)} + \left.\frac{\partial h}{\partial e}\right|_{\substack{x=x(t)\\e=e(t)}}$$

$$\frac{\partial x(t+1)}{\partial e(t)} = \left.\frac{\partial f}{\partial x}\right|_{\substack{x=x(t)\\e=e(t)}} \frac{\partial x(t)}{\partial e(t)} + \left.\frac{\partial f}{\partial e}\right|_{\substack{x=x(t)\\e=e(t)}}$$

which is a linear time-varying system based on a linearization around the trajectory described by $x(t)$ and $e(t)$. The trajectory described by $x(t)$ and $e(t)$ is obtained from the inversion resulting in $e(t)$ which has to be obtained first. In other words the elements of $\frac{dP_N}{de^N}$ can be calculated by a linear time-varying system. This will be further studied in Section 4.4 and in Appendix B. Note that computing the whole matrix $\frac{dP_N}{de^N}$ can be quite cumbersome.

3.3 Frequency domain identification

This section serves as a background to the spectral based parameter estimation methods that will be introduced in Chapter 7. In the end of this section the relationships between the log terms in the time and frequency domain ML criterion, will be considered. In the linear case it will be shown how they relate to the variance of the input.

Frequency domain data can be used for fitting linear models as stated in, e.g., (Pintelon *et al.* 1994, Ljung 1999, Pintelon and Schoukens 1999). Originally, frequency domain methods were developed and recommended for cases with periodic excitations. For arbitrary excitations, time domain methods were suggested, (Pintelon *et al.* 1994), since the main drawback of the frequency domain methods for arbitrary excitations is leakage (error) in the calculation of the frequency domain data. In (Pintelon *et al.* 1994) frequency domain methods are motivated for the case where periodic excitation is used, by:

- Easy noise reduction. The non-excited frequency lines can be eliminated.
- Data reduction. A large number of time-domain samples can be replaced by a smaller number of spectral lines.
- The initial states of the system does not have to be estimated.

- Easy to combine data from different experiments.

Also, a motivation for applying frequency domain methods are when frequency domain measurements are available. In e.g., the mechanical engineering community and vibrational analysis this is common, (Ljung 1999).

It can be noted that frequency domain methods have recently been applied to cases with arbitrary excitations (Pintelon and Schoukens 1997, Pintelon and Schoukens 1999, Schoukens *et al.* 1999). The main idea is to use an extended transfer function taking leakage into account. In (Pintelon and Schoukens 1999) frequency domain methods are used for ARMA model identification.

Let us briefly study the basic ideas of frequency domain identification covered in (Ljung 1999). In the general, linear discrete-time, case a model of the following form is assumed

$$y(t) = G(q,\theta)u(t) + H(q,\theta)e(t), \tag{3.22}$$

where $u(t)$ is an applied control signal, $e(t)$ is white noise with zero mean and variance σ^2 and $y(t)$ is the measured output. $G(q,\theta)$ and $H(q,\theta)$ are transfer functions parameterized by θ, q is the time shift operator. In the frequency domain we have

$$Y(\omega_k) = G(e^{i\omega_k},\theta)U(\omega_k) + H(e^{i\omega_k},\theta)E(\omega_k)$$

which actually should be extended with an error term unless the signals are periodic and observed over an integer number of periods.

As pointed out in (Ljung 1999) it is tempting to use the cost function

$$V_N(\theta) = \sum_{k=1}^{N} |Y(\omega_k) - G(e^{i\omega_k T},\theta)U(\omega_k)|^2 \cdot \frac{1}{|H(e^{i\omega_k T},\theta)|^2}, \tag{3.23}$$

where $Y(\omega_k)$ and $U(\omega_k)$ are the discrete Fourier transform of $y(t)$ and $u(t)$ $(t = 1,\ldots,N)$. However, the approach in (3.23) will only give a consistent estimate of θ under certain conditions that will be given below. In the case of no input signal the cost function in (3.23) correspond to *Whittle-type* estimators (Whittle 1951). An alternative to (3.23) is presented in (Ljung 1999) which is an ML approach based on the fact that

$$\begin{aligned} E(\omega) &\in N_c(0,\sigma^2) \\ Y(\omega_k) &\in N_c(G(e^{i\omega_k},\theta)U(\omega_k), \sigma^2|H(e^{i\omega_k},\theta)|^2) \\ Y(\omega_k) &\text{ and } Y(\omega_l) \text{ are asymptotically independent for } k \neq l. \end{aligned}$$

where N_c denotes the normal distribution and the subscript c indicates complex noise. The cost function based on the negative logarithm becomes

$$V_N(\theta) = N \log \sigma + \sum_{k=1}^{N} \log |H(e^{i\omega_k}, \theta)| + \frac{1}{2\sigma^2} \sum_{k=1}^{N} |Y(\omega_k) - G(e^{i\omega_k}, \theta) U(\omega_k)|^2 \frac{1}{|H(e^{i\omega_k}, \theta)|^2}, \quad (3.24)$$

and the ML estimate is given by

$$\hat{\theta} = \arg\min_{\theta} V_N(\theta).$$

If we only consider the case when only H is modeled, the cost function would reduce to

$$V_N(\theta) = N \log \sigma + \sum_{k=1}^{N} \log |H(e^{i\omega_k}, \theta)| + \frac{1}{2\sigma^2} \sum_{k=1}^{N} \frac{|Y(\omega_k)|^2}{|H(e^{i\omega_k}, \theta)|^2}. \quad (3.25)$$

The simplification which led to (3.25) gives us a cost function based on spectral components. In the literature a number of different cost functions are developed from the idea of matching transfer functions to measured frequency domain data. The methods are developed to gain computational cost and improve sensitivity to different errors, see (Pintelon *et al.* 1994) for a survey and evaluation. Further on, aspects on the unimodality of the cost function (existence of only one global minimum) and the stability of fitted models with lower order than the actual system are taken using a spectral domain approach in (Tugnait and Tontiruttananon 1998). In (Pillai and Shim 1993), ARMA system identification and model order selection using spectral information is covered. It can finally be noted that there is a `MATLAB` toolbox for frequency domain identification of linear models (Kollàr 1994).

Relations between the $\log|\cdot|$ terms in the frequency and the time domain

The occurrence of the log terms in (3.25) is similar to the log terms in the time-domain ML criterion in (3.16). There are two log terms in (3.25), $N \log \sigma$ and $\sum_{k=1}^{N} \log |H(e^{i\omega_k}, \theta)|$. If the variance of the disturbance is

known then the first term can be omitted from the cost function. Also the second term can be omitted if $H(q,\theta)$ is monic[1], stable and inversely stable, since

$$\sum_{k=1}^{N} \log|H(e^{i\omega_k},\theta)| = 0, \tag{3.26}$$

assuming that the frequencies are equally spaced, $\omega_k = \frac{2\pi k}{N}$, (Ljung 1999). If (3.26) holds then (3.23) is identical to (3.24) and, hence, (3.23) yields consistent estimates.

If, on the other hand, the variance σ^2 is unknown the problem can be reparameterized by assuming $\sigma = 1$ for the first log-term and instead assume that $H(q,\theta) = \lambda\bar{H}(q,\theta)$ where $\bar{H}(q,\theta)$ is monic. Hence, the log-term remaining in (3.25) is $N\log\lambda$. The factor λ is similar to $\frac{\partial W_N(y^N,\theta)}{\partial y(t)}$ that occurs in the time-domain ML criterion, even though no particular distribution is assumed. In fact if the system is linear then W_N is a Toeplitz matrix based on the impulse response coefficients of $H(q,\theta)$. We have, $\frac{\partial W_N(y^N)}{\partial y(t)} = 1/\lambda$, where the inverse corresponds to the negative sign of the term in (3.16).

In conclusion, even though the log term stems from the normal distribution in the frequency domain and the log term in the time-domain stems from the inverse derivation of the likelihood function there is close connection. This connection is related to the variance of the disturbance.

[1] A transfer function is monic if the coefficient $h_0 = 1$ when $H(q) = \sum_{k=0}^{\infty} h_k q^{-k}$.

Chapter 4

Feedback inversion

4.1 Introduction

The objective of this chapter is to study the problem of model inversion that occurs in parameter estimation in discrete-time nonlinear stochastic models. The rationale for using inversion in ML based parameter estimation was given in Section 3.2 where it was shown how the likelihood function is derived based on the inverse relationship. It is further shown how the gradients, used for the optimization of the cost function, can be generated by a linear time-varying feedback system associated with the nonlinear model. In addition, we derive sufficient conditions for the existence of a stable causal inverse as well as sufficient conditions for the initial transient to decay. These conditions are given in terms of properties for a linear time-varying system associated with the nonlinear model.

The models under study are of the type

$$\begin{aligned} x(t+1) &= \bar{g}(x(t), e(t), u(t), \theta), \quad x(0) = x_0(\theta) \\ y(t) &= \bar{p}(x(t), e(t), u(t), \theta) \end{aligned}$$

where $\theta \in D_{\mathcal{M}} \subset \mathbb{R}^d$ is an unknown parameter vector, $x(0) \in \mathbb{R}^n$ is the initial state, $e(t) \in \mathbb{R}$ is the unknown stochastic input which is assumed to be white, $u(t) \in \mathbb{R}^q$ is a measured input and $y(t) \in \mathbb{R}$ is the output.

Defining $g(x(t), e(t), \theta, t) = \bar{g}(x(t), e(t), u(t), \theta)$ and

$p(x(t), e(t), \theta) = \bar{p}(x(t), e(t), u(t), \theta, t)$ transforms the model above into

$$x(t+1) = g(x(t), e(t), \theta, t), \quad x(0) = x_0(\theta) \tag{4.1}$$
$$y(t) = p(x(t), e(t), \theta, t) \tag{4.2}$$

where the t-dependence reflects the possible dependence on a known input. Since it turns out that the measured input $u(t)$ does not play a role in the context below we will use (4.1)–(4.2) as our basic model.

The study will be limited to invertible models, thus, models with a one-to-one relationship between the stochastic input and the output.

It is assumed that the probability density function (PDF) of the stochastic input is known save for possibly some unknown parameters. In Figure 4.1, a schematic of the problem set-up is shown.

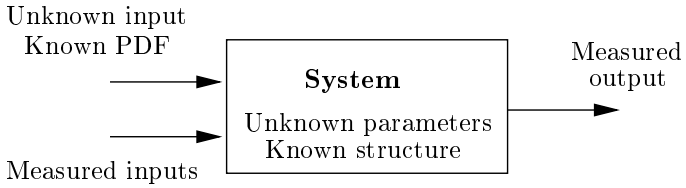

Figure 4.1: A schematic of the problem, where the unknown parameters of the system are to be estimated.

A necessary step in computationally efficient prediction error and maximum likelihood estimation of nonlinear stochastic models is that the model has to be inverted. For a linear model this is trivial but for nonlinear models this can be a quite difficult, or even impossible, task if done symbolically. This problem of inversion is the theme of this chapter.

Example 4.1. *Consider the static system*

$$y(t) = \exp(e(t)) + \sin(e(t)) \tag{4.3}$$

where $|e(t)| < 0.5$. *The function* $P(x) = \mathrm{e}^x + \sin(x)$ *is monotonic on* $[-0.5, 0.5]$ *and hence invertible. There is, however, no explicit expression for the inverse so trying to find the inverse using symbolic software such as Mathematica is futile.*

In the previous example it was not possible to do the inversion symbolically. Instead, one has to use a numerical equation solver to solve (4.3) for $e(t)$. As we will show later, the same situation arises when causal

inversion of discrete time dynamical systems is considered. This means that model inversion can be computationally very demanding since one algebraic equation has to be solved numerically at each point in time.

In Section 4.3 it is clarified when an algebraic equation solver has to be employed in causal inversion of (4.1)–(4.2). A feedback characterization of the inverse is also derived. This configuration enables simple implementation of the inverse itself and the gradients of the ML criterion in simulation environments such as Matlab/Simulink and Matrix$_X$/Systembuild. The latter is discussed in Section 4.4. Sufficient conditions for the existence of a causal inverse are derived in Section 4.5. The transient due to the initial state in the model inverse may affect the statistical properties, such as consistency and asymptotic variance, of the parameter estimates in nonlinear model identification. Section 4.5 provides sufficient conditions for when this is not the case. Finally, numerical examples are shown in Section 4.6. Different parts of the results in this chapter are presented in (Markusson and Hjalmarsson 1998) and (Markusson and Hjalmarsson 2000*a*), and the results are summarized in (Markusson and Hjalmarsson 2001*b*).

4.2 Unknown initial states and ML

In ML estimation, the initial state x_0 should be treated as an unknown parameter and estimated together with θ. However, it is well known, see, e.g., (Ljung 1999), that initial states cannot be identified consistently. Hence, it is common to fix the initial state in the model, e.g. to zero. The algorithm is then commonly referred to as conditional ML (Söderström and Stoica 1989). Provided that the transient effect of the initial state vanishes sufficiently fast, the conditional ML inherits the asymptotic statistical properties of the ML method such as consistency and efficiency (Söderström and Stoica 1989).

To illustrate this, consider for simplicity the ML criterion (3.16) and consider the case where the true system is in the model class, i.e. there is a parameter $\theta = \theta_0$, an initial state x_0 and a white Gaussian input signal $e(t)$ such that the output is given by (4.1)–(4.2). It is then well known, (Söderström and Stoica 1989), that $\theta = \theta_0$ and $x(0) = x_0$ minimizes the criterion (3.16) as $N \to \infty$. Denote by $w(t)$ the model residuals that are obtained when the model is based on an erroneous initial state $\overline{x}_0$ but that $\theta = \theta_0$. Suppose now that $|e(t) - w(t)| < C\ \lambda^t$ for some $0 \leq \lambda < 1$ and $C < \infty$, i.e. the transient due to the erroneous initial

state vanishes exponentially fast. Then the absolute difference between the criteria using correct and erroneous initial state, respectively, is given by

$$\begin{aligned}
&\left| \frac{1}{N} \sum_{t=0}^{N-1} |w(t)|^2 - \frac{1}{N} \sum_{t=0}^{N-1} |e(t)|^2 \right| \\
&= \left| \frac{1}{N} \sum_{t=0}^{N-1} |w(t) - e(t)|^2 + 2e(t)(w(t) - e(t)) \right| \\
&\leq D \frac{1}{N} \sum_{t=0}^{N-1} (\lambda^{2t} + \lambda^t) \to 0 \text{ as } N \to \infty.
\end{aligned}$$

Above D is a finite positive constant. Hence, the criterion does not depend on the initial state asymptotically and under suitable assumptions (Söderström and Stoica 1989) the conditional ML is consistent. Since the asymptotic covariance matrix of the ML estimates depends only on the second derivative of the cost function and the noise variance, (Ljung 1999), it is also possible to show that the conditional ML is asymptotically efficient when the transient vanishes sufficiently fast, e.g. exponentially, as above. In Section 4.5 we will provide sufficient conditions for when the transient due to initial conditions vanishes exponentially fast.

In Section 4.3, we will consider how to compute the model residuals, i.e. how to invert the model. We will therefore assume the initial state to be given, either as a parameter as in ML or as a fix state as in the conditional ML.

4.3 Inversion of nonlinear stochastic models

From (3.16) and (3.11) it is clear that in ML (and PEM) estimation of nonlinear stochastic models, model inversion is crucial since the likelihood (3.8) is based on the model input.

In (3.18) we have seen that nonlinear autoregressive models

$$y(t) = f(y^{t-1}, \theta) + e(t)$$

are easily inverted (recall $y^{t-1} = (y(t-1), \ldots, y(1))^T$). However, for models where the input does not appear explicitly at the output, the computation can be complicated. For example, in the introduction we saw that for the static system (4.3) in Example 4.1 no explicit inverse can be computed so that this has to be done numerically.

In this section we will show a way to implement the inverse that is ideally suited for numerical simulation environments.

4.3.1 Model description

We will study discrete-time systems where the scalar output $y(t)$ is generated by a system of the type (4.1)–(4.2). We also introduce the notation

$$y(t) = P(e^t, t), \tag{4.4}$$

where now, in addition to the initial state, we have suppressed the parameter dependence to indicate that we are considering one particular model corresponding to some arbitrary θ. We also remind the reader that the $t-$dependence in P allows for known inputs, c.f., the discussion preceding (4.1). For a particular initial state x_0, the input $\{e(t)\}_{t=0}^{N-1}$ generates the output sequence y^N. Inputs that correspond to other initial conditions but which generate the same output y^N, collectively, will be denoted by $w(t)$.

We also assume that the model is invertible, i.e. for a given initial state, the map W_N in (3.12) exists and is unique. We further assume that the state vector $\{x(t)\}_{t=0}^{\infty}$ and the output $\{y(t)\}_{t=0}^{\infty}$ in (4.1)–(4.2) are bounded when the input sequence $\{e(t)\}_{t=0}^{\infty}$ is bounded.

4.3.2 Inversion by equation solving

Let us return again to the simple static case in Example 4.1. Determining the input $e(t)$ for a particular time t and a particular output $y(t)$ amounts to solving

$$y(t) = P(e(t))$$

for $e(t)$ which, of course, is equivalent to solving

$$y(t) - P(e(t)) = 0. \tag{4.5}$$

Equation (4.5) can be displayed in block diagram form as in Figure 4.2.a where $\varepsilon(t) = y(t) - P(e(t))$. Here, the algebraic equation solver finds the value $e(t)$ which satisfies $0 = \varepsilon(t) \triangleq \varepsilon(t, e(t))$, which is the same as computing the inverse of $P(e(t))$.

Thus for static systems, the entire input trajectory can be determined by simulating the feedback system in Figure 4.2.a forward in time. This

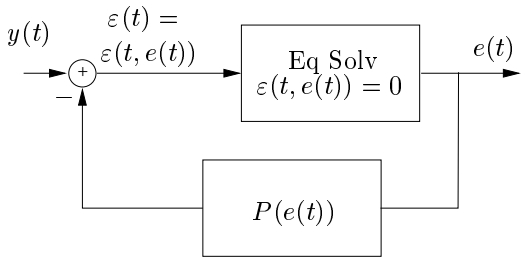

a - Static case

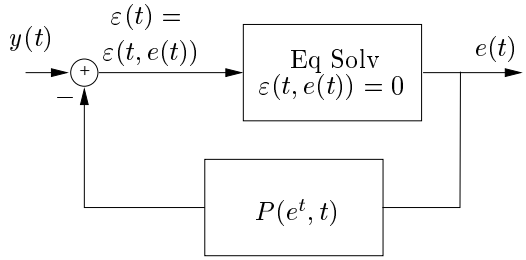

b - Dynamic case

Figure 4.2: Inversion by equation solving both in the static (a) and the dynamic (b) case.

suggests a very easy way to obtain the input trajectory for static nonlinear systems using simulation environments capable of handling algebraic equations.

The key observation is now that for dynamical causal nonlinear systems

$$y(t) = P(e^t, t),$$

exactly the same simulation set-up can be employed, see Figure 4.2.b. Let us describe the dynamical case by an example.

Example 4.2. *Consider an extension of Example 4.1 where dynamics is added to the system*

$$x(t+1) = \sin(x(t)e(t)) \tag{4.6}$$

$$y(t) = e(t) + \exp(e(t)) + \sin(e(t)) + x(t). \tag{4.7}$$

If we now apply the setting in Figure 4.2.b then

$$\varepsilon(t) = y(t) - e(t) - \exp(e(t)) - \sin(e(t)) - x(t) \tag{4.8}$$

Assume that the initial state $x(0)$ is known. For $t = 0$, the algebraic equation $\varepsilon(0) = 0$ reads $y(0) - e(0) - \exp(e(0)) - \sin(e(0)) - x(0) = 0$ and can be solved for $e(0)$ since all other quantities are known. Hence, the algebraic equation solver gives $e(t)$ for $t = 0$. Using $e(0)$ and $x(0)$ in (4.6) then gives $x(1)$. Now, the algebraic equation $\varepsilon(1) = 0$ contains no other unknowns than $e(1)$ which can be solved for $t = 1$. The procedure can now be repeated for $t = 2, 3, \ldots$ and the inverse $e(t)$, $t = 0, 1, 2, \ldots$ is obtained.

Example 4.2 shows that for a state-space model with a given initial condition, inversion requires an algebraic equation to be solved for at each point in time. At time t, the input $e(t)$ is the only unknown and all other variables such as e.g. the state vector, are known.

We thus have a very simple way of computing the inverse of nonlinear causal dynamical models: Implement the system in Figure 4.2.b in a simulation environment that is capable of handling algebraic loops such as Matlab and Matrix$_X$. Thus, the burden of solving the algebraic equation is delegated to the simulation software.

Some remarks are appropriate at this point:

- The feedback system in Figure 4.2.b is somewhat non-standard since it explicitly includes an algebraic equation solver.
- A simulation using the structure in Figure 4.2.b generates a *causal* inverse.
- The existence of a *bounded* causal inverse depends on the stability of the feedback system in Figure 4.2.b. For linear time-invariant systems this is equivalent to that P is minimum-phase. For a general nonlinear system the stability issue is more complicated – it depends both on the system itself and the excitation signal $y(t)$ (Isidori 1995). Due to the equation solver in Figure 4.2.b it is not obvious how to analyze the stability.
- Unless the initial conditions in $P(e^t, t)$ in Figure 4.2.b are identical to those of the true system, the output of the feedback system will not be identical to the true input $e(t)$. It is not obvious how to base an analysis of the initial conditions using the structure in Figure 4.2.b.

In Section 4.3.4 we will recast the inversion structure in Figure 4.2.b into a feedback structure which is more tractable for analysis of e.g. the influence of initial conditions and the existence of a stable causal inverse. Based on this structure a linear time-varying system is derived in Section 4.5 whose stability is sufficient for the existence of a causal inverse. This alternative inversion structure will also be used to show that no algebraic equation has to be solved for a certain class of partitioned models.

4.3.3 Solving algebraic equations

As we have seen above, model inversion for systems with a scalar output and one unknown input requires solving one algebraic equation for each point in time. This can be done numerically using standard iterative search algorithms such as Newton's method (Dennis and Schnabel 1996). Many of these algorithms are available in numerical software packages such as, e.g., LINPACK, Matlab/Simulink and Mathematica. For example, Matlab/Simulink uses Newton's method with weak line search and rank one updates of a Jacobian approximation.

For non-convex problems, which frequently occur in nonlinear identification, there is no guarantee that these iterative search methods will find a solution even if it exists. To enhance the possibility of finding a solution and to increase the convergence speed, it is necessary to provide an initial guess of the solution that is as close as possible to the solution. One possibility in our application is to use the previous (in time) value of the computed inverse as initial guess.

Also, one should notice that in general there is no guarantee that there *exists* a solution to the algebraic equation. Non-existence of a solution implies that the model is not suitable either because that the model itself is incorrect (wrong θ) or that the measured signal is influenced by other signals such as, e.g., unmodeled sensor noise. A model for which the inverse does not exist should be discarded since it cannot explain the observed data. Here, since our focus is on the inversion, we will assume that the model is invertible and, hence, that there is a solution.

The solution may also be non-unique, which means that different initial start values may give different solutions. Notice that non-uniqueness of the inverse by-itself is typically not a problem since often different input sequences (corresponding to the same model) can be discriminated by the likelihood function – the problem is instead that one has to find all the solutions and this may be difficult.

4.3.4 Model inversion by feedback

Let us define an arbitrary linear time-invariant system which is stable and minimum-phase and denote the system by

$$L(q^{-1}) = \sum_{l=0}^{\infty} c_l \, q^{-l}, \tag{4.9}$$

where q^{-1} is the time-shift operator, i.e., $(q^{-1}e(t) = e(t-1))$ and $c_0 \neq 0$. Now we can write (4.4) as

$$\begin{aligned} P(e^t, t) &= L(q^{-1})e(t) + (P(e^t, t) - L(q^{-1})e(t)) \\ &\triangleq L(q^{-1})e(t) + N(e^t, t). \end{aligned} \tag{4.10}$$

We have thus partitioned the system into two parallel parts as shown in Figure 4.3.

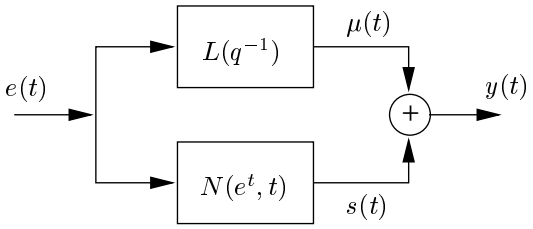

Figure 4.3: Block diagram of a partitioned parallel system, $P(e^t)$.

Following (Doyle *et al.* 1995), we can also write P as

$$P = L(I + L^{-1}N),$$

which gives that the inverse of P can be expressed as

$$(I + L^{-1}N)^{-1}L^{-1}, \tag{4.11}$$

where the t dependence is suppressed. In Figure 4.4, (4.11) is shown in block diagram form where the input to the inverse is $y(t)$ and the output is $w(t)$. The reason for denoting the output of the inverse by $w(t)$ is that, as pointed out in Section 4.2, it will not be exactly equal to $e(t)$ if the initial state is different in the model inverse compared to the model. We see that the causal inverse is obtained from a feedback system consisting

of the inverse of the linear part L in the forward path and the nonlinear part N in the feedback path. Notice that N, and hence P, *does not have to be inverted*. The feedback structure in Figure 4.4 thus suggests an alternative way of obtaining the causal inverse without explicit computation of the inverse of the nonlinear part N which also easily can be implemented in block diagram based simulation environments.

Remarks:

- In general there is an algebraic loop in the set-up in Figure 4.4 which has to be solved by the simulation software. This loop corresponds to the equation solver in Figure 4.2.b.
- The existence of a causal inverse depends on the stability of the feedback loop in Figure 4.4. Notice that since this feedback loop is explicit as opposed to the loop in Figure 4.2.b, the analysis of the inverse is simplified as we will see in Section 4.5.

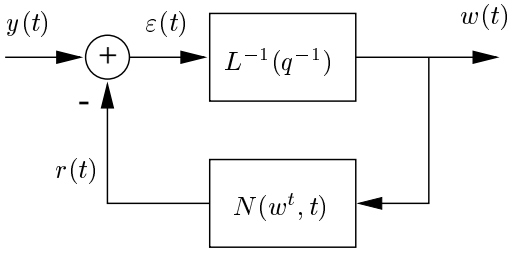

Figure 4.4: Realization of the nonlinear model inverse.

Let us now study an example where the feedback structure shown in Figure 4.4 can be applied to a general nonlinear model.

Example 4.3. *To illustrate the procedure let us return to Example 4.2. Rewriting (4.6) according to (4.10) using* $L(q^{-1}) = 1$ *gives that the model is given by*

$$\begin{aligned} x(t+1) &= \sin(x(t)e(t)) && (4.12)\\ s(t) &= \exp(e(t)) + \sin(e(t)) + x(t) && (4.13)\\ \mu(t) &= e(t) && (4.14)\\ y(t) &= s(t) + \mu(t), \end{aligned}$$

where (4.12) and (4.13) represents the nonlinear part and (4.14) represents the linear part. The inverse is illustrated in Figure 4.4 and, denoting the state by $z(t)$, we have

$$\begin{aligned} z(t+1) &= \sin(z(t)w(t)) \\ r(t) &= \exp(w(t)) + \sin(w(t)) + z(t) \\ \varepsilon(t) &= y(t) - r(t) \\ w(t) &= \varepsilon(t). \end{aligned}$$

Assuming $z(0) = x(0)$, we can identify $z(t)$ with $x(t)$, $r(t)$ with $s(t)$ and $w(t)$ with $e(t)$, i.e. the feedback loop in Figure 4.4 generates the inverse when the correct initial state is used.

4.3.5 Partitioned models

Assume that $c_0 \neq 0$ in (4.9) and that $N(e^t, t)$ in (4.10) does not depend on $e(t)$ but only on previous inputs $e(t-1), e(t-2), \ldots$, in other words, P can be decomposed into a linear time-invariant part L with a direct term and a nonlinear part N with at least one time-delay

$$P(e^t, t) = L(q^{-1})e(t) + N(e^{t-1}, t).$$

For such partitioned models there will be no algebraic loop in Figure 4.4 which means that the inversion of such models is *extremely simple*. In its turn, this means significantly lower computational complexity.

Remark: It is only the relative time-delay between the linear and the nonlinear part that matters in the case of parameter estimation with unknown stochastic inputs since the time-index may be shifted arbitrarily. Hence, in the general case there will be no algebraic loop if the time-delay in N is larger than the time-delay in L.

4.3.6 Summary

In this section we have considered inversion of nonlinear dynamical models. We have shown that, in general, this requires solving an algebraic equation for each point in time of the input trajectory. Our contribution has been to show that the inversion can be implemented as a feedback loop based on the model which fits into the framework of today's simulation environments. In this configuration, the actual inversion is delegated to the simulation software's equation solver.

Using this structure of the inverse, we also showed that for models partitioned as a linear part L in parallel with a nonlinear part N with a larger time-delay than the linear part, the inversion is very simple since no equation solver is necessary.

In Section 4.4 we will use the feedback configuration of the model inverse to derive the gradients of the cost function. We will further benefit from this structure in Section 4.5 where we will analyze the effect of erroneous initial conditions.

4.4 Computation of derivatives

Efficient numerical minimization of the cost function (3.16) requires use of the gradient of the cost function, see e.g. (Dennis and Schnabel 1996). It turns out that using the scheme in Figure 4.2.b, it can be shown that the gradient can be obtained by simulating a linear time-varying feedback system. This is related to the ideas in (De Bruyne *et al.* 1996) where tuning of nonlinear controllers is considered and (De Bruyne *et al.* 1999) where identification of nonlinear models in closed loop are considered.

To simplify matters and be explicit we will assume that the input is Gaussian. Let us use $w(t) = w(t, \theta)$ to simplify notation, then the ML criterion is given by (3.16)

$$V(\theta) = \sum_{t=1}^{N} \frac{1}{2}|w(t)|^2 - \sum_{t=1}^{N} \log \left| \frac{\partial w(t)}{\partial y(t)} \right|.$$

Furthermore we assume a state-space representation of the nonlinear operator N in (4.10) so that $r(t)$ in Figure 4.4 is given by

$$\begin{aligned} z(t+1) &= f(z(t), w(t), \theta, t) \\ r(t) &= h(z(t), w(t), \theta, t). \end{aligned} \tag{4.15}$$

These restrictions are not essential and the method can easily be adapted to other cost functions and model structures. Note that in (4.15) the parameter dependence appears explicitly and in the following we will do so when appropriate.

The derivative of the cost function with respect to one parameter θ_k is given by

$$\frac{\partial V(\theta)}{\partial \theta_k} = \sum_{t=1}^{N} \frac{\partial w(t)}{\partial \theta_k} w(t) + \sum_{t=1}^{N} \left| \frac{\partial w(t)}{\partial y(t)} \right|^{-1} \frac{\partial}{\partial \theta_k} \left(\frac{\partial w(t)}{\partial y(t)} \right). \tag{4.16}$$

Hence, to calculate the cost function and the derivatives of the cost function used for the optimization we need to calculate $\frac{\partial w(t)}{\partial \theta_k}$, $\frac{\partial w(t)}{\partial y(t)}$ and $\frac{\partial}{\partial \theta_k}\left(\frac{\partial w(t)}{\partial y(t)}\right)$.

In Appendix B we show that $\frac{\partial w(t)}{\partial \theta_k}$ can be obtained as in Figure 4.5. This is a feedback system consisting of the linear part L in series with the linearization of the nonlinear part N. The linearization is taken along the trajectory that is obtained when the feedback system in Figure 4.4 is simulated, i.e.,

$$\begin{aligned}\frac{\partial z(t+1)}{\partial \theta_k} &= \frac{\partial f}{\partial z(t)}\frac{\partial z(t)}{\partial \theta_k} + \frac{\partial f}{\partial \theta_k} + \frac{\partial f}{\partial w(t)}\frac{\partial w(t)}{\partial \theta_k} \\ \frac{\partial r(t)}{\partial \theta_k} &= \frac{\partial h}{\partial z(t)}\frac{\partial z(t)}{\partial \theta_k} + \frac{\partial h}{\partial \theta_k} + \frac{\partial h}{\partial w(t)}\frac{\partial w(t)}{\partial \theta_k},\end{aligned} \tag{4.17}$$

where the derivatives are computed along the trajectory $z(t)$ and $w(t)$, i.e. e.g.,

$$\frac{\partial f}{\partial z(t)} = \frac{\partial f(z(t), w(t), \theta, t)}{\partial z(t)}.$$

This gives the following procedure for obtaining the derivative $\frac{\partial w(t)}{\partial \theta_k}$

i) Simulate the feedback system given in Figure 4.4. Record the trajectories $z(t)$, $w(t)$ and $\varepsilon(t)$ during the simulation.

ii) Use the trajectories obtained in i) to do one simulation according to Figure 4.5 for each parameter θ_k.

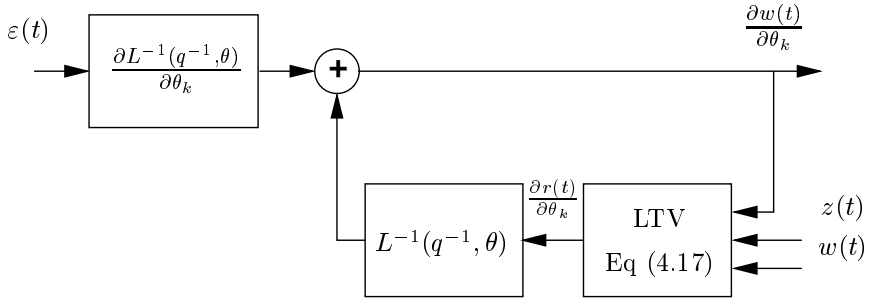

Figure 4.5: Linear time-varying filter calculating the derivative $\frac{\partial w(t)}{\partial \theta_k}$.

In conclusion, the derivatives used in (4.16) can be obtained using $\frac{\partial w(t)}{\partial \theta_k}$ as shown in Figure 4.5. In Appendix B it is also shown how to compute $\frac{\partial w(t)}{\partial y(t)}$ and $\frac{\partial}{\partial \theta_k}\left(\frac{\partial w(t)}{\partial y(t)}\right)$, see (B.5) and (B.6).

4.5 Existence of the inverse and analysis of unknown initial conditions

In this section we will analyze the existence of a stable causal inverse. This issue is linked to the stability of the feedback system in Figure 4.4. Also linked to the stability of this feedback loop is the influence of an erroneous initial state on the inverse. In this section we will use the feedback structure in Figure 4.4 to establish sufficient conditions for 1) the existence of a stable causal inverse and 2) the influence of the initial conditions to vanish. The conditions will be based on a linear time-varying system associated with the feedback system in Figure 4.4.

4.5.1 Model description

We will assume that the system is in the state space form (4.1)–(4.2) but we will partition it according to (4.10), cf. Figure 4.3. We assume relative degree zero of the linear system, and hence the whole system. We introduce the following notation

$$\begin{aligned} \zeta(t+1) &= A\zeta(t) + Be(t) \\ \mu(t) &= C\zeta(t) + De(t), \quad D \neq 0 \\ x(t+1) &= f(x(t), e(t), t) \\ s(t) &= h(x(t), e(t,t)) \\ y(t) &= \mu(t) + s(t) \end{aligned} \tag{4.18}$$

where $\zeta(t)$ and $x(t)$ are the state vectors of the linear part L and the nonlinear part N, respectively. The input to both parts is denoted $e(t)$ and the output of each subsystem is $\mu(t)$ and $s(t)$, respectively, summed together to give the total output $y(t)$. Since we will analyze the stability and transient for one particular model we have dropped the θ dependence as well.

Remark: The assumption $D \neq 0$ corresponds to that $c_0 \neq 0$ in (4.9).

4.5.2 Inverse model description

In Figure 4.6 the forward and the inverse systems are shown with the internal signals presented. The states of each block are given within parenthesis.

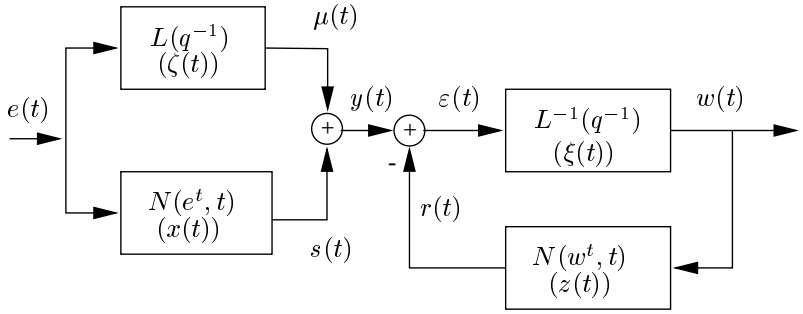

Figure 4.6: Block diagram of the forward and the inverse system.

With the inverse and the notation as in Figure 4.6, the state-space equations of the inverse system are

$$\begin{aligned} \xi(t+1) &= (A - BD^{-1}C)\xi(t) + BD^{-1}\varepsilon(t) \\ w(t) &= -D^{-1}C\xi(t) + D^{-1}\varepsilon(t) \\ z(t+1) &= f(z(t), w(t), t) \\ r(t) &= h(z(t), w(t), t) \\ \varepsilon(t) &= y(t) - r(t) \end{aligned} \tag{4.19}$$

assuming D is nonzero. However, since the states of the inverse model are unknown

$$\zeta(0) \neq \xi(0) \tag{4.20}$$

$$x(0) \neq z(0), \tag{4.21}$$

the output of the inverse $w(t)$ will not be equal to $e(t)$. The initial errors due to (4.20) and (4.21) will be analyzed in the next section.

4.5.3 Error analysis

To analyze the dependence of erroneous initial state of the inverse model, we consider the differences between $\zeta(t)$, $s(t)$, $e(t)$, and $x(t)$ versus $\xi(t)$,

$r(t)$, $w(t)$ and $z(t)$ which we define as

$$\rho(t) \triangleq \zeta(t) - \xi(t) \tag{4.22}$$

$$\sigma(t) \triangleq s(t) - r(t) \tag{4.23}$$

$$\delta(t) \triangleq w(t) - e(t) \tag{4.24}$$

$$\Delta(t) \triangleq z(t) - x(t). \tag{4.25}$$

We will use the following assumptions

$A1$: The input signals of the system $e(t)$ are bounded as well as the internal dynamics of the system $\zeta(t), x(t)$ and the output of the system $y(t)$.

$A2$: The nonlinear functions $f(z(t), w(t), t)$ and $h(z(t), w(t), t)$ have continuous derivatives w.r.t. $z(t)$ and $w(t)$ up to order 2.

$A3$: $D \neq 0$.

Theorem 4.1. *Under Assumptions A1, A2 and A3 , the inverse will exist and the errors (4.22) - (4.25) due to unknown initial conditions will vanish if the linear time-varying system*

$$\begin{array}{ll} \Delta(t+1) & = \Gamma^{\Delta}(t)\Delta(t) + \Gamma^{\rho}(t)\rho(t) \\ \rho(t+1) & = \Sigma^{\Delta}(t)\Delta(t) + \Sigma^{\rho}(t)\rho(t) \end{array}, \tag{4.26}$$

is asymptotically stable. The components of (4.26) are given by

$$\Gamma^{\Delta}(t) = \frac{\partial f}{\partial z(t)} + \frac{\partial f}{\partial w(t)} \left(-D^{-1} \frac{\partial h}{\partial z(t)} \left(1 + D^{-1} \frac{\partial h}{\partial w(t)} \right)^{-1} \right) \tag{4.27}$$

$$\Gamma^{\rho}(t) = \frac{\partial f}{\partial w(t)} D^{-1} C \left(1 + D^{-1} \frac{\partial h}{\partial w(t)} \right)^{-1} \tag{4.28}$$

$$\Sigma^{\Delta}(t) = B D^{-1} \frac{\partial h}{\partial z(t)} \left(1 + D^{-1} \frac{\partial h}{\partial w(t)} \right)^{-1} \tag{4.29}$$

$$\Sigma^{\rho}(t) = A - B D^{-1} C + B D^{-1} \frac{\partial h}{\partial w(t)} D^{-1} C \left(1 + D^{-1} \frac{\partial h}{\partial w(t)} \right)^{-1}, \tag{4.30}$$

where the derivatives w.r.t. $z(t)$ and $w(t)$ are computed along the trajectory $z(t) = x(t)$ and $w(t) = e(t)$, i.e. e.g.,

$$\frac{\partial f}{\partial z(t)} = \left. \frac{\partial f(z(t), w(t), t)}{\partial z(t)} \right|_{\substack{z(t)=x(t) \\ w(t)=e(t)}}.$$

Proof. The proof is given in the first part of Appendix B. □

According to Theorem 4.1, $w(t)$ will converge towards $e(t)$ if the linear time-varying system (4.26) is asymptotically stable. Thus, we are now concerned with the stability analysis of a LTV system with zero-input. Let us define

$$F(t) = \begin{pmatrix} \Gamma^{\Delta}(t) & \Gamma^{\rho}(t) \\ \Sigma^{\Delta}(t) & \Sigma^{\rho}(t)) \end{pmatrix}, \tag{4.32}$$

such that (4.26) can be written as

$$\begin{pmatrix} \Delta(t+1) \\ \rho(t+1) \end{pmatrix} = F(t) \begin{pmatrix} \Delta(t) \\ \rho(t) \end{pmatrix}. \tag{4.33}$$

The stability of (4.33) can be analyzed with a number of methods, see (Rugh 1996). As an example, the LTV system in (4.33) is uniformly exponentially stable if there exists a finite constant γ and a constant $0 \leq \nu \leq 1$ such that the largest point-wise eigenvalue of $F^T(t)F(t)$, denoted $\lambda_{max}(t)$, satisfies

$$\prod_{i=j}^{t} \lambda_{max}^{1/2}(i) \leq \gamma \, \nu^{t-j} \tag{4.34}$$

for all t, j such that $t \geq j$ (Rugh 1996). This stability result and Theorem 4.1 gives the following corollary.

Corollary 4.1. *The inverse of the nonlinear system (4.18) exists and the output of the inverse $w(t)$ converges towards $e(t)$ as $t \to \infty$ exponentially fast if there exists a finite constant γ and a constant $0 \leq \nu \leq 1$ such that the largest point-wise eigenvalue of $F^T(t)F(t)$ obeys the inequality in (4.34), where $F(t)$ is given by (4.32).*

In Section 4.2 we concluded that, provided the transient due to an erroneous initial state vanishes exponentially fast, the conditional ML estimator in general inherits the nice statistical properties of the ML

estimator asymptotically as $N \to \infty$. Hence, consistency and asymptotic efficiency in nonlinear dynamic ML estimation is normally ensured if the conditions of the corollary above are satisfied (and the system is identifiable).

4.6 Numerical examples

To illustrate the estimation of parameters using the above described inversion technique we will consider two different models. The first model is partitioned as a linear model in parallel with a nonlinear model as shown in Figure 4.3. The second model is a model of air flow as a function of a known valve setting and a stochastic pressure drop. Thus, in the second example there is both a measured input and an unknown stochastic input. These examples were simulated using Matlab 5.3 and Simulink 3.0. The initial value of the algebraic equation solver was zero in all cases.

4.6.1 Example 1

This example is a model with only one unmeasured stochastic input, partitioned as a linear model in parallel with a nonlinear model. The linear part is described by a first order model, $\mu(t) = L(q^{-1}, \theta)e(t)$, where

$$L(q^{-1}, \theta) = \frac{1 + bq^{-1}}{1 + aq^{-1}},$$

where a and b are real valued parameters. The nonlinear part is described by

$$\begin{aligned} x(t+1) &= cx(t) + e(t)/(1 + de(t)^2) \\ s(t) &= x(t) + ge(t)\exp(-he(t)^2) \end{aligned}$$

and the measured output is

$$y(t) = s(t) + \mu(t).$$

The input, $e(t)$, was white Gaussian distributed noise with unit variance.

It is not straightforward to solve manually for $e(t)$ in the model equations above. However, implementation in Simulink, using the methodology presented in Section 4.3, presents no problem.

The parameters, $\theta = (a, b, c, d, g, h)^T$, were simultaneously estimated using the ML method. The true value of θ is given in Table 4.1. One hundred input realizations were used, each containing 1000 samples.

The log-term in (3.16) is given by

$$\frac{\partial w(t)}{\partial y(t)} = \left(1 + g\exp\{-hw(t)^2\}(1 - 2hw^2(t))\right)^{-1}.$$

The estimation results are shown in Table 4.1.

	True value θ_0	$mean(\hat{\theta})$	$std(\hat{\theta})$
a	0.90	0.89	0.02
b	0.60	0.59	0.04
c	0.80	0.79	0.03
d	1.00	1.01	0.20
g	0.70	0.71	0.06
h	0.20	0.20	0.03

Table 4.1: *Example 1, estimation results (100 trials).*

4.6.2 Example 2

In this example we study a part of a ventilation system in a house with a large number of rooms. In particular we study the flow of air into one room. The flow is a function of the control valve setting and the pressure drop over the valve. While the valve setting is known as a measured input, the pressure drop is modeled as an unknown stochastic signal. There are two nonlinear components in the model. An exponential function describes the valve in its range of operation and the air flow is a square root function of the ratio between the pressure drop and the valve setting. The air flow model is given by

$$\begin{aligned} p(t) &= -ap(t-1) + (1+a)e(t) \\ y(t) &= -by(t-1) + (1+b)\sqrt{\frac{p(t)}{\exp\{\alpha(r(t-1)-100)\}}}, \end{aligned} \tag{4.35}$$

where $p(t)$ denotes the pressure and $y(t)$ the air flow. The unknown stochastic input, the pressure drop, is denoted by $e(t)$ and the measured input, the valve setting, is denoted by $r(t)$. The parameters to be estimated are $\theta = (\alpha, a, b)^T$. A block diagram of the air flow model is shown in Figure 4.7.

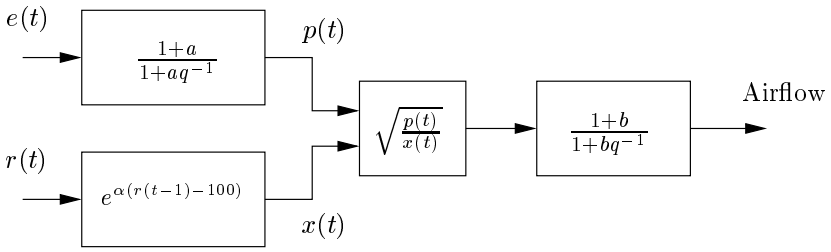

Figure 4.7: A block diagram of the air flow model.

The stochastic input was white Gaussian noise with unit variance and mean $m = 10$. The measured input $r(t)$ varies stepwise in the range $[0, 100]$ as shown in an example in Figure 4.8, where also one example of a realization of the pressure drop is shown along with the output.

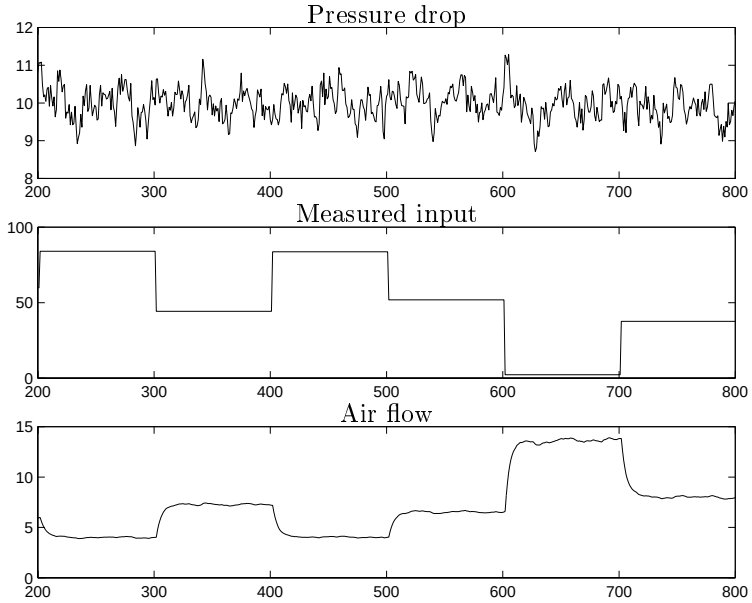

Figure 4.8: Simulated data used in Example 2. Top: Pressure drop $p(t)$, Middle: Measured input $r(t)$, Bottom: Air flow (The output).

Parameter	θ_0	$mean(\hat{\theta})$	$std(\hat{\theta})$
α	0.03	0.030	0.0005
a	-0.7	-0.67	0.049
b	-0.8	-0.80	0.006

Table 4.2: *Example 2, estimation results (100 trials).*

The log-term in (3.16) is given by

$$\frac{\partial w(t)}{\partial y(t)} = \frac{2\sqrt{p(t)}\exp\{0.5\alpha(r(t-1)-100)\}}{(1+a)(1+b)}.$$

As should be clear, solving for $e(t)$ manually in (4.35) requires some effort. However, the implementation in Simulink is straightforward and the estimation results are shown in Table 4.2.

4.7 Summary

In this chapter we have characterized model inversion in terms of a feedback loop. One of the benefits of the feedback configuration is that it can be directly implemented in simulation tools like e.g., Matlab/Simulink or Matrix$_X$/Systembuild. Using the feedback configuration we showed that inversion can be done without involving an equation solver if the model can be partitioned as a linear part in parallel with a nonlinear part where the time-delay in the nonlinear part is larger than in the linear part. Another benefit of the feedback structure is that the computation of the derivatives, used for the optimization of the cost function, can be implemented as a linear time-varying filter. This further simplifies the implementation of a parameter estimator for a nonlinear model structure. Also, this feedback formula was used to derive sufficient conditions for the existence of a stable causal inverse and for the decay of initial errors. Finally, the feedback configuration was used in ML estimation on two numerical examples.

Chapter 5

A general framework for Iterative Learning Control

Iterative learning control (ILC) has proven to be a useful tool for feedforward based tracking problems where high precision is desired and where the system is so complex that normal feedback control is insufficient, c.f. robotics (Gunnarsson and Norrlöf 2001). It is thus of general interest to understand how the design variables should be selected to obtain fast and reliable convergence. Placing ILC in the regime of optimization clarifies the role played by the design variables and how they are related to, e.g., the convergence properties. In addition this also leads to a model based interpretation of one of the design variables. A sufficient condition for convergence of the algorithm for nonlinear systems is also given. The condition has the intuitive interpretation that the design variables have to be chosen such that the desired performance is traded against modeling accuracy. This sheds further light on how the design variables should be chosen. We also point-out that the batch-wise operation of ILC can be used for non-causal feedforward control. Although this has been recognized before, we provide a comprehensive coverage of how the design variables should be chosen to achieve this and also highlight the advantages of this when non-minimum phase systems are concerned.

The main idea behind ILC is to iteratively find an input sequence such that the output of the system is as close as possible to a desired

output. Although ILC is directly associated with control, it is important to note that the end result is that the system has been inverted as will become clear later. Especially the results on stable inversion of nonlinear non-minimum phase systems are worth noting. Hence, ILC can be used as a tool for ML based parameter estimation since ILC offers means for inversion. However, the results of this chapter are general and can be applied to either control or estimation.

Some of the early results on ILC for non-minimum phase nonlinear systems are presented in (Markusson *et al.* 2001) but the main part of the results are submitted as (Markusson *et al.* 2002).

5.1 Introduction to ILC

The ILC method can be applied when the reference signal is given over a finite time interval and thereafter repeated. The idea is to use information about the control error from previous iterations to improve performance in the next iteration (Moore 1999). Many publications have been written on ILC and (Moore 1993), (Moore 1999) and (Norrlöf 2000) provide good introductions. A commonly used example is a robot arm, see e.g., (Norrlöf 2000), where the trajectory of movement is repeated over and over again.

In Figure 5.1 a general description of the ILC method is depicted. The system is given by

$$y_k(t) = P(u_k^t), \tag{5.1}$$

where $u_k^t = [u_k(1) \dots u_k(t)]^T \in \mathbb{R}^t$ is the input to the system P and $y_k(t)$ is the corresponding output, both at the kth iteration of the ILC algorithm. Here, P is a general discrete-time single-input single-output (SISO) system which may be linear or a nonlinear[1]. The signal $y_d(t)$ is the desired output and is given over a finite interval $t \in [1, N]$. Provided it exists, we will denote the corresponding input by $u_d(t)$, i.e. $y_d(t) = P(u_d^t)$.

The system input at the next iteration, $u_{k+1}(t)$, is computed as a function of the desired output $y_d(t)$ and the system output $y_k(t)$ at the kth iteration. Hence, the objective is to iteratively refine the input $u_k(t)$ such that $y_k(t)$ becomes close to $y_d(t)$.

[1]With some abuse of notation we will use $P(u(t))$ to denote the output of a nonlinear *dynamical* system with $u(t)$ as input.

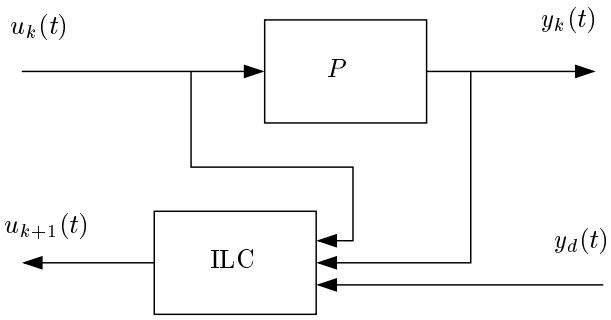

Figure 5.1: Block diagram of the iterative learning control (ILC) method. The output of the system is denoted by $y_k(t)$ and the desired output by $y_d(t)$. The applied control signal is denoted by $u_k(t)$. Note that ILC works with batches of data.

Remark 1: Note that if, at convergence, $u_\infty(t) = u_d(t), \forall t \in [1, N]$ and if the closed loop system is one-to-one then $u_\infty(t)$ is the inverse of the system given $y_d(t)$ as output.

Remark 2: The system is usually already under some kind of feedback control. In this case P denotes the closed loop system.

5.2 ILC - general idea and notation

A standard first order ILC algorithm can be described by

$$\begin{aligned} u_{k+1}(t) &= Q\left(u_k(t) + Le_k(t)\right) \\ e_k(t) &= y_d(t) - y_k(t), \end{aligned} \tag{5.2}$$

where Q and L denotes linear or nonlinear operators which can be seen as design variables chosen by the user. Notation such as u_k will be short-hand for $\{u_k(t)\}_{t=1}^{\infty}$. Note that for a *first order* ILC algorithm the operators Q and L are applied for one iteration (a single k), e.g., in the linear case

$$Qu_k(t) = \sum_{l=t-1}^{t-N} q_l u_k(t-l) \tag{5.3}$$

where q_l are real coefficients. Higher order ILC algorithms, where the result of previous iterations are directly utilized, will not be considered here.

With $u_i^N = [u_i(1), \ldots, u_i(N)]^T \in \mathbb{R}^N$ and e_k^N defined similarly, the algorithm in (5.2) can also be described as

$$u_{k+1}^N = Q_N \left(u_k^N + L_N(e_k^N) \right) \tag{5.4}$$

where $Q_N, L_N : \mathbb{R}^N \to \mathbb{R}^N$. When Q and L are linear, Q_N and L_N becomes matrices, $Q_N, L_N \in \mathbb{R}^{N \times N}$. For example, with $L = L(q)$ (q denotes the time-shift operator) being causal and linear time-invariant, then L_N is given by a lower Toeplitz matrix

$$L_N = \begin{pmatrix} h(0) & 0 & \ldots & 0 \\ h(1) & h(0) & 0 & \vdots \\ \vdots & & \ddots & 0 \\ h(N-1) & h(N-2) & \ldots & h(0) \end{pmatrix}$$

based on the impulse response coefficients $h(i)$ of $L(q)$.

5.3 ILC from an optimization perspective

In this section we will consider the problem of finding a good feedforward control sequence from the perspective of optimization.

5.3.1 Numerical optimization

One way to determine a suitable input would be to form some cost function based on the difference between y_d and y such as

$$V(u^N) = \frac{1}{2} \| y_d^N - y^N \|^2$$

and try to minimize this function with respect to u^N using gradient based numerical optimization methods. This leads to algorithms of the type

$$\begin{aligned} u_{k+1}^N &= u_k^N - \gamma_k \, R_k \frac{dV(u^N)}{du^N} \\ &= u_k^N + \gamma_k \, R_k \frac{dy^N}{du^N} (y_d^N - y^N), \end{aligned}$$

where the step-size γ_k is a scalar and R_k is some matrix. Note that the choice of step-size and the matrix R_k has a profound impact on the properties of the above algorithm.

Now assume that the system is linear such that $y^N = P_N u^N$ where P_N is a lower Toeplitz matrix consisting of the N first impulse response coefficients of the system[2]. Then $dy^N/du^N = P_N$ and hence

$$u_{k+1}^N = u_k^N + \gamma_k \; R_k P_N (y_d^N - y^N).$$

Here we clearly see that since knowledge of P_N is required, the algorithm cannot be used directly unless the system is known. Below we will discuss different approaches to circumvent this problem.

5.3.2 Iterative Feedback Tuning

The term $P_N(y_d^N - y^N)$ can be obtained by doing a new experiment with the error $y_d^N - y^N$ as input to the system. This is very much in the spirit of Iterative Feedback Control (Hjalmarsson *et al.* 1998), where this idea is explored for tuning feedback controllers.

5.3.3 Iterative Learning Control

With $\gamma_k = 1$ and $R_k = L_N \; P_N^{-1}$ we recover the ILC algorithm (5.2) with Q_N the identity. Hence we can interpret ILC in the framework above with a *very* special choice of the matrix R_k.

A common choice of R_k is to use the inverse of the Hessian of V which in the linear case is $(P_N P_N^T)^{-1}$. This gives

$$u_{k+1}^N = u_k^N + P_N^{-1}(y_d^N - y^N)$$

which converges in one step, since the cost function is quadratic in u^N when the system is linear. In ILC this corresponds to using $L_N = P_N^{-1}$ and Q_N the identity.

When the system is nonlinear, the cost function is no longer quadratic in u^N and even if the Hessian is used, convergence in a finite number of steps cannot be expected.

An interesting observation here is that if the ILC algorithm is modified slightly, then convergence in one step can also be obtained. Instead of using the control error $e_k(t)$ explicitly as in (5.4) the ILC algorithm can be written as

$$u_{k+1}^N = Q_N \left(u_k^N + L_N(y_d^N) - L_N(y_k^N) \right). \tag{5.5}$$

[2]We have here assumed zero initial conditions.

For a linear L this makes no difference compared to (5.4) but for a nonlinear L this is not true. Taking Q_N identity and $L_N(y_k^N) = P_N^{-1}(y_k^N) \triangleq u_k^N$ gives convergence in one step for a general L_N. We will therefore use the update (5.5) in the following.

5.3.4 Stochastic approximation

If the observations of dV/du^N are noisy, the step size $\gamma_k = 1/k$ can be used to average out the noise contribution asymptotically (under certain conditions). This idea can also be applied to ILC. However, this will not be further analyzed here.

5.3.5 Design variables in ILC

From the previous discussion in this section, it should be clear that, in order to optimize the convergence rate, L_N should be taken as an inverse model of the system P. In the next section we will see that L_N can be given this interpretation also from a stability point of view. Without loss of generality we will set $L_N = \hat{P}_N^{-1}$ so that

$$u_{k+1}^N = Q_N \left(u_k^N + \hat{P}_N^{-1}(y_d^N) - \hat{P}_N^{-1}(y_k^N) \right). \tag{5.6}$$

Thus Q and $\hat{P}$ are the two design variables and in the following we will examine how they influence stability and convergence of the algorithm.

5.4 Convergence points

We will begin our analysis of ILC by looking at the possible convergence points of (5.6). We will use u_∞ and y_∞ to denote the convergence points of the signals. Using operator notation and assuming that $Q = 1$ gives that $\hat{P}^{-1}(y_d) = \hat{P}^{-1}(y_\infty)$ and hence, if $\hat{P}^{-1}$ is bijective, that $y_\infty = y_d$, i.e. perfect tracking. In this case, of course, the problem must be well posed in the sense that there must be an input trajectory such that the output matches the desired trajectory y_d.

If $Q \neq 1$ but still linear, then

$$\begin{aligned} u_\infty(t) &= Q(q)u_\infty(t) + Q(q)\left(\hat{P}^{-1}(y_d(t)) - \hat{P}^{-1}(y_\infty(t))\right) \\ &= \frac{Q(q)}{1-Q(q)}(\hat{P}^{-1}(y_d(t)) - \hat{P}^{-1}(y_\infty(t))) \end{aligned} \tag{5.7}$$

This corresponds to the feedback system in Figure 5.2. If in addition $\hat{P}^{-1}$ and P are linear we get that the error $e(t) = y_d(t) - y(t)$ can be written as

$$e(t) = \frac{1}{1 + \frac{Q(q)}{1-Q(q)}\hat{P}^{-1}(q)P(q)} y_d(t). \tag{5.8}$$

From this we see that both Q and $\hat{P}^{-1}$ influence the tracking accuracy. Notice that even if $\hat{P} = P$ the tracking error will be non-zero when $Q \neq 1$.

Looking at (5.8) we see that a small tracking error at a particular frequency can be ensured by letting Q be close to 1 at that frequency. From now on we will assume that Q is linear.

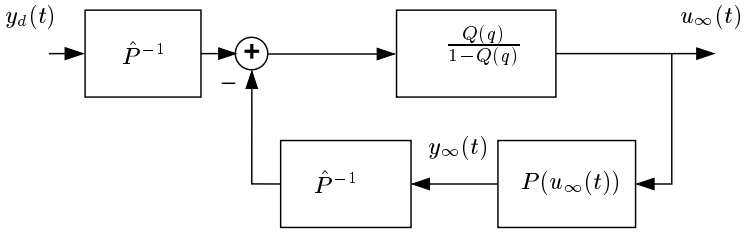

Figure 5.2: Block diagram of the ILC algorithm as $k \to \infty$ in the case $Q \neq 1$.

5.5 Convergence results for linear systems

Let us first summarize the convergence results for linear systems given in (Norrlöf 2000). First we restate the following definitions:

Definition 5.1. ϵ - convergence
A system using ILC is ϵ - convergent in a norm $\|\cdot\|$ if

$$\lim_{k\to\infty} \sup \|u_d - u_k\| < \epsilon.$$

A system using ILC is called *stable* if it is ϵ-convergent with $\epsilon < \infty$. Thus, stability does not imply that the error decays to zero as $k \to \infty$.

Definition 5.2. Asymptotic stability
A system using ILC is asymptotically stable if

$$\lim_{k\to\infty} \sup \|u_d - u_k\| = 0.$$

Linear iterative systems

Consider the matrix formulation of the ILC algorithm in (5.4) applied to a linear system G

$$\begin{aligned} u_{k+1}^N &= Q_N u_k^N + Q_N L_N e_k^N \\ e_k^N &= y_d^N - G_N u_k^N, \end{aligned} \tag{5.9}$$

where $Q_N, L_N, G_N \in \mathbb{R}^{N\times N}$, are Toeplitz matrices. The relationships in (5.9) can be rewritten as

$$u_{k+1}^N = Q_N \left(I_N - L_N G_N\right) u_k^N + Q_N L_N y_d^N, \tag{5.10}$$

which is depicted in Figure 5.3, where q_k denotes the shift operator with respect to iteration index k, i.e., $q_k^{-1} z_k(t) = z_{k-1}(t)$. The stability of

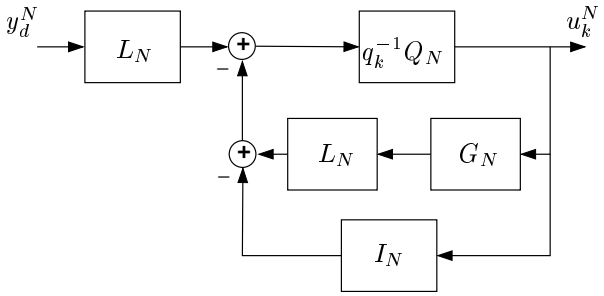

Figure 5.3: Block diagram of the ILC matrix updating in the linear case given by (5.10). Note that q_k denotes the shift operator with respect to iteration index k.

(5.10) can be studied using a linear iterative system given by

$$z_{k+1} = F_k z_k + F_y y_d, \tag{5.11}$$

where $z_k, y_d \in \mathbb{R}^N$ and $F_k, F_y \in \mathbb{R}^{N\times N}$. The stability analysis of (5.11) can be divided into two different cases, iteration invariant systems ($F_k = F \ \forall k$) and iteration variant systems. We will here restate the results for iteration invariant systems and refer to (Norrlöf 2000) for further details on the iteration variant case.

Let us first study the homogeneous part of (5.11) $z_{k+1} = F z_k$, and start by considering the maximum singular value $\bar{\sigma}(F)$ defined as

$$\bar{\sigma}(F) = \sqrt{\rho(F^T F)}. \tag{5.12}$$

In (5.12) $\rho(A)$ is the spectral radius defined as

$$\rho(A) = \max_{i=1,\ldots,N} |\lambda_i(A)|,$$

where λ_i denotes the ith eigenvalue of the matrix $A \in \mathbb{R}^{N\times N}$. Now the maximum singular value gives a bound on the gain of a matrix such that

$$\|Fx\| \leq \bar{\sigma}(F)\|x\|.$$

Thus, the homogeneous part of (5.11), $z_{k+1} = Fz_k$, will be decreasing if $\bar{\sigma}(F) < 1$, which gives

$$\|z_{k+1}\| < \|z_k\|.$$

BIBO stability

A linear iterative system is bounded-input bounded-output (BIBO) stable if a bounded input $\|y_d\| < \infty$ gives a bounded output $\|z_k\| < \infty \ \forall k$. From (Rugh 1996) it follows that the iterative system in (5.11) is BIBO stable if the spectral radius satisfies $\rho(F) < 1$.

If the system (5.11) is BIBO stable (Norrlöf 2000) then, as $k \to \infty$, we get

$$z_\infty = Fz_\infty + F_y y_d. \tag{5.13}$$

Thus, assuming that (5.13) holds, then the difference $\tilde{z}_k = z_k - z_\infty$ can be studied to obtain the conditions for convergence since

$$\begin{aligned}\tilde{z}_{k+1} &= z_{k+1} - z_\infty \\ &= Fz_k - Fz_\infty + F_y y_d - F_y y_d \\ &= F\tilde{z}_k. \end{aligned} \tag{5.14}$$

Hence, the importance of the homogeneous part of (5.11). It can finally be noted, for the ILC algorithm in (5.10), that BIBO stability implies $\epsilon-$convergence for $\epsilon < \infty$.

Asymptotic results

Asymptotic results, as $N \to \infty$, can be stated in the frequency domain by a condition on the scalar iterative system

$$z_{k+1}(t) = F(q)z_k(t) + F_y(q)y_d(t),$$

since if $F(q)$ is stable, causal and satisfies

$$\sup_{\omega\in[0,\pi]} |F(e^{i\omega})| < 1, \tag{5.15}$$

then the largest singular value of the matrix representation (5.11) fulfills

$$\bar{\sigma}(F) < 1$$

and hence $\|z_{k+1}\| < \|z_k\|$. This follows from the result

$$\bar{\sigma}(F_N) \leq \bar{\sigma}(F_{N+1}) \leq \cdots \leq \lim_{N\to\infty} \bar{\sigma}(F_N) = \sup_{\omega\in[0,\pi]} |F(e^{i\omega})|, \tag{5.16}$$

shown in (Grenander and Szegö 1984). Note that the condition in (5.15) is stricter than demanding BIBO stability.

Results for the linear ILC algorithm

The results given for the linear iterative system can now be applied to the ILC algorithm in (5.10). First we note that u_∞ is bounded if

$$\rho\left(Q_N(I_N - L_N G_N)\right) < 1,$$

thus, the algorithm is at least ϵ-convergent if this is satisfied. Second we denote the difference $\tilde{u}_k = u_k - u_\infty$ which gives

$$\tilde{u}_{k+1} = Q_N(I_N - L_N G_N)\tilde{u}_k.$$

Hence, $\|\tilde{u}_{k+1}\| < \|\tilde{u}_k\|$ is guaranteed if

$$\bar{\sigma}\left(Q_N(I_N - L_N G_N)\right) < 1.$$

As $N \to \infty$, the result in (5.16) gives the condition

$$\|Q(e^{i\omega})(1 - L(e^{i\omega})G(e^{i\omega}))\|_\infty < 1, \tag{5.17}$$

where $\|\cdot\|_\infty$ is given by

$$\|F(e^{i\omega})\|_\infty = \sup_{\omega\in[0,\pi]} |F(e^{i\omega})|.$$

The result in (5.17) is implied by the stricter condition

$$\|Q(e^{i\omega})\|_\infty \|1 - L(e^{i\omega})G(e^{i\omega})\|_\infty < 1, \tag{5.18}$$

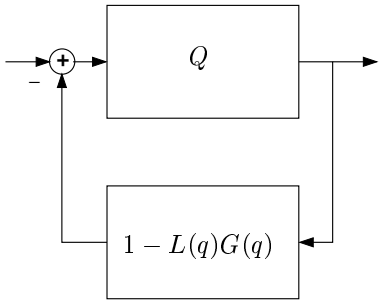

Figure 5.4: The feedback system on which the small gain condition (5.18) can be applied.

which can be interpreted as a small gain condition on the feedback system in Figure 5.4.

With our notation $L = \hat{P}^{-1}$, the convergence criterion in (5.18) can be written

$$\|Q\|_\infty \left\|(1 - \hat{P}^{-1}P)\right\|_\infty = \|Q\|_\infty \left\|\frac{\hat{P} - P}{\hat{P}}\right\|_\infty < 1, \qquad (5.19)$$

where $\frac{\hat{P}-P}{\hat{P}}$ is the relative model error. This reinforces our interpretation of $L = \hat{P}^{-1}$ as the inverse of a model $\hat{P}$ of the system P. Going back to (5.17) we see that the ILC algorithm will converge if and only if the relative model error is sufficiently small compared to Q. In light of Section 5.4 we see that the tracking accuracy will be limited by the relative model uncertainty. If the relative error is larger than one at some frequency, the tracking cannot be perfect at that frequency.

Notice also that if the system has a zero on the unit circle such that $P(e^{i\omega}) = 0$ at the frequency $\omega = \omega_z$, then the stability condition is not satisfied and convergence cannot be achieved unless the desired output is zero at that particular frequency. Consider the linear case where we can study the ILC algorithm in the frequency domain. Thus

$$\begin{aligned} U_{k+1}(\omega_z) &= U_k(\omega_z) + \hat{P}^{-1}(e^{i\omega_z})\left(Y_d(\omega_z) - P(e^{i\omega_z})U_k(\omega_z)\right) \\ &= U_k(\omega_z) + \hat{P}^{-1}(e^{i\omega_z})Y_d(\omega_z) \end{aligned}$$

which will be increasing as $k \to \infty$. This is intuitive since the algorithm tries to compensate for the zero output by increasing the input.

5.6 Convergence results for non-linear systems

The stability and convergence of the ILC method is a central issue and therefore covered in most publications on ILC. Robustness and convergence rates are, e.g., analyzed in (Wang 1998) and (Saab 1999) for nonlinear systems described by

$$\begin{aligned} x_k(t+1) &= f(x_k(t)) + B(x_k(t),t)u_k(t) \\ y_k(t) &= C(t)x_k(t) \end{aligned} \tag{5.20}$$

where $u_k(t)$ and $y_k(t)$ are the input and the output, respectively, $f(\cdot)$ and $B(\cdot)$ are nonlinear functions while the output is a linear function of the states $x_k(t)$. In (Saab 1999) and (Wang 1998) the stability condition is shown to hold under certain conditions. The most limiting condition on the system, however, is that the functions $f(\cdot)$ and $B(\cdot)$ both have to satisfy global Lipschitz conditions. This assumption does, e.g., not hold for certain robotic applications as pointed out in (Saab 1999). It is therefore of interest to derive convergence criteria without the global Lipschitz assumptions.

The contraction mapping approach has previously been used to establish convergence properties for ILC using the specific choices of $Q = 1$ and $L = 1$, (Wang and Horowitz 1985). Below we will first use a feedback interpretation to establish the convergence criterion. This will be followed by a comparison showing that these results can be interpreted as an extension of the results in (Wang and Horowitz 1985). Thus the similarity between the feedback interpretation and the contraction mapping approach will be highlighted (in Section 5.6.2). A motivation for using the feedback approach is that it provides a stepwise derivation of the criterion which gives valuable insight. The approach taken will also provide connections to the results in the linear domain.

Boundedness

Consider first the block diagram of the ILC algorithm (5.6) depicted in Figure 5.5.

To establish a condition for boundedness of the sequence $\{u_k\}_{k=1}^{\infty}$ we first let $\|\cdot\|_2$ denote the two-norm defined by $\|u\|_2 = \sqrt{\sum_{t=0}^{\infty} |u(t)|^2}$. Let us further define the concept of BIBO stability in the ℓ_2 sense (ℓ_2-stable).

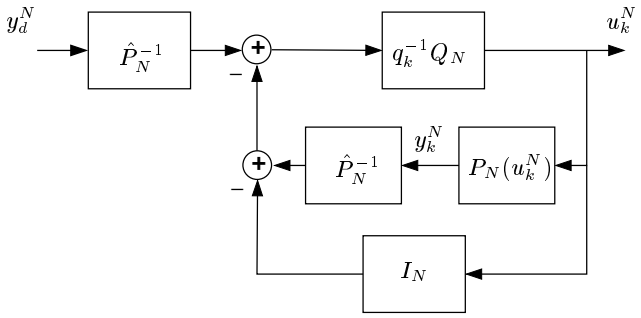

Figure 5.5: Block diagram of the ILC algorithm in the nonlinear case given by (5.6). The system is denoted by P_N transforming the vector u_k^N into y_k^N, the model inverse $\hat{P}_N^{-1}$ acts in similar way. Note that the shift operator q_k acts w.r.t. the iteration index k ($q_k^{-1}u_k(t) = u_{k-1}(t)$).

Definition 5.3. BIBO ℓ_2-stability
A system is BIBO ℓ_2-stable if the output has a finite two-norm provided that the input has a finite two-norm, (Vidyasagar 1993).

Now we can state the following theorem.

Theorem 5.1. *Assume that the system P is BIBO ℓ_2-stable. Then the system in (5.6) and Figure 5.5 is BIBO ℓ_2-stable (in the iteration domain k) if*

$$\alpha\beta < 1,$$

where

$$\alpha = \sup_{u\neq 0} \frac{\|Qu\|_2}{\|u\|_2} = \|Q\|_\infty, \tag{5.21}$$

where Q is a linear mapping, and

$$\beta = \sup_{u\neq 0} \frac{\|u - \hat{P}^{-1}(P(u))\|_2}{\|u\|_2}. \tag{5.22}$$

Proof: Using the small gain theorem for non-linear systems, see (Khalil 1996), the system (5.6) is BIBO stable if

$$\alpha^N\beta^N < 1,$$

where α^N and β^N are the induced norms

$$\alpha^N = \sup_{u^N \neq 0} \frac{\|Q_N u^N\|_2}{\|u^N\|_2}$$
$$\beta^N = \sup_{u^N \neq 0} \frac{\|u^N - \hat{P}_N^{-1}(P_N(u^N))\|_2}{\|u^N\|_2},$$

c.f. Figure 5.5. However, it is trivial that $\alpha^N < \alpha$ and $\beta^N < \beta$ (in fact e.g. $\alpha^N \to \alpha$ as $N \to \infty$) since the allowable inputs corresponding to α^N (β^N) corresponds to a subset of the inputs that define α (β). Hence, BIBO stability for (5.6) follows. □

Existence

We next ask the question when $u_\infty(t)$ and the corresponding output $y_\infty(t) = P(u_\infty(t))$ defined by (5.7), c.f. Figure 5.2, are well-defined in the case $Q \neq 1$. The following theorem applies in this case.

Theorem 5.2. *Assume that the conditions of Theorem 5.1 hold, that $Q \neq 1$ and that $\hat{P}^{-1}$ is BIBO stable. Then the system (5.7) (c.f. Figure 5.2) is BIBO ℓ_2-stable and the corresponding signals u_∞ and y_∞ are well defined.*

Proof: The system in Figure 5.2 satisfies

$$\begin{aligned} u_\infty(t) &= \frac{Q(q)}{1-Q(q)}(\hat{P}^{-1}(y_d(t)) - \hat{P}^{-1}(P(u_\infty(t))) \\ &= Q(q)\left(u_\infty(t) - \hat{P}^{-1}(P(u_\infty(t))) + \hat{P}^{-1}(y_d(t))\right). \end{aligned}$$

Now, this system is also BIBO stable if $\alpha\beta < 1$ which proves that the signals u_∞ and y_∞ in Figure 5.2 are well defined. □

The case when $Q = 1$ will also be covered below.

5.6.1 Convergence

In this section we present a convergence result very similar to (5.19) in the linear case. Suppose that y_d is bounded, that the conditions of Theorem 5.1 are satisfied such that the system (5.6) is BIBO stable and suppose also that u_∞ is well defined, meaning that the conditions for existence are fulfilled as given above.

Under these assumptions it is possible to define

$$\Delta_k(t) \triangleq u_k(t) - u_\infty(t)$$

and

$$\Phi_N(u_\infty^N, \Delta_k^N) \triangleq \hat{P}^{-1}\left(P_N(\Delta_k^N + u_\infty^N)\right) - \hat{P}^{-1}\left(P_N(u_\infty^N)\right). \tag{5.23}$$

Now, combining (5.5) and (5.23), gives

$$\begin{aligned}\Delta_{k+1}^N &= u_{k+1}^N - u_\infty^N \\ &= Q_N\Delta_k^N - Q_N\hat{P}^{-1}\left(P_N(u_k^N)\right) - \hat{P}^{-1}\left(P_N(u_\infty^N)\right) \\ &= Q_N\Delta_k^N - Q_N\Phi_N(u_\infty^N, \Delta_k^N).\end{aligned} \tag{5.24}$$

The system in (5.24) is an unforced system, initialized with a nonzero initial condition ($\Delta_0^N \neq 0$). Convergence of the ILC algorithm in the nonlinear case will be achieved if the origin is a globally asymptotically stable equilibrium of the system in (5.24).

Theorem 5.3. *Assume that the conditions in Theorem 5.1 are satisfied such that (5.5) is BIBO stable and u_∞ is well-defined for $Q \neq 1$. For $Q = 1$ assume that the system is invertible, for the desired output y_d, such that $u_\infty = u_d$ exists.*

Assume that

$$\alpha\gamma < 1 \tag{5.25}$$

where α is the induced norm of Q (5.21) and γ is the induced norm of $1 - \Phi(\cdot)$ given by

$$\gamma = \sup_{\Delta \neq 0} \frac{\|\Delta - \Phi(u_\infty, \Delta)\|_2}{\|\Delta\|_2}. \tag{5.26}$$

The input error $u_\infty^N - u_{k+1}^N$ in the ILC algorithm in (5.6) fulfills

$$\|u_\infty^N - u_{k+1}^N\| < \alpha\gamma\|u_\infty^N - u_k^N\|$$

i.e., it is a monotonically decreasing difference with

$$\lim_{k\to\infty} \sup \|u_\infty^N - u_k^N\| = 0. \tag{5.27}$$

Proof: Clearly $\Delta_k(t)$ is well-defined and bounded. From (5.24),

$$\begin{aligned}\|\Delta_{k+1}^N\|_2 &< \|Q_N\|_2 \sup_{\Delta^N \neq 0} \frac{\|\Delta^N - \Phi_N(u_\infty^N, \Delta^N)\|_2}{\|\Delta^N\|_2} \|\Delta_k^N\|_2 \\ &\leq \alpha\gamma \|\Delta_k^N\|_2,\end{aligned}$$

where the last inequality follows in the same way as in the proof of Theorem 5.1. Since $\alpha\gamma < 1$, the result in (5.27) follows. □

A couple of remarks are worth pointing out next.

Remarks:

- When $\hat{P}^{-1}$ and P are linear, the norms (5.22) and (5.26) are identical and the boundedness, existence and convergence conditions all become

  $$\|Q\|_\infty \|1 - \hat{P}^{-1}P\|_\infty < 1.$$

  Thus the sufficient condition here is very close in spirit to the necessary and sufficient condition (5.19).

- Notice the similarity between (5.26) and the relative model error

  $$\|1 - \hat{P}^{-1}P\|_\infty,$$

  in the linear case. Hence, also in the nonlinear case $\hat{P}$ should approximate the system dynamics as well as possible in a relative sense. Notice, however that in the perfect tracking case ($Q = 1$) a relative model error of up to 100% can be tolerated. This is, probably, one of the main reasons for the success of ILC. An accurate model is not required!

- The guaranteed convergence rate is geometric with rate $\alpha\gamma$. Hence, for a given modeling accuracy γ, the convergence rate can be increased by reducing α, i.e. by increasing the tracking error.

5.6.2 The contraction mapping approach

There is a clear relationship between the results above and the contraction mapping theorem (Vidyasagar 1993). Recall the ILC algorithm rep-

resented as

$$u_{k+1}^N = Q_N \left(u_k^N - \hat{P}_N^{-1}(P_N(u_k^N)) \right) + Q_N \hat{P}_N^{-1}(y_d^N),$$

which is rewritten as

$$\begin{aligned} u_{k+1}^N &= Q_N \left(u_k^N - \hat{P}_N^{-1}(P_N(u_k^N)) \right) + Q_N \hat{P}_N^{-1}(y_d^N) \\ &\triangleq \tilde{T}(u_k^N) + Q_N \hat{P}_N^{-1}(y_d^N) \\ &\triangleq T(u_k^N). \end{aligned} \tag{5.28}$$

At convergence, (5.28) satisfies

$$u_\infty^N = T(u_\infty^N),$$

hence, u_∞^N is a fixed point to the mapping T. The question is now under what conditions this is true and under what conditions the fixed point can be reached using the iterations

$$u_{k+1}^N = T(u_k^N).$$

The contraction mapping theorem (Vidyasagar 1993) states that assuming that there exists a fixed positive constant $\rho < 1$ such that

$$\|T(x) - T(y)\| \leq \rho \|x - y\|, \quad \forall x, y \in S, \tag{5.29}$$

where S denotes the set such that $x, T(x) \in S$. Under these conditions there exists only one fixed point x^*, satisfying $x^* = T(x^*)$, and this fixed point will be reached at convergence by

$$x_{k+1} = T(x_k).$$

A strength of the contraction mapping approach is that it implicitly gives conditions for both existence and convergence.

To compare the criterion for convergence derived by the feedback approach we first consider the criterion for a bounded solution. In Theorem 5.1 it was stated that the mapping

$$u_{k+1}^N = Q_N \left(u_k^N - \hat{P}^{-1}(P(u_k^N)) \right) + Q_N \hat{P}^{-1}(y_d^N)$$

is bounded if $\alpha\beta < 1$, where α is defined in (5.21) and β in (5.22). This is similar to the condition

$$\|\tilde{T}(u_k^N)\| \leq \eta \|u_k^N\|, \quad 0 < \eta < 1,$$

which is a relaxation of (5.29) with T as in (5.28), $x = u_k^N$ and with $y = 0$. In this case

$$\|u_{k+1}^N\| \leq \eta \|u_k^N\| + \|Q_N \hat{P}_N^{-1}(y_d^N)\|,$$

assuming that $\|Q_N \hat{P}_N^{-1}(y_d^N)\| < \infty$.

The criterion for existence of a fixed point in the case $Q \neq 1$ is stated in Theorem 5.2 but there does not seem to be any specific relation to the contraction mapping approach in this case.

Assuming that a fixed point u_∞^N exists, the condition of the contraction mapping approach can be relaxed to

$$\|T(u_k^N) - T(u_\infty^N)\| \leq \eta \|u_k^N - u_\infty^N\|, \;\; 0 < \eta < 1,$$

which is similar to the criterion in Theorem 5.3.

By strengthening the condition in Theorem 5.3 to (5.29), i.e.,

$$\begin{aligned} &\left\| Q_N \left((u_k^N - z_k^N) - \left(\hat{P}_N^{-1}(P_N(u_k^N)) - \hat{P}_N^{-1}(P_N(z_k^N)) \right) \right) \right\| \\ &\leq \eta \|u_k^N - z_k^N\|, \;\; 0 < \eta < 1, \end{aligned} \tag{5.30}$$

for any inputs u_k^N and z_k^N, the assumption that $u_\infty^N = u_d^N$ exists when $Q = 1$ can be dispensed with. The existence of the inverse then follows from the contraction mapping theorem, i.e. (5.30) implies existence of the inverse.

It can further be pointed out that if

$$\sup_x \left\| \frac{dT(x)}{dx} \right\| \leq \alpha < 1,$$

on a convex set S then T is a contraction mapping, which follows from the mean value theorem (Luenberger 1969). With T as in (5.28), we have

$$\frac{dT}{du^N} = \frac{d\tilde{T}}{du^N} = Q_N \left(I_N - \frac{d}{du^N} \hat{P}_N^{-1}(P_N(u^N)) \right).$$

Now define the sequence

$$\delta(t) = u(t) - \hat{P}^{-1}(P(u(t))),$$

then

$$\frac{d\delta^N}{du^N} = I_N - \frac{d}{du^N} \hat{P}_N^{-1}(P_N(u^N)).$$

Since

$$\left\| \frac{d\delta^N}{du^N} \right\| \leq \lim_{N\to\infty} \left\| \frac{d\delta^N}{du^N} \right\|,$$

we now have the following result.

Corollary 5.1. *Assume that $\hat{P}^{-1}$ and P are two times continuously differentiable. Define*

$$\bar{\gamma} = \lim_{N\to\infty} \sup_{u^N} \left\| \frac{d\delta^N}{du^N} \right\|$$

and let α be the induced norm of Q (5.21). Then the conclusions of Theorem 5.3 hold if

$$\alpha\bar{\gamma} < 1.$$

Proof. Follows from the discussion preceding the corollary. □

It can further be noted that the condition in Theorem 5.3 and Corollary 5.1 is a generalization of a condition in (Wang and Horowitz 1985). There ILC algorithm

$$u_{k+1}(t) = u_k(t) + y_d(t) - y_k(t), \tag{5.31}$$

is analyzed, hence, $Q = L = 1$. Convergence of (5.31) is guaranteed if

$$\sup_{u^N} \left\| I_N - \frac{dP_N(u^N)}{du^N} \right\| < 1, \tag{5.32}$$

for all inputs $u \in S$ where S is a convex subset of $C[1, N]$. Here, $C[1, N]$ denotes a normed linear space consisting of continuous functions on the interval $[1, N]$.

5.7 Non-causal ILC

In (5.2) the inverse of the model is used to iteratively find the inverse of the system. If the model is non-minimum phase the inverse will be unstable if causal filtering is used. However, by using non-causal filtering (exploring the batch nature of ILC) the inverse will be stable. This is one *very* interesting and useful feature of ILC.

Inversion of linear systems

Let us start by recalling the inversion of linear systems as described in Section 2.1.2. Consider a bounded signal $u(t)$ with z-transform $U(z)$ filtered through a stable, *albeit not necessarily minimum-phase*, linear system $G(z)$ and denote the resulting output $y(t)$ with transform $Y(z)$. Then, $Y(z) = G(z)U(z)$ in the region of convergence which under the given assumptions is a disc which includes the unit disc so that $y(t)$ is bounded. Consequently it holds that $U(z) = G(z)^{-1}\ Y(z)$. Since both u and y are bounded, G^{-1} is here a stable operator, i.e. its region of convergence includes the unit disc. Hence, when $G(z)$ has zeros outside the unit circle, $G^{-1}(z)$ must be interpreted as a *stable* but *non-causal* operator and to recover u from y non-causal filtering has to be performed. This is done as follows:

Factorize $G(z)$ as

$$G(z) = G_+(z)G_-(z)$$

where $G_+(z)$ includes the minimum phase zeros and $G_-(z)$ includes the non-minimum phase zeros. In this case the stable inverse of $G_+(z)$ will be causal while the stable inverse of $G_-(z)$ is anti-causal and u is recovered by first filtering y through the stable causal filter $G_+^{-1}(z)$

$$w(t) = G_+^{-1}(q)\ y(t)$$

and then anti-causal filtering of this result. The latter can be performed by filtering the reversed sequence $\bar{w}(t) = w(N-t)$ (N is the total number of data) through the stable causal filter $\bar{u}(t) = G_-^{-1}(q^{-1})\bar{w}(t)$ and then reversing the result, i.e. $u(t) = \bar{u}(N-t)$, see Chapter 2 for more details.

Nonlinear systems

Applying the inverse of nonlinear models to (5.5) can be complicated, especially when the model is non-minimum phase. There is, e.g., no obvious way to separate a nonlinear non-minimum phase system into a stable causal and a stable anti-causal subsystem. However, recall the result above stating that perfect tracking can be obtained even if the relative model error is 100 %. Based on this we suggest that a linear approximation of the system (or model) is used for the inversion in (5.5). The usage of a linear approximation of a nonlinear system will be further motivated in Section 5.8.

Hence, in case of a nonlinear non-minimum phase system it is the linearized model which is inverted, by the method described above, and applied to the ILC algorithm in (5.5). It can be noted that in this case (5.2) is equal to (5.5) since the operator L is linear.

Related work

The conventional ILC method, based on direct inversion of the model and causal filtering, becomes unstable in the case of non-minimum phase models. Even though the signals are bounded due to a finite time-horizon they are not practical to implement. This has led to erroneous conclusions in e.g., (Owens and Munde 2000) where it is claimed that the success of ILC depends on minimum-phase properties of the system. However, some ideas to improve performance in the cases of direct inversion are published. In, e.g., (Ghosh and Paden 1999*b*) a method based on the pseudo-inverse of the plant is discussed, (Amann and Owens 1994) uses an quadratic criterion optimization based ILC, and in (Roh *et al.* 1996) a best approximation of a stable inverse system is found by applying H_∞ optimization. The tracking results in these publications are however degraded as stated in (Choi and Jeong 2001).

In (Sogo *et al.* 2000), an ILC method for nonlinear non-minimum phase systems is presented based on optimization. The optimization is solved using an adjoint system which is time-reversed, hence, stable in the case of maximum phase systems (see Section 2.2). The idea of using time-reversed filtering for maximum phase systems is also explored in (Choi and Jeong 2001).

The idea of using a linear model which is split into a causal and an anti-causal part is also suggested in (Ghosh and Paden 1999*a*) for continuous time systems. In (Jeong and Choi 2001) a similar matrix based method is presented. However, the matrix based filtering method introduces limitations for systems with pairs of zeros that are reflected in the unit circle, one inside and the other outside the unit circle.

5.8 Models suited for ILC

We have seen that $L = \hat{P}^{-1}$ plays a crucial role in the properties of ILC. This quantity can be interpreted as a model of the system which, both from a stability and convergence rate perspective, should be chosen *as close as possible to the inverse of the true system.* In the previous section it was suggested that a linear model can be used in the case of a nonlinear

non-minimum phase system. In this section we will further provide ideas for how to apply and in some cases also obtain a model.

The level of a priori knowledge of a model might range from almost no information at all up to a model nearly describing the system completely. For example, the knowledge might span from a linear model only valid for a restricted set of input data, to a nonlinear model being valid for almost all types of inputs. Recall the result of Theorem 5.3 and Corollary 5.1 where it is shown how model accuracy can be traded against tracking performance.

For a nonlinear system we suggest that the following classification of the model to be used for the ILC implementation.

1 A nonlinear model is available which is suitable for inversion, e.g., not non-minimum phase.

2 A linear model is available either from

   a . linearization of a nonlinear model, or

   b . previous identification

3 A model is not available prior to applying the ILC algorithm.

These items will be further explained below where it is assumed that the factor Q is chosen such that convergence is maintained.

1. Using a nonlinear model

First of all, if a nonlinear model is available and its inverse suitable for implementation, that inverse should be used. Recall that a nonlinear inverse should be applied to the ILC algorithm in (5.5).

2. Using a linear time invariant model

As we have seen in Section 5.7, linear time invariant models, even non-minimum phase ones, are easily inverted. However, if a nonlinear model is non-minimum phase, it may be difficult to compute a stable inverse. In the latter case a linear model can be used to represent the nonlinear system. One option is to use a linearization of the nonlinear model at the origin. This linearization can be used if the difference $\|e_k^N\| = \|y_d^N - y_k^N\|$ is small. Here, the notion small implies that the higher order terms of a series expansion of $P^{-1}(e_k(t))$ are negligible. If this is not fulfilled, due

to unfortunate initialization of the ILC algorithm or depending on the accuracy of the model, other ways of choosing the linear model can be used.

Note that using a linear time-invariant model to represent a nonlinear system makes the linear model depend on the characteristics of the input-output data. If the characteristics are changed the linear model may no longer be valid. This motivates the idea of some sort of adaptive choice of the linear models. An idea could be to use a first approximation suited for large error signals but as the error decreases a linearized model at the origin can be used. Let us exemplify this idea for Wiener and Hammerstein systems.

Example 5.1. Wiener and Hammerstein systems

Here we will study the choice of $\hat{P}$ in the case of Wiener or Hammerstein systems. A Wiener system is described by a linear dynamic system followed by a static nonlinearity. A Hammerstein system consists of the same components but here the static nonlinearity is followed by a dynamic linear system, consider Figure 5.6.

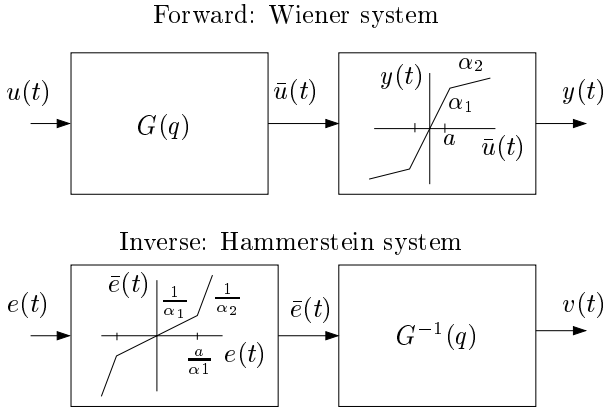

Figure 5.6: Example of a Wiener system (top) and its inverse which is an Hammerstein system (bottom).

It can be observed that if the system is described by a Wiener system then the inverse will be described by a Hammerstein system with separate inversion of the nonlinearity and the linear system. The opposite holds for the inversion of a Hammerstein system. We consider the case when

the system describe a one-to-one relationship between the input and the output, and thus is invertible.

As an example we consider the case when P is a Wiener system such that the inverse is given by the Hammerstein system in Figure 5.6. The gain α of the static nonlinearity is amplitude dependent $\alpha = \alpha(u)$ and by studying the signal examples in Figure 5.7 it is clear that a suitable approximation of the Hammerstein system will depend on the applied input signal. If the input is a square wave as in Figure 5.7, then it is clear that if $a > 1$ then the nonlinearity should be represented by the gain $\alpha = \alpha_1$ and if $a < 1$ then $\alpha = \alpha_1 a + (1 - a)\alpha_2$. On the other hand, the distribution of the mixed sinusoidal signal in Figure 5.7 is more spread out and it is less obvious to choose the correct gain.

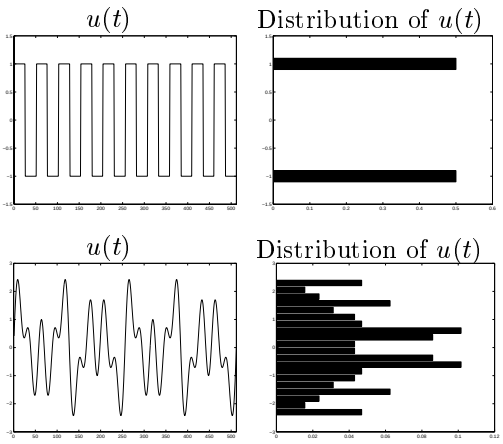

Figure 5.7: Example of different input signals and their normalized distribution.

We here suggest a heuristic way to choose the gain according to the distribution of the input. First denote the normalized distribution *of the input $e(t)$ by $q(x)$ such that*

$$q(x) = \frac{p_x}{N},$$

where x is the amplitude, p_x is the number of samples within the bin $x \pm \delta x$ and N denotes the total number of samples. The suggested gain

β is then chosen as a weighted gain according to

$$\beta = \sum_{l=1}^{m} q(x_l)\alpha(x_l), \tag{5.33}$$

where m denotes the number of bins. Hence, the choice of the approximate gain will depend on the input signal and because of that it can be adjusted for each iteration. A similar approach can be used if the inverse model is described by a Wiener system.
Remark: *If the input to the inverse system $e(t)$ is zero then the gain is chosen to be zero which seems to be a problem. On the other hand, this case corresponds to zero error which is the desired final result.*

A numerical example using the suggested idea in this section is presented in Section 5.9.3.

3. When a model is not initially available

If, initially, a model is unknown, it is natural to use the data from the ILC-iterations to identify a model. For a linear system and a flexible enough model structure, all data collected up to the current iteration can be used to identify a new model to be used in the next iteration. However, this case is of less interest since then little can be gained by ILC compared to taking $u = \hat{P}^{-1}y_d$.

For a nonlinear system the identified linear model will depend on the specific set of input-output data. If the initialization is made such that the error is small, then it is likely that the identification of a single time-invariant model is sufficient. If, on the other hand, the input at initialization u_0 differs considerably from the input at convergence u_∞ it may be beneficial to estimate new linear models as the iterations are continued. This approach is further described by an example below.

Related work is found in, e.g., (Nijsse *et al.* 2001) where a subspace method is presented for the identification at successive iterations. The method is used for applying ILC on linear systems. The approach is based on optimization and the method treats the input update between iterations as a random walk.

5.9 Numerical examples

In this section, some numerical examples will be presented. First a linear non-minimum phase system will be studied where stable inversion

of non-minimum phase systems is illustrated. The second example is on a nonlinear non-minimum phase system where it is shown that a linear non-minimum phase model is useful for inversion.

The adaptive choice of a linear model for Wiener and Hammerstein systems is exemplified in the third example. In the fourth example, the control of an inverted pendulum, which is a "real world" non-minimum phase system, is studied via simulation.

The trade-off between the relative error and the choice of the Q filter to obtain convergence is highlighted in the final example which considers a resonant flexible structure. The numerical simulations are computed with Matlab 5.3 and Simulink 3.0.

5.9.1 Linear non-minimum phase

As a first numerical example we will study a low-order linear system which is known almost correctly. The main objective with this example is to show non-causal inversion but also to show how the relative model error is connected to the convergence.

The system is given by

$$P(z) = \frac{(z+0.5)(z-1.2)}{z^2 - 1.6z + 0.8},$$

with one zero inside the unit circle ($z = -0.5$), one zero outside the unit circle ($z = 1.2$) and both poles inside the unit circle ($z = 0.8 \pm i0.4$).

Two different models are tested with the ILC algorithm. Model A is given by

$$\hat{P}_A(z) = \frac{(z+0.3)(z-1.3)}{z^2 - 1.55z + 0.8},$$

with zeros $z = -0.3$, $z = 1.3$ and poles $z = 0.775 \pm i0.4465i$. Model B is given by

$$\hat{P}_B(z) = \frac{(z+0.3)(z-1.3)}{z^2 - 1.5z + 0.8},$$

with poles $z = 0.75 \pm i0.4873$ and the same zeros as $\hat{P}_A(z)$.

In Figure 5.8 the Bode diagrams for the system and both models are shown. In addition, the relative model error is plotted in Figure 5.9 and it is clear that the infinity norm of the relative error for $\hat{P}_B(z)$ is larger than one.

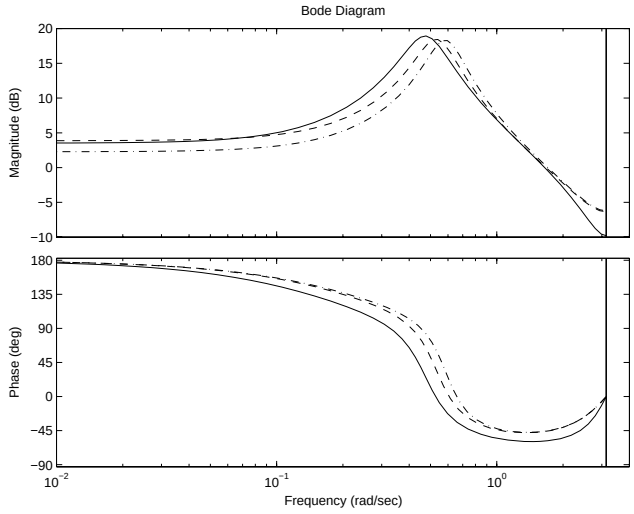

Figure 5.8: Bode diagrams for $P(z)$ (solid line), $\hat{P}_A(z)$ (dashed line) and $\hat{P}_B(z)$ dash-dotted line.

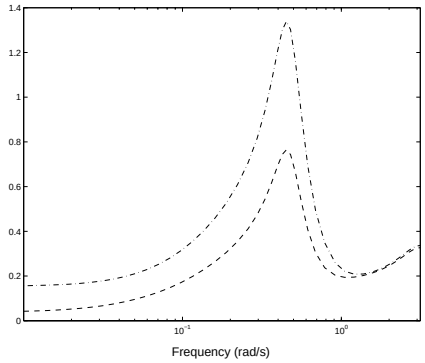

Figure 5.9: The relative error $\left|\frac{\hat{P}_k(e^{i\omega})-P(e^{i\omega})}{\hat{P}_k(e^{i\omega})}\right|$ where the relative error for $\hat{P}_A(z)$ is represented by a dashed line and for $\hat{P}_B(z)$ by a dash-dotted line.

In the ILC algorithm, we use $Q = 1$ so that

$$u_{k+1}(t) = u_k(t) + \hat{P}_k^{-1}(q)\left(y_d(t) - y_k(t)\right), \tag{5.34}$$

where $k = A, B$. Since $\hat{P}$ is non-minimum phase, direct causal inversion will be unstable. Therefore, the models are factorized as $\hat{P}_k = \hat{P}_+(z)\hat{P}_-(z)$, where $\hat{P}_+(z)$ contains minimum phase characteristics and $\hat{P}_-(z)$ contains the non-minimum phase characteristics. Here, we factorized the models with

$$\hat{P}_{-,k}(z) = z - 1.3,$$

$$\hat{P}_{+,A}(z) = \frac{z + 0.5}{z^2 - 1.55z + 0.8}$$

and

$$\hat{P}_{+,B}(z) = \frac{z + 0.5}{z^2 - 1.5z + 0.8}.$$

The filtering in (5.34) is done in forward direction with $\hat{P}_+(z)$ such that first

$$v(t) = \hat{P}_{+,k}^{-1}(q)\,(y_d(t) - y_k(t))$$

then the order of $v(t)$ is reversed $\bar{v}(t) = v(N - t)$ and filtered through

$$\hat{P}_{-,k}^{-1}(q^{-1}) = \frac{1}{(q^{-1} - 1.3)}.$$

Hence, $\bar{x}(t) = \hat{P}_{-,k}^{-1}(q^{-1})\bar{v}(t)$ and the result is thereafter reversed as $x(t) = \bar{x}(N - t)$. Finally, the control signal is updated as

$$u_{k+1}(t) = u_k(t) + x(t).$$

The reference trajectory is given by a square wave type signal with "randomly" chosen amplitude which is low pass filtered through the filter $H(q) = \frac{0.5}{1-0.5q^{-1}}$. The reference signal is kept zero in the beginning and in the end to allow for non-causal control action.

In Figure 5.10 the sum of squared tracking errors are shown for both $P_A(z)$ and $P_B(z)$. It is clear that with a relative error larger than one, the convergence cannot be guaranteed. In Figure 5.11 the tracking results using $P_A(z)$ are shown.

In this example we have showed how non-causal filtering can be used to implement a stable inverse of a non-minimum phase system. The issue of convergence was also highlighted and it was shown that with the infinity norm of the relative error larger than one convergence cannot be guaranteed with $Q = 1$.

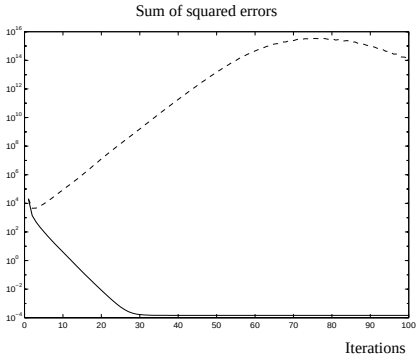

Figure 5.10: The sum of squared errors for the first 100 iterations. For $P_A(z)$ (solid line) the algorithm converges monotonically. For $P_B(z)$ (dashed line) the error increases considerably before it starts to decrease. Recall that the infinite norm of the relative model error for $P_B(z)$ is larger than one.

5.9.2 Nonlinear non-minimum phase system

Let us now study a nonlinear non-minimum phase system and exemplify how a linear non-minimum phase model can be used to in the ILC algorithm. Consider the nonlinear system $P(u)$ described by

$$\begin{aligned} x_1(t+1) =& 1.05x_1(t) + 1.085\eta_1(t) + 1.1450\eta_2(t) \\ & - \frac{x_1^3(t)}{(1+\eta_1^2(t))} + u(t) \\ \eta_1(t+1) =& \eta_2(t) - 0.05\eta_1(t)sin(x_1(t)) \\ \eta_2(t+1) =& x_1(t) + 0.6\eta_1(t) + 0.7\eta_2(t) \\ y(t) =& x_1(t), \end{aligned} \tag{5.35}$$

which is a third order nonlinear system given in normal form, with a relative degree equal to one (Califano *et al.* 1998). Linearization of (5.35), at the origin, gives the linear model

$$\hat{P}(z) = \frac{(z+0.5)(z-1.2)}{z^3 - 1.75z^2 + 1.28z - 0.455}, \tag{5.36}$$

which has poles inside the unit circle and, one zero outside the unit circle while the other zero is inside. Inversion of the model was done according

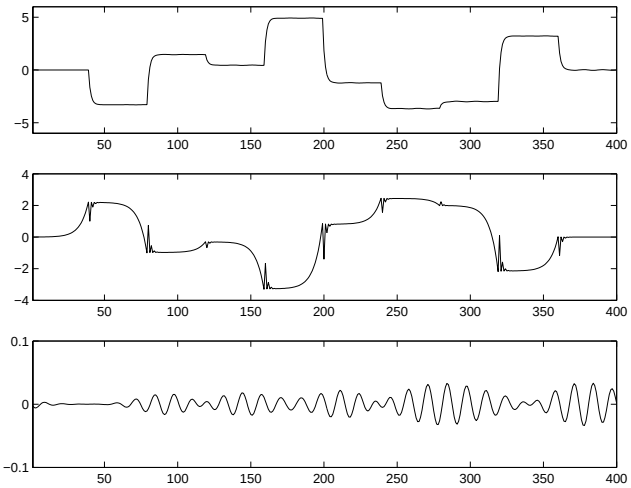

Figure 5.11: Tracking results for the linear non-minimum phase system after 10 iterations using $P_A(z)$. Top: the reference $y_d(t)$ and the output $y_{10}(t)$ (almost on top). Middle: the control signal $u_{10}(t)$. Bottom: Tracking error $e_{10}(t)$.

to Section 5.7 and the control sequences are computed as in (5.2) with $Q = 1$ and $L(z) = 0.5\hat{P}^{-1}(z)$. The reference signal $y_d(t)$ is given by

$$y_d(t) = \sin\left(5\frac{2\pi t}{N_s}\right) + \sin\left(3\frac{2\pi t}{N_s}\right) + \sin\left(6\frac{2\pi t}{N_s}\right) \tag{5.37}$$

where N_s denotes the length of the sinusoidal sequence ($N_s = 510$). Since the system is non-minimum phase the desired output has to be zero in the beginning of the reference sequence in order to allow for non-causal control action. Here the total length of the sequence is $N = 540$ samples and the reference is zero for the first 20 and the last 10 samples. The control signal was initiated as $u_0(t) = 0\ \forall t$. The ILC algorithm (5.2) was updated 20 times and the result is shown in Figure 5.12. In Figure 5.13 a simulation of the system output $y_k(t)$ is shown along with the model output using the same input $u_k(t)$ for $k = 40$. As shown in the figure, the model differs considerably from the system although it is suitable for the inversion purpose.

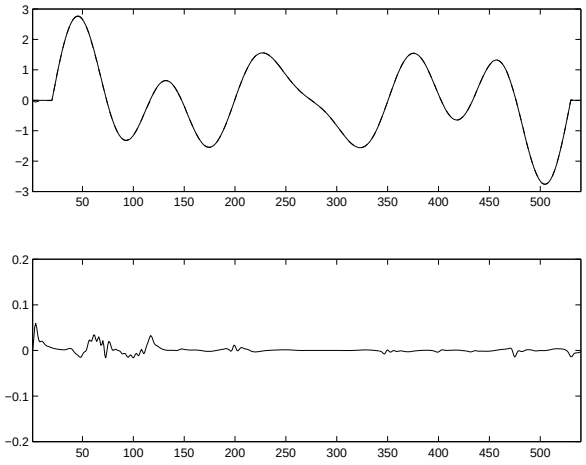

Figure 5.12: Top: Desired output (solid line) and the system output (dashed line, almost on top of the solid line). Bottom: Difference between the desired and the actual output ($e_{20}(t)$), thus the result after 20 iterations of (5.2).

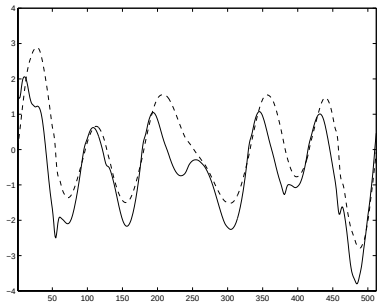

Figure 5.13: Output of the system (5.35) (dashed line) and the model (5.36) (solid line) using the input $u_k(t)$ with $k = 40$.

5.9.3 Linear representation of a Hammerstein system

In this example we will consider the Wiener system in Figure 5.6. The objective is to show that an adaptively chosen gain, based on the distribution of the input, will influence the convergence rate.

Three different models will be used for the inversion. First only the linear part $G(q)$ will be used, thus

$$\hat{P}_1(q) = G(q).$$

Second, the linear part in combination with the gain α_1 is used

$$\hat{P}_2(q) = \alpha_1 G(q).$$

which corresponds to the linearization at the origin. The third inverse will be based on the the linear model in combination with an adaptively chosen gain according to the suggested principle in Example 5.1. Hence,

$$\hat{P}_3(q) = \beta G(q),$$

where β is given by (5.33). In all three cases the used ILC algorithm is given by

$$u_{k+1}(t) = u_k(t) + \hat{P}_k^{-1}(q)\left(y_d(t) - y_k(t)\right),$$

where $k = 1, 2, 3$.

The reference signal is the mixed sinusoidal given in (5.37). The initial control signal is set to be the reference signal which gave a distribution of the error signal in the first iteration similar to the example shown at the bottom of Figure 5.7.

Important to note is that all approaches converge. The rates of convergence, however, are different. In Figure 5.14 the logarithm of the sums of the squared errors are shown as functions of the ILC iterations. The adaptive gain ($\hat{P}_3$) is faster for the first iterations although the rate of convergence is the same for $\hat{P}_3$ and $\hat{P}_2$ for iterations $k > 3$. This depends on the fact that as the error decreases the linearization at the origin becomes better. In other words, this example shows that the best choice of model approximation, in terms of the convergence rate, depends on the initialization.

5.9.4 Inverted pendulum

In this example we will study a "real world" non-minimum phase system which is the cart and the inverted pendulum depicted in Figure 5.15. We will study a simulated system and one of the objectives is to show that the tradeoff between the relative model error and Q can be utilized to obtain convergence.

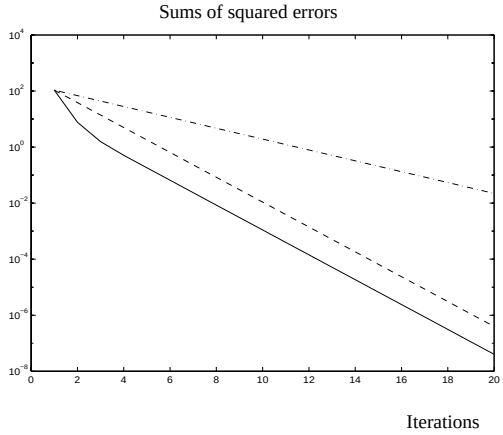

Figure 5.14: Sums of the squared errors as functions of the iterations for the Wiener system in Section 5.9.3. $\hat{P}_1(q)$ is represented by the dash dotted line, $\hat{P}_2(q)$ is represented by the dashed line, and $\hat{P}_3(q)$ is represented by the solid line.

The inverted pendulum is described by the continuous time system

$$\begin{aligned}
\dot{x}_1 &= x_2 \\
\dot{x}_2 &= \frac{-mg\sin x_3\cos x_3 + mlx_4^2\sin x_3 + f_\varphi m x_4\cos x_3 + F}{M + (1-\cos^2 x_3)m} \\
\dot{x}_3 &= x_4 \\
\dot{x}_4 &= \frac{(M+m)(g\sin x_3 - f_\varphi x_4) - (lmx_4^2\sin x_3 + F)\cos x_3}{l(M + (1-cos^2 x_3)m)}
\end{aligned} \tag{5.38}$$

where the states are chosen such that $x_1 = y$, $x_2 = \dot{y}$, $x_3 = \varphi$ and $x_4 = \dot{\varphi}$. The position of the cart is denoted by y and the angle of the pendulum is denoted by φ and the control signal is the applied force, denoted by F. The coefficients are described in Table 5.1 where also their numerical values are given.

For the numerical calculations the initial conditions were given by $x(0) = [0\ 0\ 0\ 0]^T$ and to stabilize the pendulum the system is under the state feedback control

$$F(t) = -L_f x(t),$$

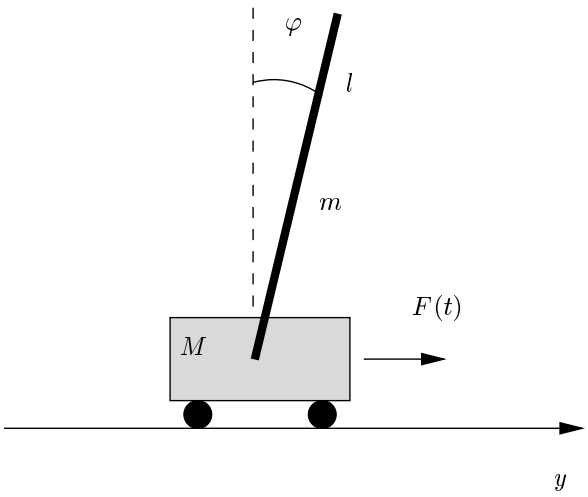

Figure 5.15: Inverted pendulum on a cart where reference tracking of the cart position is obtained by ILC.

where

$$L_f = [-2 \; -2 \; -60 \; -4].$$

Hence, the input force is given by

$$F(t) = -2x_1(t) - 2x_2(t) - 60x_3(t) - 4x_4(t) + u_k(t).$$

We have here considered the use of a discrete time ILC where the system in (5.38) is sampled with $T_s = 0.01$. The position y of the cart is further

M	2.4	mass of the cart
m	0.23	mass of the pendulum
l	0.36	length of the pendulum
f_φ	0.1	friction coefficient
g	9.81	gravitational acceleration

Table 5.1: *Parameter values for the pendulum in (5.38) depicted in Figure 5.15*

on considered as the output of the system and the reference trajectory is accordingly the desired position of the cart.

The idea is here to apply the ILC algorithm

$$u_{k+1}(t) = Q(q)\left(u_k(t) + \hat{P}^{-1}(q)(y_d(t) - y_k(t))\right). \tag{5.39}$$

However, no model is considered to be known prior to applying the first ILC iteration. A linear model was therefore identified using data from the first ILC iterations. A fourth order model was estimated as

$$\hat{P}(z) = \frac{10^{-5}(-0.038z^2 + 0.977z - 0.99)}{z^4 - 3.88z^3 + 5.65z^2 - 3.66z + 0.89},$$

and applied to the ILC algorithm.

From the first numerical experiments it followed that convergence could not be obtained with $Q = 1$. It was then assumed that the model is not so good for high frequencies and by letting Q be a low-pass filter convergence could be obtained. Numerical experiments gave that the low pass filter $Q(q) = \tilde{Q}(q)\tilde{Q}(q^{-1})$ with

$$\tilde{Q}(q) = \frac{q^2}{q^2 - 1.8q + 0.81},$$

resulted in acceptable convergence. The filter $Q(q)$ was implemented using the matlab function `filtfilt` with $\tilde{Q}(q)$.

The tracking results are shown in Figure 5.16. We conclude from the good tracking properties that a linear model, identified at the first iteration, is well suited to obtain a satisfying result. By letting $Q(z)$ be a low pass filter, model errors at higher frequencies were neglected.

5.9.5 One-link flexible arm

In this example we study the control of the one-link flexible arm depicted in Figure 5.17. The flexible arm is used in both (Doh *et al.* 1999) and (Nijsse *et al.* 2001) and the purpose of the control is to position the tip of the arm by applying a torque on the hub. One reason for studying this example is that the previously proposed methods appear less straight forward than the methods suggested here. It should however be pointed out that we have here not considered the effect of measurement noise which is studied in (Nijsse *et al.* 2001). The transfer function from the

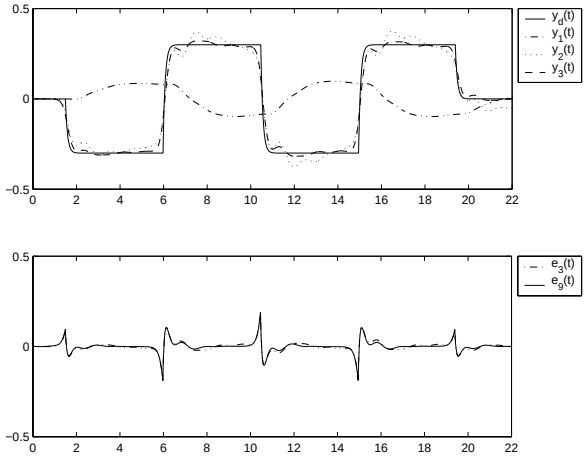

Figure 5.16: Result for the position tracking of the inverted pendulum. Top: The desired output and the actual outputs at different iterations. Bottom: Tracking errors.

torque T to the position of the tip Y_{tip} is

$$\frac{Y_{tip}(s)}{T(s)} = \sum_{i=0}^{\infty} \frac{\alpha_i}{(s+p_i)(s+q_i)}, \tag{5.40}$$

where the parameters of the first four modes used here are given in Table 5.2. The flexible arm is assumed to be under closed loop control with the controller

$$C(s) = \frac{0.1s + 0.02}{s + 0.5}.$$

mode i	p_i	q_i	α_i
0	0	0.2	2.545454
1	0.17 + i11.179	0.17 - i11.179	-7.452000
2	0.40 + i21.600	0.40 - i21.600	6.136364
3	0.70 + i48.060	0.70 - i48.060	-3.437500

Table 5.2: *Parameters for the flexible arm in (5.40)*

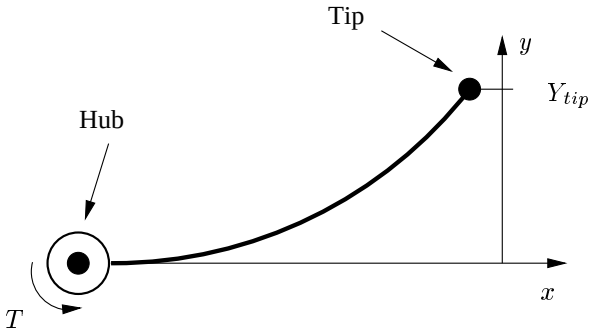

Figure 5.17: The one-link flexible arm described by the transfer function (5.40) where the input is the torque T and the output is the position of the tip, Y_{tip}.

Poles	Zeros
0.9555 ± 0.0574i	24.4176
0.9846 ± 0.0096i	1.0551

Table 5.3: *Poles and zeros of (5.41)*

The system on sampled with a period of $T_s = 0.01$.

The system is assumed to be unknown a priori and therefore data from the first ILC iteration is used to identify a fourth order linear model. The resulting model is

$$\hat{P}(q) = \frac{10^{-6} \cdot (-0.3836q^2 + 9.77q - 9.881)}{q^4 - 3.88q^3 + 5.649q^2 - 3.657q + 0.8884} \tag{5.41}$$

with poles and zeros presented in Table 5.3

In Figure 5.18, the Bode diagrams of the system and the model are presented. Since the system is quite resonant the relative model error is large for high frequencies. This should of course be considered when designing the filter $Q(q)$. Here, $Q(q)$ is designed as a low pass filter $Q(q) = \tilde{Q}(q)\tilde{Q}(q^{-1})$ with

$$\tilde{Q}(q) = \frac{0.1}{1 - 0.9q^{-1}}, \tag{5.42}$$

which is implemented using the matlab function `filtfilt` using $\tilde{Q}(q)$. In

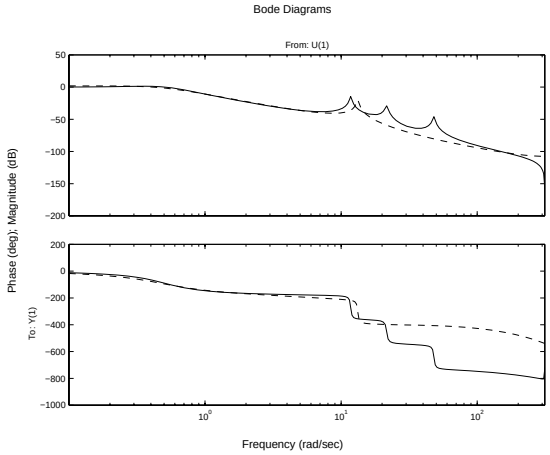

Figure 5.18: Bode diagrams of the system (solid line) and the model obtained from identification (dashed line).

Figure 5.19, the relative error as a function of frequency is shown along with the filter $Q(q)$.
Remark: The choice of the filter $Q(q)$ also reflects the performance of the tracking. It can be seen that if $Q(e^{i\omega})$ is set to be slightly larger than one for small frequencies to get the performance shown in Figure 5.20.

The tracking result after five iterations is shown in Figure 5.20 for a triangular wave similar to the desired output in (Nijsse *et al.* 2001). Exact tracking $Q = 1$ appears to be impossible with a fourth order model since then the relative error will be larger than one.

5.10 Summary

In this chapter we have highlighted the role of the design variables in ILC. We have also shown that ILC can be placed in the realm of numerical optimization. We have presented conditions for boundedness and convergence for non-linear systems which are very close in spirit to the necessary and sufficient conditions that previously have been derived for linear systems. The analysis shows that a relative model error of up to 100% can be tolerated, even when perfect tracking is desired. This is probably one of the reasons for the success of ILC in applications. The benefits of non-causal filtering for non-minimum phase systems has been elaborated upon and the implementational aspects of this covered.

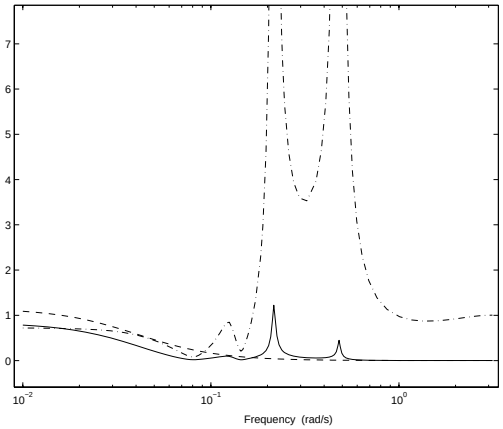

Figure 5.19: Relative model error $\left|\frac{\hat{P}(e^{i\omega})-P(e^{i\omega})}{\hat{P}(e^{i\omega})}\right|$ (dash dotted line), the filter $Q(e^{i\omega})$ (dashed line) and the total factor $\left|Q(e^{i\omega})\frac{\hat{P}(e^{i\omega})-P(e^{i\omega})}{\hat{P}(e^{i\omega})}\right|$ (solid line).

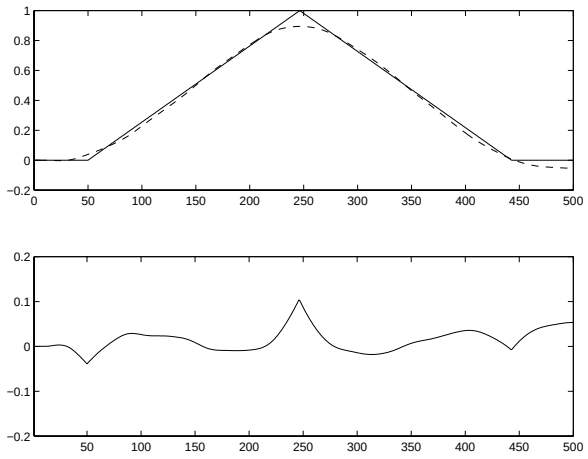

Figure 5.20: Top: Tracking result for the flexible arm, $y_d(t)$ (solid line) and $y_5(t)$ (dashed line), Bottom: Tracking error $y_d(t) - y_5(t)$.

Chapter 6

Identification of nonlinear systems by linear models for control

6.1 Introduction

In this chapter we consider control design for nonlinear systems based on linear time-invariant models. It is shown that a desired closed loop response can be obtained for a nonlinear system using a controller based on a linear model. This is possible if the linear model used in the control design is able to capture the input-output behavior of the nonlinear system for the desired response. An identification method is designed for this purpose where inversion plays an important role. By applying, e.g., the ILC algorithm for inversion, the method can be considered as an experiment design method and the achieved input signal can be used to identify a linear model. Inversion is thus one motivation for studying this problem in the context of this thesis where the results of Chapters 4 and 5 will be utilized. Parts of the results are presented in (Henriksson *et al.* 2001).

Related work

During the last decade there has been a vigorous activity to merge identification and control. The surveys (Ninness and Goodwin 1995, Gevers 1993) and (Van den Hof 1997) provide excellent introductions to

various aspects of the topic. Different methods to quantify the model uncertainty (Goodwin *et al.* 1992), (Goodwin *et al.* 1999), (Milanese and Vicino 1991) have been proposed. The role of bias and variance errors and their estimation have been discussed in (Goodwin *et al.* 1991) and (Hjalmarsson and Ljung 1992).

Several interesting model based control schemes that iteratively perform identification in closed loop and subsequent control design have been suggested (Lee *et al.* 1993, Schrama and Van den Hof 1993, Åström 1993, Hjalmarsson *et al.* 1996). These methods, and their underlying rationale for closed loop experimentation, has lead to renewed interest in closed loop identification (Gevers *et al.* 2001), (Forssell and Ljung 1999). Another direction has been taken in (Safonov and Tsao 1997) and (Kosut 1999) where direct parameterizations of the controllers are used. Much of the work in the field has been based on the assumption that the underlying system is linear and time-invariant. One of the exceptions is (Savaresi and Guardabassi 1998) in which the controller parameters are directly updated, c.f. direct adaptive control.

The purpose of this chapter is to study when linear, model based, control designs can be used on nonlinear systems and to develop an identification method that is suited for this type of problem.

6.2 Problem Statement

As a general set-up we will consider the closed-loop system depicted in Figure 6.1. The system P is an unknown nonlinear discrete-time SISO plant which we want to control and has the state-space representation

$$P \begin{cases} x(t+1) &= f(x(t), u(t)) \\ y(t) &= h(x(t)). \end{cases} \tag{6.1}$$

We assume that the system is controlled by a linear time-invariant controller $C(q, \rho)$ such that

$$u(t, \rho) = C(q, \rho)(r(t) - y(t, \rho)), \tag{6.2}$$

where $r(t)$ is an external reference signal. The controller $C(q, \rho)$ is parameterized by a parameter vector $\rho \in \mathbb{R}^l$ and q denotes the time-shift operator, i.e. $qu(t) = u(t+1)$. We will use ρ as argument when the signals are generated with $C(q, \rho)$ as the controller.

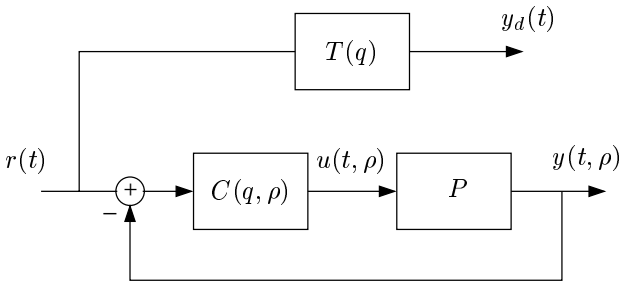

Figure 6.1: General setup of the desired closed loop system $T(\rho)$, the controller $C(q,\rho)$ and the system P.

The signal $y_d(t)$ represents the desired response and is generated from a fix linear model reference $T(q)$ as

$$y_d(t) = T(q)r(t). \tag{6.3}$$

For future reference we define the designed sensitivity function

$$S(q) = 1 - T(q).$$

The input signal which when applied to P makes the system output equal to $y_d(t)$ is denoted by $u_d(t)$. The corresponding state sequence is denoted by $x_d(t)$. Hence, $u_d(t)$ and $x_d(t)$ are defined by

$$\begin{aligned} x_d(t+1) &= f(x_d(t), u_d(t)) && (6.4)\\ y_d(t) &= h(x_d(t)). && (6.5) \end{aligned}$$

The existence of $u_d(t)$ is guaranteed if the system is invertible. We will assume that $u_d(t)$ exists and is unique.

The objective for the controller is to minimize the difference between $y_d(t)$ and $y(t,\rho)$ for a given reference $r(t)$ in the mean-square sense

$$J_N(\rho) = \frac{1}{N}\sum_{t=1}^{N} \left|y(t,\rho) - y_d(t)\right|^2, \tag{6.6}$$

and in addition we define the estimate $\hat{\rho}$ as

$$\hat{\rho} = \arg\min_{\rho} J_N(\rho).$$

We will use a model based control design. The model, which we denote by $G(q,\rho)$, is a discrete-time linear model of the nonlinear system. Model reference control will be used since the purpose is to make the closed loop close to the reference model T. This means that the controller $C(q,\rho)$ is chosen such that

$$T(q) = \frac{G(q,\rho)C(q,\rho)}{1+G(q,\rho)C(q,\rho)},$$

i.e.

$$C(q,\rho) = \frac{T(q)}{G(q,\rho)(1-T(q))}. \tag{6.7}$$

The objective of this chapter is to design an identification method, including the experimental conditions for the identification experiment, such that the identified model $G(q,\hat{\rho})$ is such that when the controller (6.7) is applied to the true nonlinear system P, the closed loop output $y(t,\hat{\rho})$ is close to the desired output $y_d(t)$, i.e. (6.6) is minimized.

The identification will be based on experimental data taken from the true system. We will consider two approaches to obtain input-output (I/O) measurements, used to identify $G(q,\rho)$. One procedure is for the situation where only one experiment is applied. The other approach is an iterative procedure based on iterative learning control (ILC). The focus in this chapter will be how to "tune" the bias error in the model such that the model becomes useful for control purposes. We will therefore assume a noise-free setting. In order to achieve good performance, we must ensure that the experimental data contains information of the nonlinear dynamics that are relevant for the control problem. In the next section we will outline how this can be done.

6.3 Method outline

To ease the notation somewhat we will from now on omit the operator argument q from the transfer functions. In order to find the model $G(\rho)$ that suits our purpose, we argue as follows. Given that the control signal $u(t,\rho)$ is given by (6.2) with the controller defined by (6.7) we can write the closed loop output $y(t,\rho)$ as

$$\begin{aligned} y(t,\rho) &= G(\rho)u(t,\rho) + y(t,\rho) - G(\rho)u(t,\rho) \\ &= G(\rho)C(\rho)(r(t) - y(t,\rho)) + y(t,\rho) - G(\rho)u(t,\rho). \end{aligned}$$

This gives

$$\begin{aligned} y(t,\rho) &= \frac{G(\rho)C(\rho)}{1+G(\rho)C(\rho)}r(t) \\ &\quad + \frac{1}{1+G(\rho)C(\rho)}(y(t,\rho)-G(\rho)u(t,\rho)) \\ &= Tr(t) + S\ (y(t,\rho)-G(\rho)u(t,\rho)) \\ &= y_d(t) + S\ (y(t,\rho)-G(\rho)u(t,\rho)). \end{aligned} \tag{6.8}$$

From (6.8) we see that whether or not the output behaves like the desired linear system $T\ r(t)$ depends on if the second term on the right-hand side is small or not. The size of this term depends on how well the nonlinear system is modeled by $G(\rho)$, for the particular control signal $u(t,\rho)$ that is used. Further notice that the modeling is particularly important at frequencies where the designed sensitivity function S is large.

By rewriting (6.8) we get

$$y(t,\rho) - y_d(t) = S\ (y(t,\rho) - G(\rho)u(t,\rho)). \tag{6.9}$$

This expression is identical to the expression for $y(t,\rho) - y_d(t)$ derived in (Åström 1993) for a linear time-invariant feedback system.

If the ρ's in $y(t,\rho)$ and $u(t,\rho)$ would have been fix, (6.9) could have been interpreted as an identification error with the designed sensitivity S as a prefilter and the ρ minimizing (6.6) could have been obtained by identification of $G(q,\rho)$ using (6.9). This resemblance has triggered attempts to match the identification objective with the control objective (6.6) in the case of a complex linear system and a restricted complexity linear model, see e.g. (Åström 1993).

The recognition that the signals y and u in (6.9) indeed depend on ρ has lead to the development of iterative identification and control algorithms which, in our model reference setting, basically works as follows:

i) Start with some model $G(q,\rho_i)$, $i=0$.

ii) With $\rho=\rho_i$, compute the controller (6.7).

iii) Generate and collect the closed loop data $y(t,\rho_i)$ and $u(t,\rho_i)$, $t = 1,\dots N$, by a closed loop experiment.

iv) Identify a new ρ_{i+1} by minimizing

$$J_{id}(\rho) = \frac{1}{N}\sum_{t=1}^{N} \left|S\left(y(t,\rho_i) - G(\rho)u(t,\rho_i)\right)\right|^2 . \tag{6.10}$$

v) If ρ_i has converged stop, otherwise goto ii).

Such schemes have given good results on a number of linear examples. There is, however, no guarantee that the optimal ρ, i.e. the one minimizing (6.6), is found with this method even if the sequence $\{\rho_i\}_{i=0}^{\infty}$ converges. This has been pointed out in (Ljung and Söderström 1983), in the context of adaptive control, and in (Hjalmarsson *et al.* 1995), in the context of iterative identification and control. In fact, for this to be true requires typically that the model can describe the system perfectly.

Our contribution will be to show that it is not necessary with a perfect match between the system and model if the model can describe the system behavior for the desired operating conditions. Hence, it is possible to use linear models also when the system is nonlinear provided that the model structure is flexible enough.

Theorem 6.1. *Let y_d and u_d be defined by (6.3) and (6.4)–(6.5), respectively. Let $G^*(q)$ be a linear time-invariant model and let*

$$x^*(t+1) = f(x^*(t), u^*(t)) \tag{6.11}$$
$$y^*(t) = h(x^*(t)) \tag{6.12}$$
$$u^*(t) = C^*(q)(r(t) - y^*(t)) \tag{6.13}$$

be the closed loop description of the system P when the controller

$$C^*(q) = \frac{T(q)}{G^*(q)(1-T(q))} \tag{6.14}$$

is operating.

Suppose that C^* stabilizes the system in the sense that u^* and y^* are bounded, then

$$y^*(t) = y_d(t),\ \forall t,$$

if and only if

$$y_d(t) = G^*(q)u_d(t),\ \forall t. \tag{6.15}$$

Proof: See Appendix C. □

The only if part of Theorem 6.1 shows that if the input in the identification experiment is chosen such that the output becomes identical to the desired output y_d, then the controller corresponding to a linear model with zero model residuals

$$\varepsilon^*(t) = y_d(t) - G^*(q)u_d(t) \tag{6.16}$$

will give the desired closed loop performance. This underpins the intuitively appealing idea that an identification experiment should be carried out under the desired operating conditions. This is also in line with the observation made by Horowitz. In (Horowitz 1992) it is shown that if a linear time-invariant equivalent (LTIE) model can be used to represent the input-output relationship of a nonlinear system, then it can be used for control design. It should be stressed that the equivalent model is valid only for a specific input signal.

The if part of Theorem 6.1 shows that if u_d and y_d are used as data in the identification and there exists a model, G^*, of the open loop system in the model set such that the corresponding controller C^* gives the desired closed loop behavior, then this model will be identified. Hence, in this case we are guaranteed to find the optimal model (and controller) in one shot and no iterative procedure is necessary.

For a nonlinear system, it may seem unrealistic that there exists a linear model G^* which gives a perfect match between y_d and G^*u_d. However, the result indicates that even if the model residuals (6.16) are nonzero but small, close to optimal performance will be obtained. It will be shown in the next theorem that this is a valid statement when the system is linear.

Theorem 6.2. *Suppose that the system (6.1) is linear time-invariant with transfer function $P(q)$. Also, suppose that the controller C^* (6.14) stabilizes the closed loop system, i.e.*

$$y^*(t) = P(q)\, u^*(t) \tag{6.17}$$

$$u^*(t) = C^*(q)(r(t) - y^*(t)) \tag{6.18}$$

is stable. Then

$$y^* - y_d = \frac{T^*}{T}\, S\, (y_d - G^*u_d) \tag{6.19}$$

where $T^* = PC^*/(1 + PC^*)$.

Proof: See Appendix C. □

Notice that T^*/T will be approximately unity at low frequencies since, approximately, both T^* and T will be unity assuming that the control design (6.14) includes an integrator. The frequency contents of both y_d and u_d will be small at high frequencies for sensible control designs.

Hence, $S\ (y_d - G^* u_d)$ will be a good measure of $y^* - y_d$. This suggests that, for linear time-invariant systems, a model which makes the identification criterion

$$J_{\mathrm{id}}(\rho) = \sum_{t=1}^{N} |S\ (y_d(t) - G(\rho)u_d(t))|^2 \tag{6.20}$$

small, makes the control criterion (6.6) small. In other words, (6.20) is an identification criterion suitable for control. In addition it can be observed that (6.20) can be related to (6.9) with y and u being the desired input and output.

In the identification criterion (6.20), the desired response $y_d(t)$ is known from (6.3). However, $u_d(t)$ is unknown and although essential for the optimization of $J_{\mathrm{id}}(\rho)$. Recall that $u_d(t)$ is the input to the true system when $y_d(t)$ is the output. Hence, to obtain $u_d(t)$ the system has to be inverted and this will be the topic of the next section.

6.4 Experimental system inversion

As noted in Section 6.3, the identification criterion (6.20) requires $u_d(t)$. The natural way to retrieve the input corresponding to a specific output is to apply inversion. The problem here is that no model of the system is available and, hence, inversion has to be based on the system itself. Two approaches will be considered, first an approach based on Iterative Learning Control (ILC) introduced in Chapter 5, and then an approximative method is suggested. The main difference between these approaches is that ILC is an iterative method while the approximative method will depend on only one set of input-output data. The second method is related to the method presented in Chapter 4. Notice, however, that here we work with the actual system.

Experiment design

It should be noted that the methods presented below to obtain $u_d(t)$ can be interpreted as experiment design methods. In other words, the

methods suggest what inputs to apply such that the data is suitable for identification.

6.4.1 Inversion by ILC

Although iterative learning control (ILC) is mainly associated with control it also provides means for inversion. At convergence, the method gives the input corresponding to a desired output. Even though the ILC algorithm is presented to great extent in Chapter 5 we will highlight some of the relevant parts below.

First of all, a first order ILC algorithm is given by

$$u_{k+1}(t) = Q(u_k(t) + \hat{P}^{-1}(y_d(t)) - \hat{P}^{-1}(y_k(t)), \tag{6.21}$$

where $u_k(t)$ is the input at the kth iteration and the corresponding output is denoted by $y_k(t)$. In (6.21), $\hat{P}^{-1}$ denotes the inverse of an estimated model of the system and Q is an operator chosen such that convergence is obtained. In Figure 6.2, the ILC algorithm for a sequence of length N is shown.

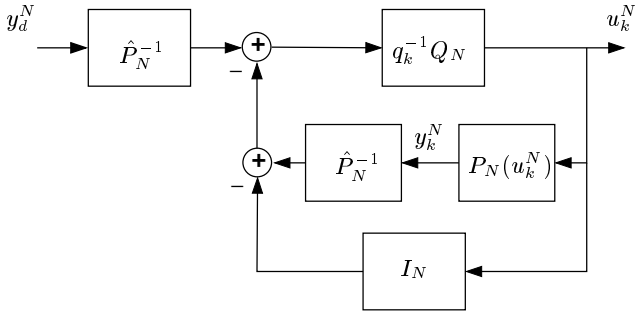

Figure 6.2: Block diagram of the ILC algorithm in the nonlinear case given by (5.6). The system is denoted by P_N transforming the vector u_k^N into y_k^N, the estimated inverse $\hat{P}_N^{-1}$ acts in similar way. Note that the shift operator q_k^{-1} acts w.r.t. the iteration index k ($q_k^{-1}u_k(t) = u_{k-1}(t)$).

Assuming that no model is available a priori the data from the first ILC iteration can be used to identify a model according to the ideas in Section 5.8. The identified model is assumed to be linear which is partly motivated by the fact that a linear model is easily inverted as shown in Chapter 2.

The choice of the operator Q is made such that it satisfies the criterion for convergence as formalized in Theorem 5.3 and Corollary 5.1. Recall also the tradeoff between the relative model error and the operator Q in the linear case.

At least two things are worth pointing out here. First of all, perfect inversion will only be obtained with $Q = 1$. Second, even if $Q = 1$, perfect inversion is hard to achieve since ILC is an iterative method and only a finite number of iterations can be applied in practice. However, as previously stated, the inversion must not be absolutely perfect since the cost function (6.10) is weighted with the sensitivity function S. Thus $Q = 1$ may not be a restrictive condition. By studying the numerical examples in Section 5.9 it can be seen that ILC can be applied successfully for a number of different systems.

6.4.2 Approximative inverse

In this section we will derive an approximation of the system inverse to obtain an approximation, $\hat{u}_d(t)$ of $u_d(t)$. The main property of the approach is that only a single set of input-output data will be used.

Consider the nonlinear system P, for which we will use the short-hand notation $P(u^t)$ to denote the output. As shown in Chapter 4 one gets, by adding and subtracting a linear filter $L(q)$,

$$\begin{aligned} P(u^t) &= \underbrace{P(u^t) - L(q)u(t)} + L(q)u(t) \\ &= N(u^t) + L(q)u(t). \end{aligned} \tag{6.22}$$

Inversion by feedback (Doyle *et al.* 1995) can be introduced by writing P as

$$P = L(I + L^{-1}N). \tag{6.23}$$

It is assumed that the inverse of L exists, e.g., L cannot be an ideal low pass filter. It is also further assumed that L is minimum phase.

Now, the inverse of P can be expressed as

$$P^{-1} = (I + L^{-1}N)^{-1}L^{-1}. \tag{6.24}$$

In Figure 6.3, the relationship in (6.24) is illustrated by a block diagram and it is clear that the system can be inverted without explicitly inverting the nonlinear system. It is sufficient to invert the linear part and filter the data through the nonlinear feedback system as shown in Figure 6.3. For this to work, the closed loop has to be stable, i.e. L has to be chosen such that this is the case.

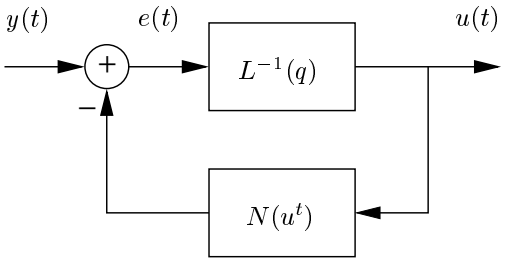

Figure 6.3: Realization of the model inverse, $P^{-1}(y^t)$.

6.4.3 Implementation and approximation

When the feedback loop shown in Figure 6.3 is implemented by means of a digital control system and the actual system, a time-delay of one sample is introduced, if not already present. From now on it will be assumed that this time-delay is included in P. The feedback also depends on the time-delay which is depicted in Figure 6.4. The feedback system is shown in Figure 6.4 where the time-delay of L is represented by the operator D (usually $D = q^{-1}$). The output $\hat{u}(t)$ from the feedback loop in Figure

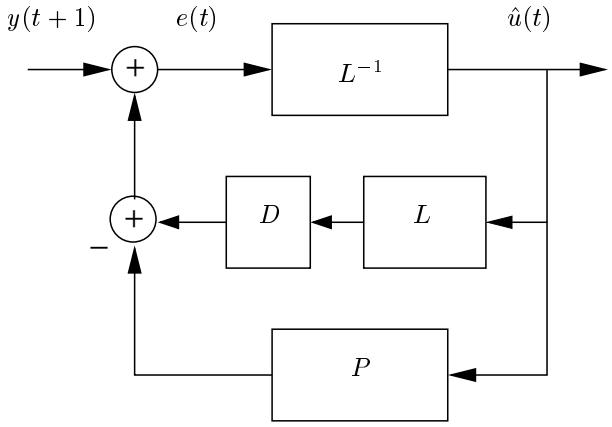

Figure 6.4: Realization of the approximative inverse of $P(u^t)$

6.4 will no longer be the exact inverse of P but an approximation. The quality of the approximation is influenced by L and the question of how to choose this filter will be covered next.

Notice that the configuration in Figure 6.4 can be interpreted as an Internal Model Control (IMC) (Morari and Zafiriou 1989*b*) feedback system where L is the system model (recall that $N = P - L$) and L^{-1} is the controller.

In conclusion, the input $u(t)$ that generates a specified output $y(t)$ of a general nonlinear system can be obtained by the closed loop experiment shown in Figure 6.4. Hence, the input $u_d(t)$ that corresponds to the output $y_d(t)$ is obtained by taking $y(t) = y_d(t)$ in the experiment in Figure 6.4.

Remark: The approximation in Figure 6.4, with $D = q^{-1}$, corresponds to an approximation as

$$y(t+1) \approx P(u^t) + L(q)(1 - q^{-1})u(t).$$

Hence, it is assumed that the innovation in $y(t)$ is a linear function of $u(t)$.

Choice of filter. In general, the objective is, of course, to choose L such that the difference between $u(t)$ and the approximation $\hat{u}(t)$ is as small as possible. Since our objective is to be able to evaluate

$$S\ (y_d(t) - G(\rho)u_d(t)), \tag{6.25}$$

we will use $y(t) = y_d(t)$ as input to the feedback loop in Figure 6.4 and our concern will be to get an as accurate approximation of $S\ G(\rho)\ u_d(t)$ as possible.

It is complicated to determine the optimal filter L in the general nonlinear case. However, in the linear time-invariant case an explicit solution can be found.

Theorem 6.3. *Assume that the system P is linear time-invariant with minimum-phase transfer function $P(q)$. Suppose that the reference signal $r(t)$ is quasi-stationary (Ljung 1999) with spectral factorization*

$$\Phi_r(\omega) = |H_r(e^{i\omega})|^2 \lambda.$$

Let the approximative inverse be given, as in Figure 6.4, by

$$\hat{u}_d(t) = \frac{q\ L^{-1}}{1 - q^{-1} + P\ L^{-1}} y_d(t).$$

Let G^* be a linear time-invariant model and define the error

$$\varepsilon(t) = S\ G^*\ (\hat{u}_d(t) - u_d(t)). \tag{6.26}$$

Let $u(t) = -L^{-1}\ y(t)$ be the minimum variance control law (Åström and Wittenmark 1984) for the system

$$y(t) = Fu(t) + Hv(t), \tag{6.27}$$

where

$$F = \frac{1}{1-q^{-1}}\ P \tag{6.28}$$

$$H = Q\ S\ T\ \frac{G^*}{P}\ H_r. \tag{6.29}$$

In (6.29), Q is such that H is monic, i.e. $Q = \alpha\ q^k$ where k is such that there is no pure time-delay in H and α is adjusted such that the first impulse response coefficient of H is unity. Above, $v(t)$ is white noise with zero mean and finite variance.

Then L minimizes

$$J_L = \mathrm{E}\left[|\varepsilon(t)|^2\right]. \tag{6.30}$$

Proof: See Appendix C, where also the choice of L^{-1} is considered in the case of measurement noise. □

Remarks:

- Notice that, quite naturally, the optimal L does depend on the (unknown) system P since F and H depend on P. However, our experience is that it is not critical to find the optimal L so instead of P a simple prior model of P can be used, e.g. obtained from a step response experiment.

- Notice also that since the optimal model will approximate P, a natural approximation in H is to replace G^*/P by 1.

- When F only contains one time-delay, the optimal L is given by

$$L = \frac{F}{H-1} = \frac{\frac{1}{1-q^{-1}}\ P}{S\ T\ \frac{G^*}{P}\ H_r - 1} \approx \frac{\frac{1}{1-q^{-1}}\ P}{S\ T\ H_r - 1}.$$

- In the case of a nonlinear system, an L that corresponds to a linear time-invariant model that approximates the system can be used. As in the linear case, the model can be quite simple and still yield a useful L. This is illustrated in Section 6.6.

In conclusion, this method tries to achieve an impossible task. Namely, to invert the system by feedback control with very poor knowledge of the system. Since the objective is to design a feedback controller which accomplish this, we are biting our tail. However, as shown by the numerical examples, useful results can be obtained using this method. The recommended method, however, is to use ILC.

6.5 Modeling linear systems

The proposed identification criterion (6.10) also makes sense when the true system is linear but when the model is of restricted complexity. Thus, the true system cannot be modeled perfectly. Theorem 6.2 shows that

$$S\left(y_d - G^* u_d\right) = \frac{T^*}{T}(y^* - y_d).$$

Hence, (6.10) minimizes, a by $\frac{T^*}{T}$, weighted version of the desired cost function (6.6). However, as argued after Theorem 6.2 the factor $\frac{T^*}{T}$ is close to unity at low frequencies and the energy in the signals is low at high frequencies. Hence, the difference between (6.10) and (6.6) can be expected to be small. Thus, using (6.10) with u_d obtained using ILC, is an interesting alternative to the iterative methods of tuning the bias, based on the approach outlined in Section 6.3, see e.g. (Zhang *et al.* 1995) and (Lu and Skelton 2001). For these methods, it has turned out to be hard to establish convergence. We will, however, not pursue this analysis further.

6.6 Numerical examples

As numerical examples we consider two different Hammerstein systems. The systems are shown in Figure 6.5 and the linear parts, which are the same in both cases, is given by

$$G(q) = \frac{q^{-1}}{1 - 1.6q^{-1} + 0.8q^{-2}}.$$

In Example 1 the nonlinear part, N, is described by a variable gain according to Figure 6.5 and in Example 2 the nonlinear part is given by

$$N(u) = sign(u)\sqrt{|u|}.$$

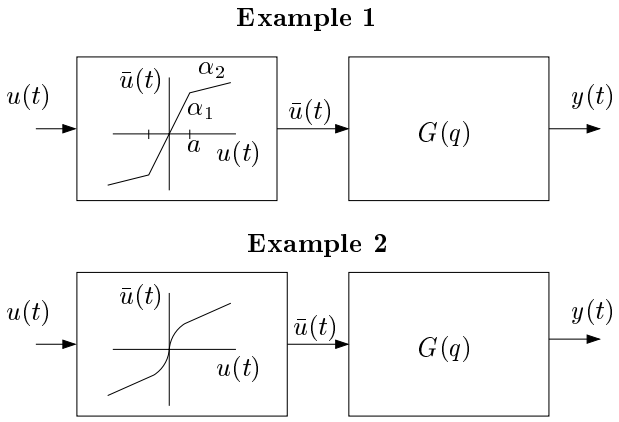

Figure 6.5: Block diagrams for Example 1 and 2.

The same reference signal $r(t)$ is applied in both cases and it is a square-wave with 100 samples period time with amplitude 5. The desired output $y_d(t)$ is given by $y_d(t) = T(q)r(t)$ where

$$T(q) = \frac{0.16q^{-1}}{1 - 0.84q^{-1}},$$

in both cases. The length of the applied sequences was 2000 samples in both cases.

As described above the control of the nonlinear system is based on a linear model given by optimizing (6.20) and the controller is calculated as in (6.7).

Three ways of obtaining $u_d(t)$ will be tested. The exact inverse is evaluated to study what is possible when the system is known exactly and the suggested methods for approximating the inverse will, of course, also be tested. The ILC method is applied according to the outlined method in Section 6.4.1 and the third approach follows the ideas for approximative inverse in Section 6.4.2. In more detail we are studying the following cases.

A. Exact inversion
Since the system is known, it is possible to calculate the input signal $u_d(t)$ directly from the desired signal $y_d(t)$. Hence, in this case we mainly study how a linear model can be used to calculate a controller for a nonlinear system given a specific reference trajectory.

B. Inversion by ILC
ILC is applied according to Section 6.4.1 assuming that no model is known a priori. Convergence is obtained by selecting the Q filter in an appropriate manner. Note that if only a finite number of iterations are applied then this type of inversion will be an approximation. Recall also that if $Q \neq 1$ the inverse will not be exact no matter how many iterations applied.

C. Inverse by feedback approximation
The feedback inverse described in Section 6.4 is applied as depicted in Figure 6.4. The filter $L(q)$ was obtained following the guidelines in Theorem 6.3.

6.6.1 Example 1 - results

The system in this example is shown at the top of Figure 6.5 with numerical values $a = 2$, $\alpha_1 = 0.5$ and $\alpha_2 = 0.1$. The three different inversion approaches listed above were applied and the resulting models $G(q, \rho)$ are presented in Table 6.1. For the case of exact inversion the correlation function for the prediction error together with confidence intervals is shown in Figure 6.6. At the bottom of the same figure, the cross-correlation between the input and the prediction error is shown. The model does not pass a standard validation test considering the strong cross-correlation, and appears to be of questionable use for control. However, as we will see below this is not the case.

The controllers corresponding to each model are also presented in Table 6.1 and the tracking results are shown in Figure 6.7. To study the robustness w.r.t. changes in the reference signals, different amplitudes are tested and shown in Figure 6.7. Recall that the model is identified for a desired output with amplitude 5.

The ILC approach was iterated ten times and it was initialized as $u_0(t) = y_d(t) \forall t$. A second order linear model $\hat{P}$ was identified using data from the first iteration and $Q = 1$ was used. By considering the estimated models in Table 6.1 it can be noted that the result of the ILC algorithm is very close to the result of the exact inverse. The feedback inversion approach resulted in a slightly different model but, as can be seen from the simulations, the corresponding controller gives a similar result as the other approaches. Hence, from the results in Figure 6.7, it can be concluded that a linear controller can be used in this example.

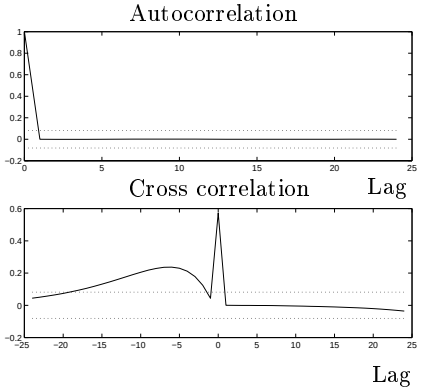

Figure 6.6: Example 1. Top: Autocorrelation of the prediction error. Bottom: Cross-correlation between the input and the prediction error. Confidence limits (99 %) are shown as dotted lines.

6.6.2 Example 2 - results

In this example the system depicted at the bottom of Figure 6.5 is studied and the estimated models $G(q, \rho)$ are presented in Table 6.2. As in the previous example the correlation function for the prediction error together with confidence intervals are shown in Figure 6.6 for the case of exact inversion. At the bottom of the same figure, the cross-correlation between the input and the prediction error is shown. In this case, the model does not pass the standard validation tests and, considering the strong cross-correlation, appears to be of questionable use for control.

The controllers corresponding to each model are also presented in Table 6.2 and the tracking results are shown in Figure 6.9. To study the robustness w.r.t. changes in the reference signals, different amplitudes are tested and shown in Figure 6.9. As in the previous example the model is identified for a reference signal with an amplitude of 5.

From studying the tracking results in Figure 6.9 it can be deduced that a linear controller can be used in this example. The estimated models in Table 6.1 are similar for the ILC and the exact inversion approaches. The feedback inversion approach, however, resulted in a different model. The application of the feedback approach is questionable in this case since the result varied considerably depending on the model structure of G. For example, a higher model order gave considerably worse result than the result shown in Figure 6.9.

Method	$G(q,\rho)$	$C(q,\rho)$
Exact	$\frac{0.8399q^{-1}-0.3523q^{-2}}{1-1.6q^{-1}+0.8002q^{-2}}$	$\frac{0.1905-0.3048q^{-1}+0.1524q^{-2}}{1-1.419q^{-1}+0.4194q^{-2}}$
ILC	$\frac{0.8395q^{-1}-0.3512q^{-2}}{1-1.6q^{-1}+0.8004q^{-2}}$	$\frac{0.1906-0.3049q^{-1}+0.1525q^{-2}}{1-1.418q^{-1}+0.4184q^{-2}}$
Feedback	$\frac{0.47q^{-1}-0.21q^{-2}}{1-1.8q^{-1}+1.1q^{-2}-0.14q^{-3}}$	$\frac{0.34-0.61q^{-1}+0.36q^{-2}-0.05q^{-3}}{1-1.4q^{-1}+0.44q^{-2}}$

Table 6.1: *Example 1: Estimated models and corresponding controllers.*

Method	$G(q,\rho)$	$C(q,\rho)$
Exact	$\frac{1.416q^{-1}-1.046q^{-2}}{1-1.734q^{-1}+0.808q^{-2}}$	$\frac{0.113-0.196q^{-1}+0.09131q^{-2}}{1-1.739q^{-1}+0.7391q^{-2}}$
ILC	$\frac{1.52q^{-1}-1.18q^{-2}}{1-1.765q^{-1}+0.8312q^{-2}}$	$\frac{0.1053-0.1858q^{-1}+0.0875q^{-2}}{1-1.776q^{-1}+0.7763q^{-2}}$
Feedback	$\frac{0.2681q^{-1}+0.05324q^{-2}}{1-1.672q^{-1}+0.765q^{-2}}$	$\frac{0.5968-0.998q^{-1}+0.4565q^{-2}}{1-0.8014q^{-1}-0.1986q^{-2}}$

Table 6.2: *Example 2: Estimated models and corresponding controllers.*

It can be noted in this case that the convergence of the ILC algorithm was improved by reidentifying the linear model $\hat{P}$ for each iteration. The operator Q was also chosen as a low-pass filter $Q(q) = \frac{0.4}{1-0.6q^{-1}}$. Ten iterations of the ILC algorithm were applied and it was initialized as $u_0(t) = y_d(t) \forall t$.

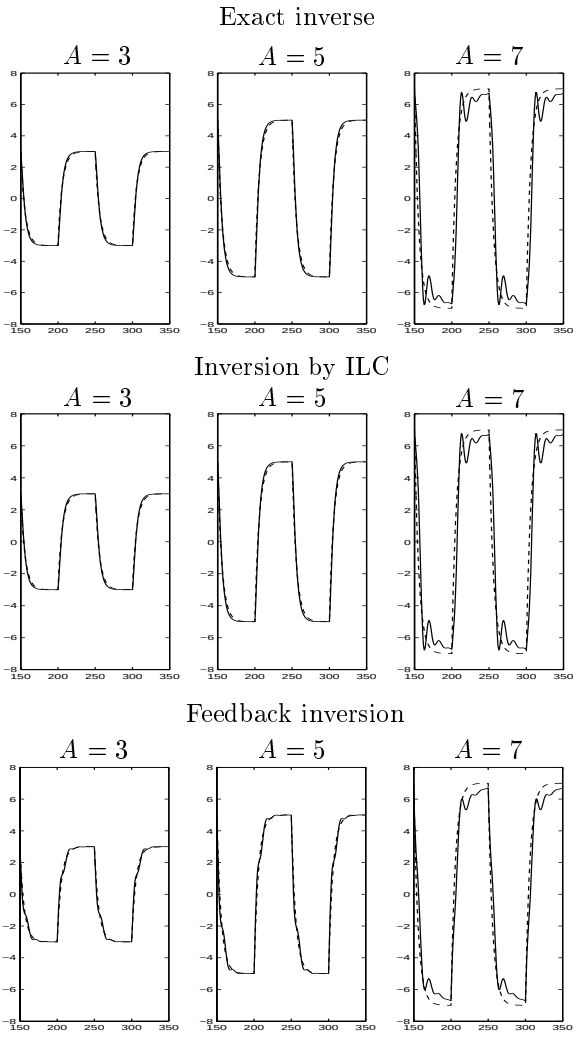

Figure 6.7: Example 1: Tracking results where the controllers are designed for $A = 5$ (middle). Dashed line: $y_d(t)$, solid line $y(t, \rho)$. To evaluate robustness the controller is also applied for $A = 3$ (left) and $A = 7$ (right).

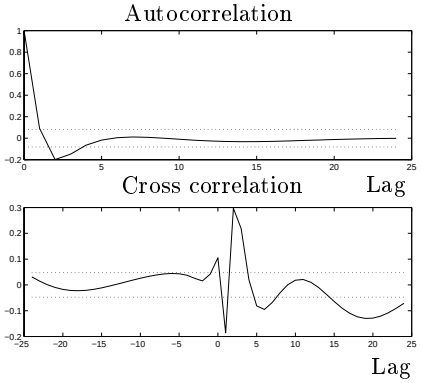

Figure 6.8: Example 2. Top: Autocorrelation of the prediction error. Bottom: Cross-correlation between the input and the prediction error. Confidence limits (99 %) are shown as dotted lines.

6.7 Summary

We have in this chapter shown that under certain circumstances it is possible to use a linear model based control design even on nonlinear systems. We have also suggested a method for how to identify a model that is suited for the model based control design. The identification procedure is based on the inversion of the system and two ways of obtaining the inverse have been suggested. The approach based on iterative learning control (ILC) results in better models and can be applied to a larger class of systems than the feedback approach. This is seen by studying the numerical examples. Noise sensitivity and robustness are two main issues that remains to be studied.

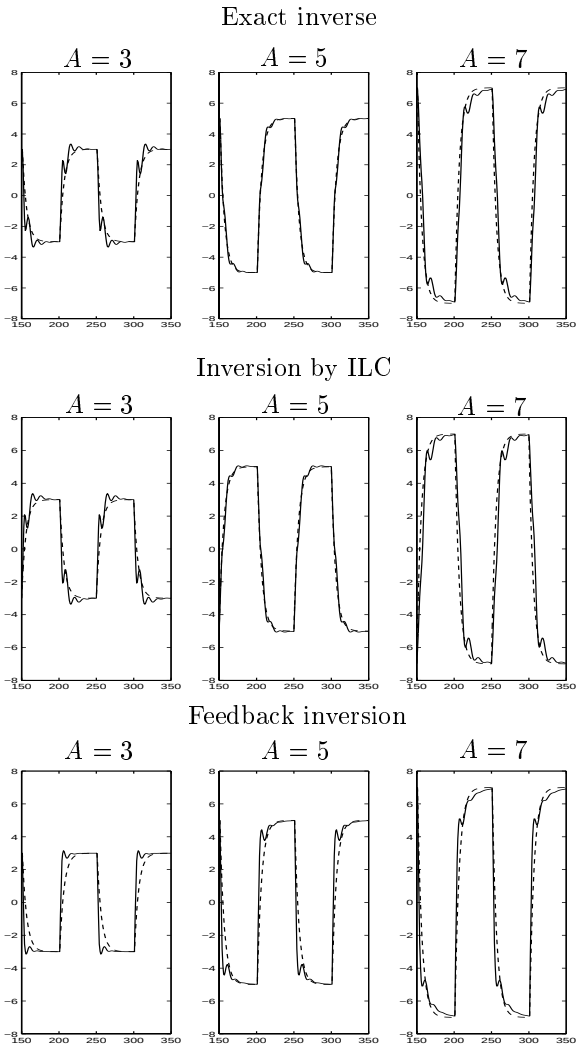

Figure 6.9: Example 2: Tracking results where the controllers are designed for for $A = 5$ (middle). Dashed line: $y_d(t)$, solid line $y(t, \rho)$. To evaluate robustness the controller is also applied for $A = 3$ (left) and $A = 7$ (right).

Chapter 7

Spectral matching for parameter estimation

7.1 Introduction

In this chapter we consider parameter estimation in nonlinear stochastic models by spectral matching. Models with a measured output and both known and unknown inputs are considered. Simulated data is used to estimate the spectrum of the nonlinear model and two different cost functions are suggested for the matching of the spectrum. Theoretical results on convergence and parameter covariance are presented. In addition, an identifiability condition for a class of nonlinear models is given. An extension of the matching idea is made using higher order statistics. The estimation methods are illustrated numerical examples.

Method outline

In this chapter we consider parameter estimation in models of systems depicted in Figure 7.1. The output of the system $y(t)$ is measured as well as the optional control input $u(t)$. The disturbance $e(t)$ is considered to be unknown. In the case of a linear model the spectrum of the model output can be calculated analytically. However, in the nonlinear case analytical calculation is more complicated. Instead of analytical calculation the spectrum of the model output is based on *simulated data*. The data is simulated using the known input signals and realizations of the unknown input signals (using their assumed PDF:s).

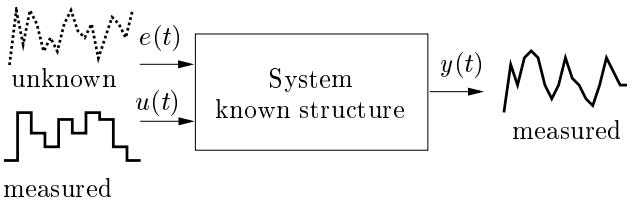

Figure 7.1: The system under consideration.

A graphical description of the suggested estimation method is shown in Figure 7.2, where the measured signal is denoted $y(t)$ and its estimated spectrum $\hat{\phi}_y(\omega)$. In parallel to the system a model is simulated using a realization $\hat{e}(t)$ of the unknown disturbance $e(t)$ and the known input $u(t)$. The output is denoted $\hat{y}(t)$. The model spectrum is computed from simulated data and denoted $\phi_{\hat{y}}(\omega, \theta)$. In the estimator block a cost function is evaluated and an update of the parameters in the model is computed, usually based on numerically estimated derivatives. In other words the suggested method is estimating the parameters of the model by minimizing a cost function comparing the spectra of the model and the system output. An advantage of this method is that we can have more sources than measured signals which is complicated when applying ML estimation based on inversion. Also the probability density function (PDF) of the noise source may be parameterized, by e.g., mean and variance. The results of this chapter are presented in (Markusson and Hjalmarsson 2000*b*), (Markusson and Hjalmarsson 2001*a*) and (Markusson and Hjalmarsson 2001*c*).

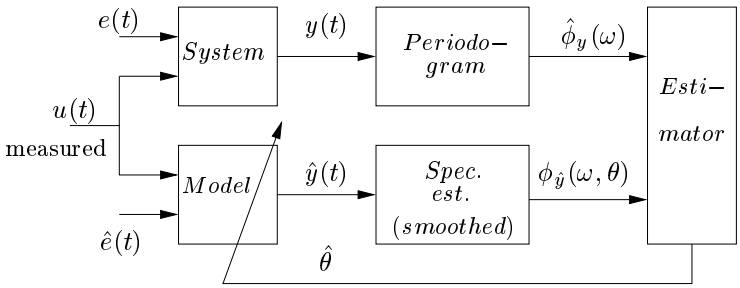

Figure 7.2: Graph of the estimation idea using spectral comparison.

Motivation

Although ML estimation is a statistically tractable method as pointed out in Chapter 3, it is sometimes difficult to implement. The motivation for the method introduced here are the cases where inversion, and thereby ML estimation, is impossible or at least difficult to apply. For example, if the model has two unknown input signals (only the PDF:s are assumed to be known) then ML is difficult to implement. The frequency domain approach can also be motivated from the fact that the periodogram is asymptotically independent for different frequencies with a χ^2 distribution with the true spectrum $\phi(\omega)$ as mean. This property can be used to establish a maximum likelihood based estimator. Also, since the statistics of the spectral estimates are known, it is possible to establish a weighted least squares criterion.

7.2 Spectral estimation

Let us first give an introduction to spectral estimation of random signals. An excellent textbook on spectral estimation is (Stoica and Moses 1997) where the following informal definition is given "from a finite record of stationary data sequence, estimate how the total power is distributed over frequency". A more formal definition is also given "From a finite-length record $\{y(1), \ldots, y(N)\}$ of a second-order stationary random process, determine an estimate $\hat{\phi}(\omega)$ of its power spectral density $\phi(\omega)$, for $\omega \in [-\pi, \pi]$". There are two broad approaches to spectral estimation, non-parametric and parametric estimation. In the first approach the idea is that the signal is applied to a narrow bandpass filter which is swept in a certain frequency range. The second, parametric approach, uses a model for the data which parameterizes the spectrum and the method estimates the parameters of the model. The advantage of the parametric method is that it provides more accurate estimates when the model assumption is correct. However, when the model assumptions fail, the non-parametric methods are superior to parametric methods. In our case we will focus on non-parametric spectral estimation and use the spectrum to estimate the parameters of the model. Below an overview of non-parametric spectral estimation is given.

The two main non-parametric spectral estimators are the periodogram and the correlogram, which are known to be equal under weak conditions (Stoica and Moses 1997). First we assume that $y(t)$ is a second-order stationary signal. In Section 7.4, a definition of second-order stationarity

is given and stationarity in the combination with nonlinear systems is also discussed. Assuming that $y(t)$ is a second-order stationary sequence, the periodogram is given by

$$\hat{\phi}_p(\omega) = \frac{1}{N}\left|\sum_{t=1}^{N} y(t)e^{-i\omega t}\right|^2, \tag{7.1}$$

where the signal under study is $\{y(t)\}_{t=1}^{N}$. The correlogram is given by

$$\hat{\phi}_c(\omega) = \sum_{k=-(N-1)}^{N-1} \hat{r}_y^N(k)e^{-i\omega k} \tag{7.2}$$

where the covariance function is computed as

$$\hat{r}_y^N(k) = \frac{1}{N}\sum_{t=|k|+1}^{N} y(t)y(t-k), \quad -(N-1) \leq k \leq N-1. \tag{7.3}$$

Remark: There are different ways of computing the covariance function. This way of computing the covariance function is biased but is the most commonly used function. In (Stoica and Moses 1997) further details are presented and it is also shown that when using (7.3) to estimate $\hat{r}(k)$ then $\phi_c(\omega)$ coincides with $\phi_p(\omega)$.

There is unfortunately a drawback with the above described spectral estimators since the variance is high and does not decay when the number of samples increases. One explanation for the high variance can be seen from the estimation of $\phi_c(\omega)$ where the estimation errors of $\hat{r}_y^N(k)$ are on the order of $\frac{1}{\sqrt{N}}$ for large N. Since $\phi_c(\omega)$ consists of $(2N-1)$ elements the difference between the real and the estimated spectrum will not die out when N is increased. For further explanation of the high variance, see (Stoica and Moses 1997). There are a number of ways to decrease the variance although at the expense of an increased bias. We will here describe two different methods; one applied to the correlogram and one applied to the periodogram. Further methods are given in (Stoica and Moses 1997).

7.2.1 Blackman-Tukey Spectral Estimate

The main idea behind the Blackman-Tukey (BT) estimator is to truncate the sequence used for the computation of $\hat{\phi}_c(\omega)$ in (7.2). This is motivated

by the erratic behavior of the estimator stemming from the summation of a large number of covariance estimation errors for large values of k ($|k| \simeq N$). The BT estimator is computed as

$$\hat{\phi}_{BT}(\omega) = \sum_{k=-(M-1)}^{M-1} w(k)\hat{r}(k)e^{-i\omega k} \tag{7.4}$$

where $w(k)$ is a weighting function called a lag window. The sequence $w(k)$ is an even function with $w(0) = 1$ and $w(k) = 0$ for $|k| \geq M$. The lag window can be chosen in many ways where length and shape are design factors. Study, e.g., (Oppenheim and Schafer 1989) for a description of different window functions. There are two main rules concerning the choice of window, (Stoica and Moses 1997):

- "The choice of window's length should be based on a tradeoff between spectral resolution and statistical variance".
- "The selection of window's shape should be based on a tradeoff between smearing and leakage effects".

Briefly, smearing reduces resolution and leakage gives an error in the estimate.

7.2.2 Welch method

To reduce the fluctuations of the periodogram there are a number of suggested methods based on splitting the data sequence, windowing the time series and performing averaging. The Welch method is based on splitting the sequence into S overlapping segments that are windowed prior to computing the periodogram as

$$\hat{\phi}_j(\omega) = \frac{1}{MP}\left|\sum_{t=1}^{M} v(t)y_j(t)e^{-i\omega t}\right|^2,$$

where M is the length of the segment and P is the power of the window

$$P = \frac{1}{M}\sum_{t=1}^{M}|v(t)|^2.$$

The final periodogram is computed as

$$\hat{\phi}_W(\omega) = \frac{1}{S}\sum_{j=1}^{S}\hat{\phi}_j(\omega).$$

Remark: When the Welch method is applied in this work we have used a Hanning window.

7.3 Related work

In the linear case, estimation with a spectral based ML cost function was presented in (Whittle 1951) and further analyzed in (Hannan 1973). This type of cost function will be evaluated below as one of two different cost functions for nonlinear models. Other approaches to fit linear models based on frequency domain data are presented in (Ljung 1999) and further described in Section 3.3.

7.4 Assumptions

Before we consider the suggested cost functions we state some assumptions.

A.1 *The signal*

It is assumed that the stochastic process $\{y(t)\}$ is weakly stationary and exponentially forgetting of order four. A stochastic process is weakly stationary if there is a constant m and a finite valued function $r(\cdot)$ such that

$$\begin{aligned} Ey(t) &= m \\ E(y(t)-m)(y(s)-m) &= r(t-s), \end{aligned}$$

hence, $r(t-s)$ is only a function of the difference $t-s$. A weakly stationary process is also called a wide sense stationary process. A stochastic process is said to be exponentially forgetting (EF) of order γ if it has a finite memory approximant of order γ. The definition of a finite memory approximant of order γ (Hjalmarsson 1993) is:

Definition 7.1. *A doubly indexed process* $\{z_s^0(t)\}$ *is said to be finite memory approximant of order* γ *to the process* $\{z(t)\}$ *if* $z_s^0(t)$ *is independent of* $\{z(k), k \leq s\}$ *and of* $\{z_l^0(k), l \leq k \leq s\}, z_t^0(t)$ *and*

$$\left\| z(t) - z_s^0(t) \right\|_\gamma \leq C\lambda^{t-s}$$

for $t \geq s$, *where* $C < \infty$ *and* $0 < \lambda < 1$.

Now let

$$H(e^{i\omega}) = \sum_{k=0}^{\infty} h_k e^{-i\omega k}, \quad h_0 = 1,$$

be the minimum phase spectral factor of $\phi_y(\omega)$, i.e.,

$$\phi_y(\omega) = \sigma^2 \left| H(e^{i\omega}) \right|^2, \ \sigma^2 < \infty.$$

Let

$$H^{-1}(e^{i\omega}) = \sum_{k=0}^{\infty} \tilde{h}_k e^{-i\omega k}$$

then the following assumptions are used.

$S1:$ $\phi_y(\omega) > \delta > 0$ for some $\delta > 0$ $\forall \omega$.

$S2:$ $|\tilde{h}_k| < C\lambda^k$, for some $C < \infty$, $0 < \lambda < 1$

Remark 1: Exponentially forgetting implies that $|h_k| < C\lambda^k$ and, hence,

$$\phi_y(\omega) < M \ \forall \ \omega \text{ for some } M < \infty.$$

Remark 2: The condition $|\tilde{h}_k| < C\lambda^k$ implies that the spectrum is uniformly continuous.

A.2 *The model*

The model structure is defined by $\{\phi(\omega, \theta), \theta \in \Theta\}$ where $\phi(\omega, \theta)$ is the spectrum of the output of the model parameterized by θ. It is assumed that $\phi(\omega, \theta)$ can be written as

$$\phi_y(\omega, \theta) = \sigma^2(\theta) \left| H(e^{i\omega}, \theta) \right|^2, \ \sigma^2(\theta) < \infty.$$

where $H(e^{i\omega},\theta)$ is the spectral factor of $\phi(\omega,\theta)$, i.e,

$$H(e^{i\omega},\theta)=\sum_{k=0}^{\infty}h_k(\theta)e^{-i\omega k},\ \ h_0(\theta)=1.$$

The following assumptions are used.

$M1:$ $\{\phi(\omega,\theta),\theta\in\Theta\}$ is an equicontinuous family, i.e,

$$\begin{aligned}&\forall\,\varepsilon>0,\ \exists\,\delta>0\ \text{s.t.}\ \ |\phi(\omega_1,\theta)-\phi(\omega_2,\theta)|<\varepsilon\\&\forall\,\theta\in\Theta,\forall\,\omega_1,\omega_2\ \text{s.t.}\ \ |\omega_1-\omega_2|<\delta\end{aligned}$$

$M2:$ $\sigma^2(\theta)<M,\ \forall\,\theta\in\Theta.$

$M3:$ $|h_k(\theta)|<C\lambda^k$, for some $C<\infty,\ 0<\lambda<1.$

$M4:$ $\phi(\omega,\theta)>\delta>0$ for some $\delta>0$

$M5:$

$$H^{-1}(e^{i\omega},\theta)=\sum_{k=0}^{\infty}\tilde{h}_k(\theta)e^{i\omega k}\ \text{where}$$
$$\left|\tilde{h}_k(\theta)\right|<C\lambda^k,\ C<\infty,\ \ 0<\lambda<1.$$

The following assumptions are also made concerning the derivatives of the model spectrum:

$M6:$ $\phi'_{\theta_i}(\omega,\theta)\ \exists\ \forall\ i,\ \forall\ \omega$

$M7:$ $\phi''_{\theta_{i,j}}(\omega,\theta)\ \exists\ \forall\ i,j,\ \forall\ \omega$

7.4.1 Stationarity

One may wonder under what conditions a nonlinear system generates a weakly stationary output. Weak stationarity is implied by stationarity and as we will argue below, nonlinear systems driven by stationary inputs often generate stationary outputs.

The definition of a stochastic process $\{y(t),t\in T\}$ is a family of random variables indexed by t. If, for any $(t_1,\ldots,t_n)$ the joint distribution of $\{y(t_1+t_0),\ldots,y(t_n+t_0)\}$ does not depend on t_0 the process is said to be stationary or strictly stationary. Examples of stationary signals are given

in (Brillinger 1981). For example, a series of independent identically distributed random variables (white noise) $x(t)$ where $(t = 0, \pm 1, \dots)$ is a stationary time series. Also a moving average process is stationary where

$$y(t) = \sum_u a(t-u)x(u),$$

where the input $x(t)$ is white noise and a is absolutely summable, i.e.,

$$\sum_{u=-\infty}^{\infty} |a(t-u)| < \infty.$$

Other linear examples are also given in (Brillinger 1981) but also functions of stationary time series are covered. If a time series is generated by a time invariant measurable function of another stationary time series, then the generated series is stationary (Brillinger 1981). This includes also nonlinear functions. As an example, Volterra functional expansions are considered in (Brillinger 1981) where it is shown that if $x(t)$ is stationary and

$$\begin{aligned} y(t) =& \sum_{u_1} a_1(t-u_1)x(u_1) + \sum_{u_1}\sum_{u_2} a_2(t-u_1, t-u_2)x(u_1)x(u_2) \\ &+ \sum_{u_1}\sum_{u_2}\sum_{u_3} a_3(t-u_1, t-u_2, t-u_3)x(u_1)x(u_2)x(u_3) + \dots \\ =& \sum_{J=0}^{L} \sum_{u_1,\dots,u_J} a_J(t-u_1, \dots, t-u_J)x(u_1)\dots x(u_J), \end{aligned} \tag{7.5}$$

then $y(t)$ is stationary. In (7.5) $L < \infty$ and a_J is absolutely summable. The solution of nonlinear stochastic difference equations can in some cases be expressed as (7.5). In conclusion, there is a large class of nonlinear models which generates a stationary output when excited with a stationary input.

7.5 The cost functions

Two different cost functions are considered. The first is a weighted least squares type function and the second is an ML based function.

7.5.1 Weighted least squares

The first cost function is based on the spectral difference between the spectrum of the measured data and the spectrum of the model output. It is of a weighted least squares type given by

$$V_{QSD,N}(\theta) = \frac{1}{2N}\sum_{k=1}^{N}(\hat{\phi}_N(\omega_k) - \phi(\omega_k,\theta))^2\frac{1}{\phi^2(\omega_k)}, \tag{7.6}$$

where $\hat{\phi}_N(\omega_k)$ is the periodogram, or equivalently the correlogram, of y based on N samples. The spectrum of the matching model is denoted $\phi(\omega_k,\theta)$. The frequency is $\omega_k = \frac{2\pi k}{N}$ and the model is parameterized by the parameter vector θ. The spectrum of the model output is a smoothed version of the periodogram. The samples of the periodogram are asymptotically uncorrelated and the asymptotic variance is $\phi^2(\omega)$ (Stoica and Moses 1997). Thus, the weighting is chosen as $\frac{1}{\phi^2(\omega_k)}$ which is estimated from a smoothed version of the measured time-series y. The subscript of the cost function $V_{QSD,N}(\theta)$ is an abbreviation for Quadratic Spectral Difference, evaluated for N samples. Note that the subscripts y and $\hat{y}$ used for ϕ in Section 7.1 have been dropped to simplify the notation.

7.5.2 Spectral Maximum Likelihood

Instead of the quadratic cost function in (7.6), an ML based spectral approach for the spectral comparison may be taken. The asymptotic distribution of the periodogram is given by

$$\hat{\phi}_N(\omega) \sim \phi(\omega)\chi_2^2/2 \tag{7.7}$$

where χ_2^2 denotes a chi squared distribution with two degrees of freedom as pointed out in (Brillinger 1981). The probability density function is given by

$$\chi_2^2(x) = \frac{1}{2}e^{-\frac{x}{2}}.$$

According to the relation in (7.7), $2\frac{\hat{\phi}_N(\omega)}{\phi(\omega)}$ is χ_2^2 distributed. Then the likelihood is given by

$$L(\phi,\theta) = \prod_k^N \chi_2^2\left(\frac{\hat{\phi}_N(\omega_k)}{\phi(\omega_k,\theta)}\right)\left|\frac{\partial}{\partial\hat{\phi}_N(\omega_k)}\left(\frac{\hat{\phi}_N(\omega_k)}{\phi(\omega_k,\theta)}\right)\right|$$

and the negative log-likelihood function is,

$$-\log L(\phi,\theta) = \sum_{k}^{N} \left\{ \log 2 + \frac{\hat{\phi}_N(\omega_k)}{\phi(\omega_k,\theta)} + \log \phi(\omega_k,\theta) \right\},$$

where the first term can be omitted for optimization purposes. This results in a negative log-likelihood function that gives a cost function described by

$$V_{SML,N}(\theta) = \frac{1}{N}\sum_{k=1}^{N} \frac{\hat{\phi}_N(\omega_k)}{\phi(\omega_k,\theta)} + \log\{\phi(\omega_k,\theta)\}. \tag{7.8}$$

In (7.8), SML denotes Spectral Maximum Likelihood.

Remark 1: In both (7.6) and (7.8), one component is $\phi(\omega,\theta)$ which usually is not straightforward to calculate, except for linear models. Here, simulated data will be used to get an estimate of this quantity.
Remark 2: The cost function $V_{SML,N}(\theta)$ in (7.8) is of Whittle-type. The novelty lies in that nonlinear models are considered and simulated data is used to calculate the spectrum of such models.
Remark 3: The cost function (7.8) is in general not the negative log-likelihood function for the original data and can thus not be expected to give optimal accuracy.

7.6 Identifiability

For the spectral based methods described in this chapter, the question of identifiability is connected to the relation between the parameters and the generated spectrum. There has to be a one-to-one mapping between the parameters and the spectrum of the model output. Notice that this puts restrictions on the excitation signals as well. The signals typically have to be persistently exciting. For spectral based methods the following definition is useful.

Definition 7.2. *A model set is second order identifiable for an excitation signal e if*

$$\phi(\omega,\theta_1,e) \equiv \phi(\omega,\theta_2,e) \;\; \omega \in [0,\infty) \Rightarrow \theta_1 = \theta_2,$$

where $\phi(\omega,\theta_i,e)$ is the second order spectrum of the output of a model with parameters $\theta = \theta_i$ $(i = 1,2)$.

This condition is somewhat restrictive. As an example, for linear systems it is important that minimum (or non-minimum) phase properties of the system are either known or assumed since the proposed cost functions are based on the second-order statistics. This is the case also for noise models identified with, e.g., prediction error methods based on least-squares criteria.

The question is now how the above identifiability condition can be characterized for nonlinear stochastic models. The approach taken here is to derive identifiability conditions in the correlation domain. Since the spectrum is the Fourier transform of the auto-correlation function (ACF) and it is a one-to-one transformation, identifiability can be studied in the correlation domain.

Let us start by studying an example.

Example 7.1. *Consider the nonlinear static system given by*

$$y(t) = c_1 x(t) + c_2 x^2(t),$$

where $x(t)$ is white Gaussian noise with unit variance. With $r_{yy}(\tau) = E\{y(t)y(t-\tau)\}$, we have that

$$r_{yy}(\tau) = (c_1 \; c_2) \begin{pmatrix} r_{xx}(\tau) & 0 \\ 0 & r_{xx}^2(0) + 2r_{xx}^2(\tau) \end{pmatrix} \begin{pmatrix} c_1 \\ c_2 \end{pmatrix},$$

and by stacking $r_{yy}(0)$ and $r_{yy}(1)$ we get

$$\begin{pmatrix} r_{yy}(0) \\ r_{yy}(1) \end{pmatrix} = \begin{pmatrix} r_{xx}(0) & 0 & 0 & 3r_{xx}^2(0) \\ r_{xx}(1) & 0 & 0 & r_{xx}^2(0) + 2r_{xx}^2(1) \end{pmatrix} \begin{pmatrix} c_1^2 \\ c_1 c_2 \\ c_1 c_2 \\ c_2^2 \end{pmatrix},$$

which can be rewritten as

$$\begin{pmatrix} r_{yy}(0) \\ r_{yy}(1) \end{pmatrix} = \begin{pmatrix} r_{xx}(0) & 3r_{xx}^2(0) \\ r_{xx}(1) & r_{xx}^2(0) + 2r_{xx}^2(1) \end{pmatrix} \begin{pmatrix} c_1^2 \\ c_2^2 \end{pmatrix}. \tag{7.9}$$

Given that we use white Gaussian noise with unit variance as $x(t)$ we get

$$\begin{pmatrix} r_{yy}(0) \\ r_{yy}(1) \end{pmatrix} = \begin{pmatrix} 1 & 3 \\ 0 & 1 \end{pmatrix} \begin{pmatrix} c_1^2 \\ c_2^2 \end{pmatrix},$$

and we note that (7.9) describes a one-to-one relationship between the squared parameters and the ACF since,

$$\det \begin{pmatrix} 1 & 3 \\ 0 & 1 \end{pmatrix} = 1 \neq 0.$$

Hence, the parameters are identifiable provided that the sign of the parameters are known.

From the example above, we see that the second order statistics of the output can in some cases be used to estimate parameters of nonlinear stochastic models.

Let us now consider a more general nonlinear system given by

$$\begin{aligned} y(t) =& c_{11}x_1(t) + c_{12}x_2(t) + \cdots + c_{1r}x_{r_1}(t) + \\ & c_{21}x_1^2(t) + c_{22}x_2^2(t) + \cdots + c_{2r_2}x_{r_2}^2(t) + \ldots \\ & c_{p1}x_1^p(t) + c_{p2}x_2^p(t) + \cdots + c_{pr_p}x_{r_p}^p(t) \\ =& c^T X(t) \end{aligned} \tag{7.10}$$

where

$$\begin{aligned} c &= \begin{pmatrix} c_{11} & c_{12} & \ldots & c_{pr} \end{pmatrix}^T \text{ and} \\ X(t) &= \begin{pmatrix} x_1(t) & x_2(t) & \ldots & x_{r_p}^p(t) \end{pmatrix}^T. \end{aligned}$$

The number of parameters is denoted by q, $(\dim(c) = q \times 1)$. It can be noted that the system description (7.10) is quite general. For example $x_k(t)$ may denote lagged versions of the input (finite impulse response, FIR case), lagged versions of the output (infinite impulse response, IIR case), or functions of the output and the input.

Next it will be derived how the ACF is related to the parameters of (7.10). It will further be shown under what conditions there is a one-to-one relationship between the squared parameters and the ACF. These conditions will be used to ensure that the model is identifiable given the second order statistics of the output. Assuming $y(t)$ to be at least weakly stationary then the second order statistics is given by

$$\begin{aligned} r_{yy}(\tau) &= E\left\{y(t)y^T(t-\tau)\right\} \\ &= c^T E\left\{X(t)X^T(t-\tau)\right\} c \\ &= c^T B(\tau) c. \end{aligned}$$

This can be rewritten as

$$\begin{aligned} r_{yy}(\tau) &= c^T B(\tau) c \\ &= \mathrm{Tr}\left\{c^T B(\tau) c\right\} \\ &= \mathrm{Tr}\left\{cc^T B(\tau)\right\} \\ &= \underbrace{\mathrm{vec}\left(B(\tau)\right)^T}_{b^T(\tau)} \underbrace{\mathrm{vec}\left(cc^T\right)}_{\tilde{c}}, \end{aligned} \tag{7.11}$$

where $\mathrm{Tr}(\cdot)$ denotes the trace operator and the notation $\mathrm{vec}(A)$ refers to a vector formed by stacking the columns of the matrix A. In (7.11) the following properties are used, $\mathrm{Tr}\ (\alpha) = \alpha$ for a scalar α, $\mathrm{Tr}(AB) = \mathrm{Tr}\ (BA)$ for matrices A and B of appropriate dimensions. Also $\mathrm{Tr}\ (AB) = \mathrm{vec}(A^T)^T\ \mathrm{vec}(B)$ and the last equality is shown in e.g., (Brewer 1978). Now, we can stack the results of (7.11) for different values of τ as

$$\begin{pmatrix} r_{yy}(0) \\ r_{yy}(1) \\ \vdots \\ r_{yy}(M-1) \end{pmatrix} = \begin{pmatrix} b^T(0) \\ b^T(1) \\ \vdots \\ b^T(M-1) \end{pmatrix} \tilde{c} \tag{7.12}$$

which is rewritten as

$$\tilde{r} = \tilde{B}\tilde{c}, \tag{7.13}$$

where $\dim(\tilde{r}) = M \times 1$, $\dim(\tilde{B}) = M \times q^2$ and $\dim(\tilde{c}) = q^2 \times 1$. Equation (7.13) describes a relationship between the parameters of (7.10) and the ACF. The question is now if this relationship is unique. Considering the dimensions of the factors in (7.13) it can be noted that the dimension of $\tilde{c}$ is $q^2 \times 1$ while we have only q unknown parameters. First consider the case when it is possible to stack M rows of $\tilde{B}$ as in (7.12) such that $\mathrm{rank}(\tilde{B}) = q^2$, then it is clear that (7.13) can be solved for $\tilde{c}$ and, hence, there is a unique relationship. If, on the other hand, $\mathrm{rank}(\tilde{B}) < q^2$, then there might still be a one-to-one relationship. To analyze this we can study the singular value decomposition of $\tilde{B}$ which gives

$$\begin{aligned} \tilde{B} &= U\Sigma V^T \\ &= \begin{bmatrix} U_1 & U_2 \end{bmatrix} \begin{pmatrix} \Sigma_1 & 0 \\ 0 & 0 \end{pmatrix} \begin{bmatrix} V_1^T \\ V_2^T \end{bmatrix} \\ &= U_1 \Sigma_1 V_1^T, \end{aligned} \tag{7.14}$$

where $\dim(\Sigma_1) = \text{rank}(\tilde{B})$. The result of the mapping $V_1^T\tilde{c}$ is denoted by $\bar{c}$ such that

$$\bar{c} = V_1^T\tilde{c} \tag{7.15}$$

where $\dim(\bar{c}) = \text{rank}(\tilde{B}) \times 1$.

An identifiability criterion can now be formulated considering the following assumptions:

A1. The output $y(t)$ and the sequence $X(t)$ are at least weakly stationary sequences.

A2. The sign of the parameters are known.

Theorem 7.1. *If, under the assumptions A1 and A2, there exists a one-to-one mapping between the original parameter vector c in (7.10) and $\bar{c}$ in (7.15), then there exists a one-to-one mapping between the parameters and the ACF.*

Proof. In (7.13) the relationship between the parameters $\tilde{c}$ and the ACF is given followed by arguments about the condition on the rank of $\tilde{B}$ to certify a unique relationship between the parameters and the ACF. Also, from (7.13), (7.14) and (7.15) we have that

$$\tilde{r} = U_1\Sigma_1\bar{c},$$

hence,

$$\bar{c} = \Sigma_1^{-1}U_1^T\tilde{r},$$

and if there is a one-to-one mapping between $\bar{c}$ and c then there is a one-to-one relationship between the parameters and the ACF. It can finally be noted that a one-to-one mapping implies that $\text{rank}(\tilde{B}) \geq q$. □

It can now be noted that if the system (7.10) satisfies Theorem 7.1 then the system is identifiable from the second order statistics of the observed output $y(t)$.

To check the identifiability condition in practice, the matrix $\tilde{B}$ in (7.13) has to be calculated. Since analytical calculation can be quite cumbersome, a numerical estimate of $\tilde{B}$ can be used. It is important to note that in the cases where $X(t)$ in (7.10) includes lagged versions of the output (IIR-case) then $\tilde{B}$ depends on the parameters. In these cases, recorded output data and realizations of the unknown input signal can

be used to numerically estimate $\tilde{B}$. Another approach is to use simulated output data, based on a sufficiently large set of parameters to estimate $\tilde{B}$.

In addition to the above identifiability condition, the experience of the authors is that the spectral based identification method can be applied to other models than (7.10). This will be further explored in Section 7.9. Below it will be assumed that the model structure is identifiable.

7.7 Convergence

As more and more data is collected the identification method should yield parameter estimates that converge. For the QSD cost function, the convergence result is stated in the following theorem.

Theorem 7.2. *Assuming that Θ is a compact set ($\theta \in \Theta$) and under the assumptions $M1$, $M2$, $M3$, $S1$ and $S2$ (in Section 7.4) then*

$$\hat{\theta}_N \to \theta^* = \arg\min_{\theta\in\Theta} \frac{1}{4\pi} \int_{-\pi}^{\pi} |\phi(\omega) - \phi(\omega,\theta)|^2 \frac{1}{\phi^2(\omega)}\, d\omega$$

for the QSD cost function.

Proof: The proof is given in Appendix D . □

For the SML cost function the convergence result is given in the following theorem.

Theorem 7.3. *Assuming that Θ is a compact set ($\theta \in \Theta$) and under the assumptions $M1$, $M2$, $M3$, $M4$, $M5$, $S1$ and $S2$ (in Section 7.4) then*

$$\hat{\theta}_N \to \theta^* = \arg\min_{\theta\in\Theta} \frac{1}{2\pi} \int_{-\pi}^{\pi} \frac{\phi(\omega)}{\phi(\omega,\theta)} + \log\phi(\omega,\theta)\, d\omega$$

for the SML cost function.

Proof: The proof is given in Appendix D □

In conclusion, assuming that there exists a parameter θ_0 such that the model spectrum perfectly matches the spectrum of y and that the model structure is identifiable, $\theta^* = \theta_0$ for both methods.

7.8 Covariance of the parameter estimates

The parameter estimate is given by

$$\hat{\theta}_N = \arg\min_{\theta} V_N(\theta)$$

where $V_N(\theta)$ is given by (7.6) or (7.8). The normalized covariance matrix $\lim_{N\to\infty} NE\{(\hat{\theta}_N - \theta^*)(\hat{\theta}_N - \theta^*)^T\}$ is given by

$$\lim_{N\to\infty} N[\overline{V}''(\theta^*)]^{-1} E\{V_N'(\theta^*)V_N'(\theta^*)^T\}[\overline{V}''(\theta^*)]^{-1}, \tag{7.16}$$

where the derivatives are taken w.r.t. the parameter vector θ, see (Ljung 1999). In (7.16),

$$\overline{V}''(\theta^*) = \lim_{N\to\infty} V_N''(\hat{\theta}_N),$$

under the assumption that, $\hat{\theta}_N \to \theta^*$ as $N \to \infty$. To calculate the covariance matrix, $V'_{QSD,N}(\theta)$ is first considered,

$$V'_{QSD,N}(\theta) = \frac{1}{N}\sum_{k=0}^{N-1} -\left(\hat{\phi}_N(\omega_k) - \phi(\omega_k,\theta)\right)\frac{\phi'_\theta(\omega_k,\theta)}{\phi^2(\omega_k)}, \tag{7.17}$$

where $\omega_k = \frac{2\pi k}{N}$. Next $V'_{SML,N}(\theta)$ is considered

$$V'_{SML,N}(\theta) = \frac{1}{N}\sum_{k=0}^{N-1} -\left(\hat{\phi}_N(\omega_k) - \phi(\omega_k,\theta)\right)\frac{\phi'_\theta(\omega_k,\theta)}{\phi^2(\omega_k,\theta)}.$$

The expressions for $V'_{SML,N}(\theta)$ and $V'_{QSD,N}(\theta)$ are equal when $\phi(\omega,\theta) = \phi(\omega)$, i.e. when the model matches the true output spectrum perfectly. This suggests that the covariance will asymptotically be the same for the two cost functions. However, the covariance for small N may be different since $V_{QSD,N}(\theta)$ is different from $V_{SML,N}(\theta)$. The weighting used in $V_{QSD,N}(\theta)$ must be a smoothed version of the spectrum computed from the measured data. In the case when N is small this might give different results compared to $V_{SML,N}(\theta)$. This difference will be noted in the numerical examples in Section 7.9. The results are summarized as follows.

Theorem 7.4. *Under the assumptions S1, S2, M4, M6 and M7 (in Section 7.4) and assuming that*

$$\lim_{N\to\infty} \hat{\theta}_N = \theta_0,$$

where $\phi(w,\theta_0) = \phi(w)$. *Then the normalized covariance matrix of the parameter estimates of* $V_{QSD,N}$ *and* $V_{SML,N}$ *is*

$$NE\{(\hat{\theta}_N - \theta_0)(\hat{\theta}_N - \theta_0)^T\} = 2A^{-1} + A^{-1}DA^{-1},$$

asymptotically as $N \to \infty$, *where*

$$A = \frac{1}{2\pi}\int_{-\pi}^{\pi} \frac{\phi'_\theta(\omega,\theta)(\phi'_\theta(\omega,\theta))^T}{\phi^2(\omega)} d\omega \Big|_{\theta=\theta_0}$$

and

$$D = \frac{1}{2\pi}\int_{-\pi}^{\pi}\int_{-\pi}^{\pi} \phi'_\theta(\omega,\theta)(\phi'_\theta(\omega,\theta))^T \phi_4(\omega,-\omega,\mu) \frac{1}{\phi^2(\omega)}\frac{1}{\phi^2(\mu)} d\omega d\mu \Big|_{\theta=\theta_0}$$

where $\phi_4(\omega,-\omega,\mu)$ *denotes the fourth-order cumulant spectrum.*

Proof: See Appendix E where the results of (Chiu 1988) are explored. □

The lower limit of the parameter covariance, also called the Cramér-Rao lower bound (CRLB), is given by

$$N\mathrm{var}(\hat{\theta}) \geq 2A^{-1} = 2\left[\frac{1}{2\pi}\int_{-\pi}^{\pi} \frac{\phi'_\theta(\omega,\theta)(\phi'_\theta(\omega,\theta))^T}{\phi^2(\omega)} d\omega\right]^{-1}$$
$$= 2\left[\frac{1}{2\pi}\int_{-\pi}^{\pi} \frac{d\log\phi(\omega,\theta)}{d\theta}\left(\frac{d\log\phi(\omega,\theta)}{d\theta}\right)^T d\omega\right]^{-1}$$

as derived in, e.g., (Kay 1993) for Gaussian signals. Thus for Gaussian signals the proposed spectral matching methods will reach the Cramér-Rao bound since $D = 0$.

7.9 Numerical examples

Example 1:
First we study a system given by

$$y(t) = c_{11}\sin(y(t-1)) + c_{12}e_1(t) + c_{23}e_2^2(t), \tag{7.18}$$

Cost function	Parameter	θ_0	$mean(\hat{\theta})$	$std(\hat{\theta})$
QSD	c_{11}	1	1.03	0.05
	c_{12}	-1.5	-1.45	0.21
	c_{23}	0.8	0.79	0.02
SML	c_{11}	1	1.04	0.05
	c_{12}	-1.5	-1.46	0.21
	c_{23}	0.8	0.8	0.02

Table 7.1: *Example 1: Estimation results for 100 trials (N=4096).*

where $e_1(t)$ is known and $e_2(t)$ is unknown. Both inputs are white Gaussian noise with zero mean and unit variance. To check identifiability of (7.18), the matrix $\tilde{B}$ in (7.13) is estimated numerically as discussed in Section 7.6. Using $M = 9$ gives that $\tilde{B}$ will have full rank and therefore there is a one-to-one correspondence between the second order statistics of the output and the squared parameters. In other words the model satisfies Theorem 7.1 and is therefore identifiable provided that the sign of the parameters are known. The estimation results are shown in Table 7.1 and they are based on 4096 samples. The results of the two methods are very similar which is partly due to the large number of samples.

Example 2:
In this example we study a part of a ventilation system in a house with a large number of rooms. In particular we study the flow of air into one room. The flow is a function of the control valve setting and the pressure drop over the valve. While the valve setting is known as a measured input, the pressure drop is modeled as an unknown stochastic signal. There are three nonlinear components in the model. An exponential function describes the valve in its range of operation and the air flow is a square root function of the ratio between the pressure drop and the valve setting. There is also a saturation of the air flow, modeled as a sigmoidal function. The saturation function makes inversion impossible and time-domain ML estimation difficult. The air flow model is given by

$$p(t) = -ap(t-1) + (1+a)e(t)$$
$$y(t) = -by(t-1) + S\left[(1+b)\sqrt{\frac{p(t)}{\exp\{\alpha(r(t-1)-100)\}}}\right]$$

Cost function	Parameter	θ_0	$mean(\hat{\theta})$	$std(\hat{\theta})$
QSD	α	0.03	0.03	0.002
	a	-0.7	-0.8	0.1
	b	-0.8	-0.84	0.3
SML	α	0.03	0.029	0.002
	a	-0.7	-0.73	0.2
	b	-0.8	-0.8	0.003

Table 7.2: *Example 2: Estimation results for 100 trials (N=2048).*

where $p(t)$ denotes the pressure and $y(t)$ the air flow. The saturation $S[x]$ is given by

$$S[x] = \frac{1 - e^{-5x}}{1 + e^{-5x}}.$$

The unknown stochastic input, the pressure drop, is denoted by $e(t)$ and the measured input, the valve setting, is denoted by $r(t)$. The parameters to be estimated are $\theta = (\alpha, a, b)^T$. A block diagram of the air flow model is shown in Figure 7.3. The stochastic input was white Gaussian noise with unit variance and mean $m = 10$. The measured input $r(t)$ varies randomly in the range $[0, 100]$ with a uniform distribution. The estimation results of 100 trails are shown in Table 7.2. In this case the identifiability condition in Theorem 7.1 cannot be applied, however, the results are quite satisfying. As also shown by the results, the SML method seems more accurate which might be explained by that the weighting in the QSD method is based on the too few data samples.

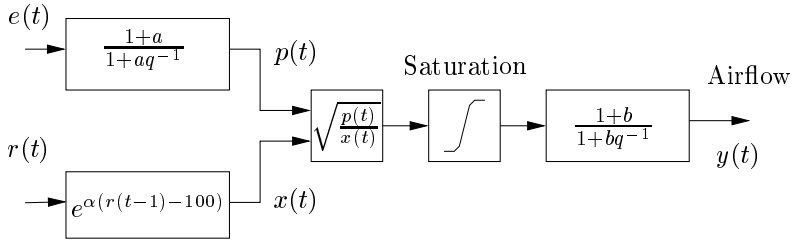

Figure 7.3: A block diagram of the air flow model.

7.10 Higher order statistics

Up to this point, we have only considered second order statistics for the matching. In this section we will take a somewhat heuristic approach to the extension of the previously presented method to higher order statistics. This extension will only include time-series but the matching idea is the same as before, using a similar set up as in Figure 7.2. We suggest that a cost function based on higher order cumulant matching can be used for the parameter estimation instead of only using the second order statistics. In addition, since the estimation of higher order statistics can be numerically cumbersome, cost functions using low-dimensional slices of the cumulant functions are suggested.

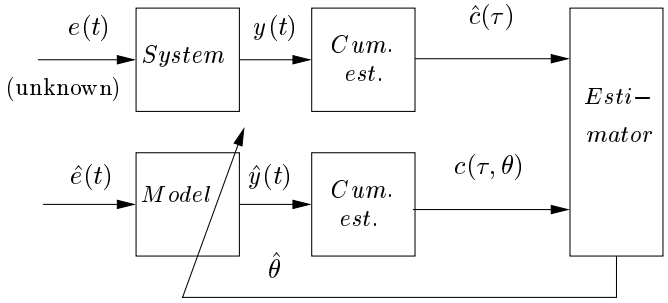

Figure 7.4: Estimation using cumulant comparison.

The method is shown in Figure 7.4 where the measured signal is denoted $y(t)$ and the corresponding estimated cumulants are denoted $\hat{c}(\tau)$. In parallel to the system, a model is simulated using a realization $\hat{e}(t)$ with the assumed PDF of $e(t)$. The output of the model is denoted $\hat{y}(t)$ and the cumulants of the model output are denoted $c(\tau,\theta)$. It should be noted that the number samples of simulated data, used to calculate the cumulants $c(\tau,\theta)$, is independent of the number of recorded samples. In the estimator block in Figure 7.4 a cost function is evaluated and an update of the parameters in the model is computed. In other words the suggested method is estimating the parameters of the model by minimizing the cost function comparing the cumulants of the model and system outputs. In addition to the model parameters, the probability density function (PDF) of the noise source may be parameterized.

Motivation

Higher order statistics can be useful for the analysis of time-series produced by nonlinear systems. It is, e.g., well known that if the input to a linear system is Gaussian then also the output is Gaussian. It is also known that a Gaussian process can be completely described by the first and second order statistics (i.e., mean and autocorrelation). However, nonlinear systems rarely produce outputs with Gaussian statistics, not even when the input is Gaussian. Hence, to describe the statistics of the output of a nonlinear system also higher order statistics, i.e., higher order than two, are motivated from a statistical efficiency, as well as an identifiability, point of view.

Related work

A general introduction to higher order statistics is given in (Nikias and Petropulu 1993) where also the properties and methods for estimation of higher order statistics are given. Identification based on higher order statistics is presented in (Tugnait 1987) for linear models where a cost function based on second and fourth order cumulants is used and the input to the model is considered to be non-Gaussian. In (Lii 1996) the analysis of nonlinear models, and the discrimination between them, are based on cumulant matching. The discrimination between a priori given models is based on stepwise comparing higher and higher orders of the cumulants.

7.10.1 Moments and cumulants of stationary processes

Higher order statistics are often considered in terms of moments and cumulants. For a real random process denoted by $\{y(k)\}$ the moments of order n, denoted m_n are given by

$$m_n(y(k), y(k+\tau_1), \ldots, y(k+\tau_{n-1})) = E\{y(k)y(k+\tau_1)\cdots y(k+\tau_{n-1})\}.$$

If stationarity is assumed this implies that the moments will only depend on the time differences denoted by τ_i $(i = 1, \ldots, n-1)$. Hence, the moments, denoted by $m_n(\tau_1, \tau_2, \ldots, \tau_{n-1})$ are given by

$$m_n(\tau_1, \tau_2, \ldots, \tau_{n-1}) = E\{y(k)y(k+\tau_1)\cdots y(k+\tau_{n-1})\}.$$

Cumulants are usually preferred when analyzing stochastic processes. One of the reasons being that cumulants of two independent stationary random processes is the sum of their individual cumulants. Another reason is that if the process is Gaussian then the cumulants of order higher than two are zero. In combination these two arguments gives that additive Gaussian measurement noise does not have an impact on cumulants of order higher than two (Mendel 1991).

The cumulants will be denoted $c_n(\tau_1, \tau_2, \ldots, \tau_{n-1})$, where n is the order of the cumulant. There are certain relationships between the moments and the cumulants, and for a zero mean process these relationships are given by

$$\begin{aligned} c_1 &= m_1 = 0 \\ c_2(\tau) &= m_2(\tau) \\ c_3(\tau_1, \tau_2) &= m_3(\tau_1, \tau_2) \\ c_4(\tau_1, \tau_2, \tau_3) &= m_4(\tau_1, \tau_2, \tau_3) - m_2(\tau_1)m_2(\tau_3 - \tau_2) \\ &\quad - m_2(\tau_2)m_2(\tau_3 - \tau_1) - m_2(\tau_3)m_2(\tau_2 - \tau_1). \end{aligned}$$

A notable property of cumulants is that symmetric distributions only are represented by the even orders of the cumulants, see (Nikias and Petropulu 1993) for further properties.

7.10.2 Cost function

The suggested cost function is given by

$$V(\theta) = \sum_{i=2}^{M} \lambda_i \sum_{\tau \in \bar{L}_i} \tilde{c}_i^2(\tau, \theta) \tag{7.19}$$

where $\bar{L}_i$ denotes the summation region, given by

$$\begin{aligned} \bar{L}_i = \{ & -L_i \leq \tau_1 \leq 0 \\ & \tau_1 \leq \tau_2 \leq 0 \\ & \ldots \\ & \tau_{i-2} \leq \tau_{i-1} \leq 0\}, \end{aligned}$$

for an integer constant L_i. The summation region is chosen as above due to the symmetry regions of the cumulants. The notation $\tau = \{\tau_1, \tau_2, \ldots, \tau_{i-1}\}$ will also be used and finally

$$\tilde{c}_i = \hat{c}_i(\tau) - c_i(\tau, \theta), \quad \forall \tau \in \bar{L}_i. \tag{7.20}$$

In (7.20), $\hat{c}_i(\tau)$ are the estimated cumulants of the recorded data and $c_i(\tau, \theta)$ are the cumulants obtained from the simulated data. For example, using the second and third order cumulants, the cost function is given by

$$V(\theta) = \lambda_2 \sum_{\tau=-L_2}^{0} \tilde{c}_2^2(\tau, \theta) + \lambda_3 \sum_{\tau_1=-L_3}^{0} \sum_{\tau_2=\tau_1}^{0} \tilde{c}_3^2(\tau_1, \tau_2, \theta)$$

where

$$\tilde{c}_2(\tau) = \hat{c}_2(\tau) - c_2(\tau, \theta)$$
$$\tilde{c}_4(\tau_1, \tau_2) = \hat{c}_3(\tau_1, \tau_2) - c_3(\tau_1, \tau_2, \theta).$$

Thus the weights λ_2 and λ_3 (or at least their ratio) and the integers $L_{2,3}$ has to be chosen by the user.

Remark: The cost function in (7.19) is a general form of the cost function suggested in (Tugnait 1987) for the estimation of linear models using second and fourth order cumulants given by

$$V(\theta) = \sum_{\tau=-L_2}^{0} \tilde{c}_2^2(\tau, \theta) + \lambda \sum_{\tau_1=-L_4}^{0} \sum_{\tau_2=\tau_1}^{0} \sum_{\tau_3=\tau_2}^{0} \tilde{c}_4^2(\tau_1, \tau_2, \tau_3, \theta). \qquad (7.21)$$

This cost function is suitable for the case when the distribution is symmetric since then cumulants of odd orders are zero. The choice of λ is suggested in (Tugnait 1987), as

$$\lambda = \lambda_0 \frac{\sum_{\tau=-L_2}^{0} \hat{c}_2^2(\tau)}{\sum_{\tau_1=-L_4}^{0} \sum_{\tau_2=\tau_1}^{0} \sum_{\tau_3=\tau_2}^{0} \hat{c}_4^2(\tau_1, \tau_2, \tau_3)}.$$

In this case the parameters λ_0, and the summation region L_2, L_4 must be chosen by the user. In (Tugnait 1987) it is shown that choosing L_2 and L_2 to be twice the model order gives consistent estimates in the linear case. In the nonlinear case, a possible way to obtain guidance in the choice of these parameters can be retrieved from estimation trials with known parameters. This will be considered in the numerical examples in Section 7.10.4.

7.10.3 Reduced cost function

To reduce the computational burden in the estimation of the cumulants, a cost function based on slices of the cumulants can be used. A slice of a cumulant can be constructed using a reduced number of dimensions of the cumulant, e.g., $c_3(\tau_1, \tau_2 = 0)$. One dimensional slices of the cumulants are used in the identification of linear systems (Mendel 1991).

7.10.4 Numerical examples - HOS

We will study three different cost functions. First a cost function based on second and third order cumulants will be used. Next, two cost functions, based on the second and fourth order cumulants, will be studied. One is the complete version and the other is a reduced version, using slices of cumulants.

Example 3:
In this example the model is given by

$$y(t) = -0.5y(t-1) + ay(t-1)e(t-1)^3 + be(t-1)^2e(t-2), \quad (7.22)$$

where a and b are the unknown parameters. The input e is a stochastic zero mean input which is based on a mixed Gaussian PDF given by

$$p_x(x,\rho) = (1-\rho)p_1(x) + \rho p_2(x).$$

The PDF p_i is given by

$$p_i(x) = \frac{1}{\sqrt{2\pi\sigma_i^2}} e^{-\frac{1}{2\sigma_i^2}(x-m_i)^2}, \quad (7.23)$$

where in this example $\sigma_i = 1$ for $i = 1, 2$ and $m_1 = 10$, $m_2 = -1$ and $\rho = 0.5$. The input $e(t)$ is taken as $e(t) = x(t) - m_x$ where m_x is the sample mean of $x(t)$. For the cost function the parameter λ was chosen as

$$\lambda = \lambda_0 \frac{\sum_{\tau=-L_2}^{0} \hat{c}_2^2(\tau)}{\sum_{\tau_1=-L_3}^{0} \sum_{\tau_2=\tau_1}^{0} \hat{c}_3^2(\tau_1,\tau_2)}.$$

The parameters λ_0, L_2 and L_3 were chosen by testing the estimation procedure for different values and considering the variance of the estimates. In this case we used $\lambda_0 = 0.1$ and $L_2 = L_3 = 10$. The results of the estimation procedure are shown in Table 7.3.

Although the resulting estimates are close to their actual values the disadvantage of this method is the tuning of the parameters λ_0 and L_2 and L_3. Even if it is possible to simulate data and study the relation between the these parameters and the estimates an exhaustive study can be quite time-consuming. Theoretical results the choice of λ_0 and $L_{2,3}$ would therefore be desired although not further studied here.

Parameter	θ_0	$mean(\hat{\theta})$	$std(\hat{\theta})$
a	0.5	0.48	0.05
b	1	1.03	0.12

Table 7.3: *Estimation results for Example 3 (N=2000) 100 trials.*

Example 4:
In this example the complete cost function in (7.21) will be used as well as a reduced cost function. The reduced cost function is given by

$$V(\theta) = \sum_{\tau=-L_2}^{0} \tilde{c}_2^2(\tau,\theta) + \lambda \sum_{\tau_1=-L_4}^{0} \sum_{\tau_2=\tau_1}^{0} \tilde{c}_{4,r}^2(\tau_1,\tau_2,\theta) \tag{7.24}$$

where $\tilde{c}_2(\tau,\theta)$ and $\tilde{c}_4(\tau_1,\tau_2,0)$ are defined as

$$\tilde{c}_2(\tau,\theta) = \hat{c}_2(\tau) - c_2(\tau,\theta)$$
$$\tilde{c}_{4,r}(\tau_1,\tau_2,\theta) = \hat{c}_4(\tau_1,\tau_2,0) - c_4(\tau_1,\tau_2,0,\theta).$$

In this case the model is given by

$$x(t+1) = -ax(t) + e(t+1) + be(t)$$
$$y(t) = x(t) + cw(t)e^{-de(t)^2}$$

where $e(t)$ and $y(t)$ denotes the input and the output, respectively. The parameters, denoted a, b, c, d, are estimated using the two cost functions given above. The stochastic input is a, zero mean, mixed Gaussian signal generated as in the previous example with the parameters $\sigma_i = 1$ for $i = 1, 2$, $m_1 = 5$, $m_2 = -5$ and $\rho = 0.5$.

In this case the computation of the complete cost function is approximately 20 times slower than the computation of the reduced cost function, the estimation results are however very similar.

The numerical examples shown here indicate that higher order statistics can be applied in the matching procedure presented in this chapter. It should be noted that further work remains before the parameters λ and L_i can be chosen efficiently.

7.11 Summary

In this chapter it has been shown that spectral based cost functions can be applied for parameter estimation in nonlinear models. Conditions for

Parameter	θ_0	Complete cost (7.21)		Reduced cost (7.24)	
		$mean(\hat{\theta})$	$std(\hat{\theta})$	$mean(\hat{\theta})$	$std(\hat{\theta})$
a	0.9	0.9	0.02	0.89	0.04
b	0.6	0.6	0.05	0.6	0.07
c	0.7	0.71	0.18	0.69	0.23
d	0.2	0.2	0.15	0.23	0.14

Table 7.4: *Estimation results for Example 4 (N=1024) 100 trials.*

identifiability are also derived for a class of nonlinear models.

Two cost functions were suggested where a weighted least squares function was compared towards a spectral based maximum likelihood function. The statistical properties of the cost functions were shown to be asymptotically identical. However, the spectral based maximum likelihood function appears to perform better when applied to short data sequences. Although a spectral based method can be computationally burdensome, one advantage of the method is that it is easy to implement. Another advantage is that spectral matching can be applied to nonlinear models with several inputs. In the latter case time-domain ML estimation based on inversion is difficult to implement.

A heuristic approach to a cost function based on higher order statistics was also taken in this chapter. A cost function based on cumulant matching was suggested and studied by numerical examples.

Chapter 8

Summary and suggestions for future work

In this thesis we have considered different problems related to control and identification of nonlinear systems. Inversion of nonlinear systems and models plays, as the title suggests, an important part in both cases.

Chapters 1 - 3 - Introduction and Background

The Chapters 1 - 3 provide introduction and background to the different areas of this thesis. A general introduction is presented in Chapter 1 where also links between the different areas are presented. Chapter 1 also includes an overview of the main contributions. Inversion of linear and nonlinear systems are introduced in Chapter 2 where special attention is given to the stability of the inverse of non-minimum phase systems. A background to parameter estimation methods such as prediction error and maximum likelihood estimation is presented in Chapter 3.

Chapter 4 - Feedback inversion

Feedback inversion is used in Chapter 4 for the purpose of parameter estimation. The suggested approach is especially suited for simulation software such as e.g., Matlab/Simulink or Matrix$_X$/Systembuild where

the feedback structure is easily implemented and a solver of numerical equations is utilized. The conditions for when the inversion can be applied are formulated as stability conditions of a linear time varying system. It is further shown that using the feedback configuration, inversion can be done without involving an equation solver if the model can be partitioned as a linear part in parallel with a nonlinear part where the time-delay in the nonlinear part is larger than in the linear part. Another benefit of the feedback structure is that the computation of the derivatives, used for the optimization of the cost function, can be implemented as a linear time-varying filter. This further simplifies the implementation for parameter estimation.

The advantage of applying this method is that there is no need for prior calculations to rewrite the model equations on a special form suitable for inversion, e.g., the normal form presented in Chapter 2. On the other hand, a disadvantage can be that the computational speed is slower compared to using methods based on prior calculations.

Chapter 5 - Iterative learning control

Iterative learning control (ILC) can be applied to control of systems performing the same desired output over and over again. By considering the control error at one iteration the control is improved in the next iteration. It is important to note that the bottom line of ILC is inversion of the system, i.e., the input corresponding to a specific output is obtained if the method converges. In Chapter 5 the ILC algorithm is considered and the role of the design variables are highlighted. It is also shown that ILC can be placed in the realm of numerical optimization and conditions are presented for convergence of ILC for non-linear systems. The conditions are very close in spirit to the necessary and sufficient conditions that previously have been derived for linear systems. The analysis also shows that a relative model error of up to 100% can be tolerated, even when perfect tracking is desired. This is probably one of the reasons for the success of ILC in applications. The benefits of non-causal filtering for non-minimum phase systems has been elaborated upon and the implementational aspects of this covered.

Suggestions for future work are:

- Further analysis of the convergence for iteratively updated inverse models, hence, when a new model is estimated (and inverted) based

on data from more than the first iteration.

- The choice of design variables in the case of measurement noise.
- Further application of ILC to parameter estimation in nonlinear systems, especially for non-minimum phase systems.
- Application of non-causal filtering for non-minimum phase system when applying higher-order ILC algorithms. The main idea with higher-order ILC algorithms is to use control errors from more than one previous ILC iteration.
- The idea of adaptively choosing the linear model to reflect the magnitude of the tracking error was suggested in the case of Wiener and Hammerstein systems. This can be expanded to more general systems.

Chapter 6 - Identification of nonlinear systems by linear models for control

In Chapter 6 it is shown that it is possible to use a linear, model based, control design on nonlinear systems, under certain circumstances. A method is also suggested for how to identify a model that is suited for the model based control design. The identification procedure is based on the inversion of the system and two ways of obtaining the inverse are suggested. It can be noted that these methods are experiment design methods where the input is designed and the obtained data is further used for identification. An iterative method based on ILC is found to perform better than a single-shot method based on an approximative inverse.

Suggestions for future work are:

- Noise sensitivity and robustness are two main issues that needs to be studied further.
- To gain insight in the applicability of the method further numerical examples can be studied.

Chapter 7 - Spectral matching for parameter estimation

Maximum likelihood estimation based on inversion is one of the topics of this thesis. However, inversion based parameter estimation can be complicated to implement in some cases. In this part of the thesis it is shown that spectral based cost functions can be used in parameter estimation in nonlinear models. Conditions for identifiability are also derived for a class of nonlinear models. Two cost functions are suggested, a weighted least squares function was compared to a spectral based maximum likelihood function. The statistical properties of the cost functions are shown to be asymptotically identical. Although the spectral based methods presented here can be computationally burdensome, one advantage is that they are easy to implement. Another advantage is that spectral matching can be applied to nonlinear models with both known and unknown inputs.

Suggestions for future work on spectral matching are:

- Generalization of the identifiability conditions.
- Implementation of numerically efficient optimization routines including a study of possible ways to obtain easily computed gradients.

As a final part of Chapter 7, a heuristic approach is taken based on higher order statistics. A cost function based on cumulant matching was suggested and studied by numerical examples.

A lot of work remains to be done in the area of matching higher order statistics for parameter estimation and some of the suggestions are:

- A theoretical analysis of the convergence and the covariance of the parameter estimates.
- Identifiability, at least for some class of nonlinear systems.
- Methods to reduce the computational costs, e.g., an easily studied criterion for how to choose the slices used by the suggested reduced cost function.

Appendix A

Maximum likelihood estimation

Derivation of (3.13)

In Chapter 3, the PDF $p_y(y^N;\theta)$ is given by (3.13) which is derived in (Jazwinski 1970). The proof is restated below.

Let us first assume that the initial conditions of the inverse are the same as for the forward system. Further assume that $\theta = \theta_0$ and the notation of θ is further dropped to ease the notation. Thus, we have

$$y^N = P_N(e^N),$$

and

$$e^N = P_N^{-1}(y^N).$$

The distribution function $F_e(x)$ is defined such that

$$F_e(x) \triangleq \Pr\{e \leq x\}$$

where Pr denotes probability. Thus

$$F_e(x) = \int_{-\infty}^{x} p_e(e)de,$$

where $p_e(\cdot)$ is the PDF of e. Let S denote a set $S \in \mathbb{R}^N$ and note that

$$\Pr\{y^N \in S\} = \Pr\{P_N(e^N) \in S\} = \Pr\{e^N \in P_N^{-1}(S)\}.$$

But

$$\begin{aligned}\Pr\{e^N \in P_N^{-1}(S)\} &= \int_{P_N^{-1}(S)} p_e(e^N) de^N \\ &= \int_S p_e(P_N^{-1}(y^N)) \left\| \frac{dP_N^{-1}(y^N)}{dy^N} \right\| dy^N\end{aligned}$$

where the last equality follows from the transformation of variables in the integral.

Recall (3.11) and (3.12) for the case $\theta \neq \theta_0$ and different initial conditions. Then, assuming that the PDF of w^N is p_e it follows that $p_y(\cdot)$ can be computed as

$$p_y(y^N;\theta) = p_e(W_N(y^N,\theta);\theta) \left\| \frac{dW_N(y^N,\theta)}{dy^N} \right\|,$$

where $p_e(\cdot)$ is the PDF of the white disturbance input $e(t)$ and $\|\cdot\|$ denotes the absolute value of the determinant. See (Jazwinski 1970) for further details.

Appendix B

Feedback inverse

In this appendix some of the derivatives in Section 4.4 are derived. The derivatives are to be used for optimizing the ML criterion in Chapter 4. The proof of Theorem 4.1 also follows below.

Derivation of $\frac{\partial w(t)}{\partial \theta_k}$

To compute $\frac{\partial w(t)}{\partial \theta_k}$ we start with

$$\begin{aligned} w(t) &= L^{-1}(q^{-1},\theta)\varepsilon(t) \\ &= L^{-1}(q^{-1},\theta)\left(y(t) - r(t)\right), \end{aligned}$$

from figure 4.4. Hence, we can calculate $\frac{\partial w(t)}{\partial \theta_k}$ as

$$\begin{aligned} \frac{\partial w(t)}{\partial \theta_k} &= \frac{\partial L^{-1}(q^{-1},\theta)}{\partial \theta_k}\varepsilon(t) + L^{-1}(q^{-1},\theta)\frac{\partial \varepsilon(t)}{\partial \theta_k} \\ &= \frac{\partial L^{-1}(q^{-1},\theta)}{\partial \theta_k}\varepsilon(t) - L^{-1}(q^{-1},\theta)\frac{\partial r(t)}{\partial \theta_k}, \end{aligned} \tag{B.1}$$

since $y(t)$ does not depend on the parameters of the inverse model. The first term of (B.1) is represented by a separate block with $\varepsilon(t)$ as an input. The second term includes $\frac{\partial r(t)}{\partial \theta_k}$ which is obtained from (4.17). The system in (4.17) can be interpreted as a linear time-varying system with $\frac{\partial z(t+1)}{\partial \theta_k}$ as states, $\frac{\partial w(t)}{\partial \theta_k}$ as the input and $\frac{\partial r(t)}{\partial \theta_k}$ being the output. The terms $\frac{\partial h}{\partial \theta_k}$ and $\frac{\partial f}{\partial \theta_k}$ can also be seen as inputs to the LTV system, calculated using $w(t)$ and $z(t)$.

Derivation of $\frac{\partial w(t)}{\partial y(t)}$ and $\frac{\partial}{\partial \theta_k}\left(\frac{\partial w(t)}{\partial y(t)}\right)$

If the second term of the cost function (3.16) is nonzero we also have to calculate $\frac{\partial w(t)}{\partial y(t)}$ and $\frac{\partial}{\partial \theta_k}\left(\frac{\partial w(t)}{\partial y(t)}\right)$. In order to be able to give an expression for $\frac{\partial w(t)}{\partial y(t)}$ we have to specify the structure of $L(q^{-1},\theta)$. We assume that $L(q^{-1},\theta)$ is described by a rational transfer function as

$$L(q^{-1},\theta) = \frac{1 + b_1 q^{-1} + b_2 q^{-2} + ... + b_n q^{-n}}{1 + a_1 q^{-1} + a_2 q^{-2} + ... + a_n q^{-n}} = \frac{B(q)}{A(q)}. \tag{B.2}$$

To compute the derivative $\frac{\partial w(t)}{\partial y(t)}$ we start by considering

$$w(t) = L^{-1}(q^{-1},\theta)(y(t) - r(t)).$$

Since we assume that $L(q^{-1},\theta)$ is given by (B.2) we get

$$\begin{aligned}\frac{\partial w(t)}{\partial y(t)} &= \frac{\partial}{\partial y(t)}\left(y(t) - r(t)\right) \\ &= 1 - \frac{\partial h}{\partial y(t)} \\ &= 1 - \frac{\partial h}{\partial w(t)}\frac{\partial w(t)}{\partial y(t)},\end{aligned} \tag{B.3}$$

where

$$\frac{\partial h}{\partial w(t)} = \left.\frac{\partial h(z(t), w(t), t)}{\partial w(t)}\right|_{\substack{z(t)=z(t)\\ w(t)=w(t)}}. \tag{B.4}$$

In (B.3) the first term 1 comes from the assumption of monic polynomials in $L(q^{-1},\theta)$ and the second term is due to the fact that $r(t)$ depends on $y(t)$ via $L^{-1}(q^{-1},\theta)$ and $N(\theta,t)$. Notice that the second term is zero if there is a time delay in $N(\theta,t)$. It follows from (B.3) that

$$\frac{\partial w(t)}{\partial y(t)} = \left(1 + \frac{\partial h}{\partial w(t)}\right)^{-1}, \tag{B.5}$$

where $\frac{\partial h}{\partial w(t)}$ is given by (B.4).

Finally, for the optimization we need

$$\frac{\partial}{\partial \theta_k}\left(\frac{\partial w(t)}{\partial y(t)}\right) = -\left(1 + \frac{\partial h}{\partial w(t)}\right)^{-2}\frac{\partial}{\partial \theta_k}\left(\frac{\partial h}{\partial w(t)}\right), \tag{B.6}$$

where $\frac{\partial h}{\partial w(t)}$ is given by (B.4).

Proof of Theorem 4.1

We start with

$$\begin{aligned}\varepsilon(t) &= y(t) - r(t)\\ &= y(t) - h(z(t), t)\end{aligned}$$

such that

$$\xi(t+1) = (A - BD^{-1}C)\xi(t) + BD^{-1}(y(t) - h(z(t), t)).$$

Thus, the difference between $\zeta(t+1)$ and $\xi(t+1)$ can be written as

$$\rho(t+1) = \zeta(t+1) - \xi(t+1) = (A - BD^{-1}C)\rho(t) - BD^{-1}\sigma(t). \quad \text{(B.7)}$$

Denote the right-hand side of (B.7) by Σ

$$\rho(t+1) = \Sigma(\rho(t), \sigma(t)). \quad \text{(B.8)}$$

Also,

$$\begin{aligned}\varepsilon(t) &= y(t) - h(z(t), t)\\ &= C\zeta(t) + De(t) + h(x(t), t) - h(z(t), t),\end{aligned} \quad \text{(B.9)}$$

and by inserting (B.9) into the equation for $w(t)$ in (4.19) we get

$$w(t) = e(t) + D^{-1}C\rho(t) + D^{-1}\sigma(t)$$

and the difference becomes

$$\delta(t) = w(t) - e(t) = D^{-1}C\rho(t) + D^{-1}\sigma(t). \quad \text{(B.10)}$$

The right-hand side of (B.10) will be denoted Π, thus

$$\delta(t) = \Pi(\rho(t), \sigma(t)). \quad \text{(B.11)}$$

The difference $\Delta(t)$ (4.25) is a nonlinear function which can be expanded by a Taylor expansion. The expansion is based on the derivatives evaluated at $x(t)$ and $e(t)$,

$$\begin{aligned}\Delta(t+1) &= z(t+1) - x(t+1) = f(z(t), w(t), t) - f(x(t), e(t), t)\\ &= f(x(t), e(t), t) - f(x(t), e(t), t) + \frac{\partial f}{\partial z(t)}\,\Delta(t) + \frac{\partial f}{\partial w(t)}\,\delta(t)\\ &\quad + \text{H.O.T. of } (\Delta(t) \text{ and } \delta(t))\\ &= \Gamma(\Delta(t), \delta(t), t),\end{aligned} \quad \text{(B.12)}$$

where

$$\frac{\partial f}{\partial z(t)} = \left.\frac{\partial f(z(t), w(t), t)}{\partial z(t)}\right|_{\substack{z(t)=x(t)\\ w(t)=e(t)}}$$
$$\frac{\partial f}{\partial w(t)} = \left.\frac{\partial f(z(t), w(t), t)}{\partial w(t)}\right|_{\substack{z(t)=x(t)\\ w(t)=e(t)}}.$$

Above H.O.T. denotes higher order terms. The time dependence in (B.12) reflects the fact that the system is linearized along the trajectory $x(t)$ and $e(t)$.

The difference $\sigma(t)$ can be treated the same way as $\Delta(t)$ using an expansion of the function h at each iteration. We get

$$\begin{aligned}\sigma(t) &= s(t) - r(t) = h(z(t), w(t), t) - h(x(t), e(t), t)\\ &= h(x(t), e(t), t) - h(x(t), e(t), t) - \frac{\partial h}{\partial z(t)}\,\Delta(t) - \frac{\partial h}{\partial w(t)}\,\delta(t)\\ &+ \text{H.O.T. of } (\Delta(t) \text{ and } \delta(t))\\ &= \Phi(\Delta(t), \delta(t), \end{aligned} \tag{B.13}$$

where

$$\frac{\partial h}{\partial z(t)} = \left.\frac{\partial h(z(t), w(t), t)}{\partial z(t)}\right|_{\substack{z(t)=x(t)\\ w(t)=e(t)}}$$
$$\frac{\partial h}{\partial w(t)} = \left.\frac{\partial h(z(t), w(t), t)}{\partial w(t)}\right|_{\substack{z(t)=x(t)\\ w(t)=e(t)}}.$$

According to (B.11) and (B.13) we can write $\delta(t)$ and $\sigma(t)$ as functions of $\Delta(t)$ and $\rho(t)$ as

$$\sigma(t) = \Phi(\Delta(t), \Pi(\Delta(t), \rho(t)), t) \tag{B.14}$$
$$\delta(t) = \Pi(\rho(t), \sigma(t), t) \tag{B.15}$$

and by inserting (B.14) and (B.15) into (B.12) and (B.8) we get

$$\Delta(t+1) = \Gamma(\Delta(t), \Pi(\Delta(t), \rho(t)), t) \tag{B.16}$$
$$\rho(t+1) = \Sigma(\rho(t), \Phi(\Delta(t), \Pi(\Delta(t), \rho(t))), t). \tag{B.17}$$

This is a system which has no exciting term, only started at $t = 0$ with the nonzero initial conditions represented by nonzero differences: $(\zeta_0 - \xi_0,$

$s_0 - r_0$, $w_0 - e_0$, $z_0 - x_0$). Clearly, we want the differences, due to unknown initial conditions, to vanish. Thus we want the origin $\mathbf{0}$ to be a stable equilibrium of the system (B.16) and (B.17). To tackle the stability analysis of (B.16) and (B.17) we can linearize the system around the equilibrium $\mathbf{0}$. If the linearized system has a uniformly asymptotically stable equilibrium at the origin, then the nonlinear system is uniformly asymptotically stable at the origin, (Vidyasagar 1993, (5.9.42) p. 268).

The linearized system is described by

$$\begin{aligned}\Delta(t+1) &= \Gamma^{\Delta}(t)\Delta(t) + \Gamma^{\rho}(t)\rho(t)\\ \rho(t+1) &= \Sigma^{\Delta}(t)\Delta(t) + \Sigma^{\rho}(t)\rho(t)\end{aligned}$$

where

$$\begin{aligned}\Gamma^{\Delta}(t) &= \frac{\partial \Gamma}{\partial \Delta(t)} + \frac{\partial \Gamma}{\partial \Pi}\left(\frac{\partial \Pi}{\partial \Delta(t)} + \frac{\partial \Pi}{\partial \rho(t)}\frac{\partial \rho(t)}{\partial \Delta(t)}\right) \qquad \text{(B.18)}\\ \Gamma^{\rho}(t) &= \frac{\partial \Gamma}{\partial \Pi}\left(\frac{\partial \Pi}{\partial \rho(t)} + \frac{\partial \Pi}{\partial \Delta(t)}\frac{\partial \Delta(t)}{\partial \rho(t)}\right)\\ \Sigma^{\Delta}(t) &= \frac{\partial \Sigma}{\partial \Phi}\left(\frac{\partial \Phi}{\partial \Delta(t)} + \frac{\partial \Phi}{\partial \Pi}\left(\frac{\partial \Pi}{\partial \Delta(t)} + \frac{\partial \Pi}{\partial \rho(t)}\frac{\partial \rho(t)}{\partial \Delta(t)}\right)\right)\\ \Sigma^{\rho}(t) &= \frac{\partial \Sigma}{\partial \rho(t)} + \frac{\partial \Sigma}{\partial \Phi}\frac{\partial \Phi}{\partial \Pi}\left(\frac{\partial \Pi}{\partial \rho(t)} + \frac{\partial \Pi}{\partial \Delta(t)}\frac{\partial \Delta(t)}{\partial \rho(t)}\right) \qquad \text{(B.19)}\end{aligned}$$

with all derivatives with respect to $\Delta(t)$ and $\rho(t)$ evaluated at $\Delta(t) = 0$ and $\rho(t) = 0$. The derivatives in (B.18) to (B.19) are, when evaluated in

$\Delta = 0$ and $\rho = 0$,

$$\frac{\partial \Gamma}{\partial \Delta(t)} = \left.\frac{\partial f(t)(z(t), w(t))}{\partial z(t)}\right|_{\substack{z(t)=x(t) \\ w(t)=e(t)}} \tag{B.20}$$

$$\frac{\partial \Gamma}{\partial \Pi} = \left.\frac{\partial f(z(t), w(t), t)}{\partial w(t)}\right|_{\substack{z(t)=x(t) \\ w(t)=e(t)}} \tag{B.21}$$

$$\begin{aligned}\frac{\partial \Pi}{\partial \Delta(t)} &= -D^{-1} \left.\frac{\partial h(z(t), w(t), t)}{\partial z(t)}\right|_{\substack{z(t)=x(t) \\ w(t)=e(t)}} \\ &\quad \times \left(1 + D^{-1} \left.\frac{\partial h(z(t), w(t), t)}{\partial w(t)}\right|_{\substack{z(t)=x(t) \\ w(t)=e(t)}}\right)^{-1}\end{aligned} \tag{B.22}$$

$$\frac{\partial \rho(t)}{\partial \Delta(t)} = 0 \tag{B.23}$$

$$\frac{\partial \Delta(t)}{\partial \rho(t)} = 0 \tag{B.24}$$

$$\frac{\partial \Phi}{\partial \Delta(t)} = -\left.\frac{\partial h(z(t), w(t), t)}{\partial z(t)}\right|_{\substack{z(t)=x(t) \\ w(t)=e(t)}} \tag{B.25}$$

$$\frac{\partial \Phi}{\partial \Pi} = -\left.\frac{\partial h(z(t), w(t), t)}{\partial w(t)}\right|_{\substack{z(t)=x(t) \\ w(t)=e(t)}} \tag{B.26}$$

$$\frac{\partial \Pi}{\partial \rho(t)} = D^{-1}C \left(1 + D^{-1} \left.\frac{\partial h(z(t), w(t), t)}{\partial w(t)}\right|_{\substack{z(t)=x(t) \\ w(t)=e(t)}}\right)^{-1} \tag{B.27}$$

$$\frac{\partial \Sigma}{\partial \rho(t)} = A - BD^{-1}C \tag{B.28}$$

$$\frac{\partial \Sigma}{\partial \Phi} = -BD^{-1} \tag{B.29}$$

Finally by inserting (B.20) to (B.29) into (B.18) to (B.19) we get (4.27) to (4.30).

Appendix C

Proof of theorems in Chapter 6.

Proof of Theorem 6.1

To prove the only if part it is assumed that $y^* = y_d$ which according to (6.4) and (6.5) implies

$$u^* = u_d. \tag{C.1}$$

The input $u^*(t)$ can be written

$$\begin{aligned} u^*(t) &= C^*(r(t) - y^*(t)) = C^*(r(t) - y_d(t)) \\ &= C^* S\ r(t) \end{aligned}$$

and recall that

$$C^* = \frac{T}{G^*(1-T)} \Rightarrow T = G^* C^* S$$

which means that we may write the desired output y_d as

$$\begin{aligned} y_d(t) &= T\ r(t) = G^*\ C^* S\ r(t) \\ &= G^*\ u^*(t) \end{aligned} \tag{C.2}$$

Hence, (C.1) and (C.2) give that

$$y_d(t) = G^*\ u_d(t) \tag{C.3}$$

and the only if part of the theorem is proved.

Turning to the if part, $y_d(t) = G^*(q)u_d(t)$ imply, using (6.14) that

$$u_d(t) = C^*(r(t) - y_d(t)) \tag{C.4}$$

Equation (C.4) together with (6.4) and (6.5) implies that u_d and y_d are obtained as input and output, respectively, the system is operating in closed loop with the controller C^*. But by definition, the input and output with this controller are $u^*(t)$ and $y^*(t)$. Thus, $u_d(t) = u^*(t)$ and $y_d(t) = y^*(t)$ and the proof is complete.

Proof of Theorem 6.2

From (6.9) we have

$$\begin{aligned}
y^*(t) - y_d(t) &= S\ (y^*(t) - G^*u^*(t)) \\
&= S\ (P - G^*)u^*(t) \\
&= S\ (1 - G^*P^{-1})Pu^*(t) \\
&= S\ (1 - G^*P^{-1})P\frac{C^*}{1 + PC^*}r(t) \\
&= S\ (1 - G^*P^{-1})\frac{PC^*}{1 + PC^*}T^{-1}Tr(t) \\
&= \frac{PC^*}{1 + PC^*}T^{-1}\ S\ (y_d - G^*u_d) \\
&= \frac{T^*}{T}\ S\ (y_d - G^*u_d)
\end{aligned} \tag{C.5}$$

where $S^* = 1/(1 + PC^*)$.

Proof of Theorem 6.3

The problem of finding an optimal linear L in the linear case (P linear) can be described graphically as in Figure C.1. The main idea is to study the difference $\hat{u}_d(t) - u_d(t)$ in a minimal variance control setting. We assume that there is a delay of one sample in the system generating $y(t)$, this delay is represented by the D-block to the left of P in Figure C.1.

No measurement noise ($\nu(t) \equiv 0$)

In (6.26) the error $\varepsilon(t)$ is defined as

$$\varepsilon(t) = SG^*(\hat{u}_d(t) - u_d(t))$$

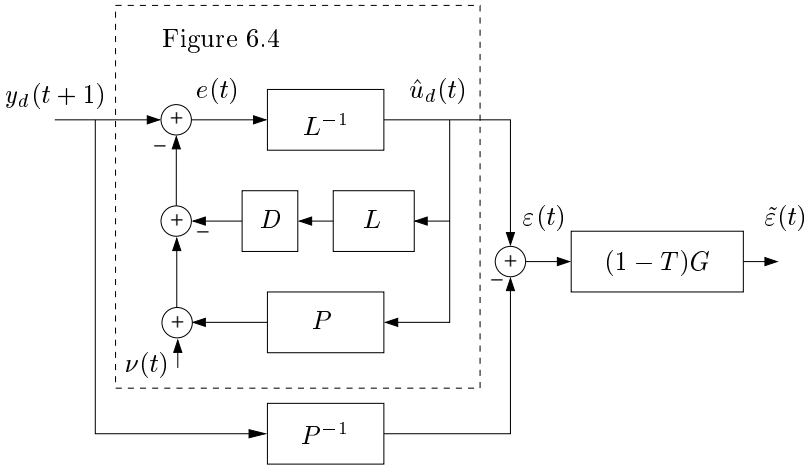

Figure C.1: Comparison of inverses.

which, with the notation in Figure C.1 can be written as

$$\varepsilon(t) = SG^*(\hat{u}_d(t) - u_d(t)).$$

Now we have that

$$\hat{u}_d(t) = \frac{D^{-1}L^{-1}}{1 - D + PL^{-1}} y_d(t)$$

and

$$\begin{aligned}
\varepsilon(t) &= \hat{u}_d(t) - D^{-1}P^{-1}y_d(t) \\
&= \frac{D^{-1}L^{-1} - D^{-1}P^{-1}(1 - D + PL^{-1})}{1 - D + PL^{-1}} y_d(t) \\
&= \frac{(D^{-1} - D^{-1})L^{-1} - D^{-1}P^{-1}(1 - D)}{1 - D + PL^{-1}} y_d(t) \\
&= \frac{-D^{-1}P^{-1}}{1 + \frac{1}{1-D}PL^{-1}} y_d(t).
\end{aligned}$$

Concequently,

$$\tilde{\varepsilon}(t) = \frac{-(1-T)GP^{-1}}{1 + \frac{1}{1-D}PL^{-1}} y_d(t). \tag{C.6}$$

In a stochastic setting the variance of $\tilde{\varepsilon}(t)$, $E\tilde{\varepsilon}^2(t)$, should be minimized. By studying (C.6) we find that the problem can be recognized as a minimum variance control problem where $(1-T)GP^{-1}$ is the noise model, $\frac{D}{1-D}P$ is the system and the controller is given by L^{-1}. Hence, we can find L^{-1} by optimization of a minimum variance criterion.

Consider a system given on the form

$$y(t) = Fu(t) + Hv(t) \tag{C.7}$$

where F and H are rational transfer functions, $y(t)$ is the output, $u(t)$ is the control signal and $v(t)$ denotes the disturbance, modeled as zero mean white noise. For a system (C.7) where the pole excess in F is equal to one, the minimum variance controller is given by $\frac{H-1}{F}$ (Söderström 1994), hence we would have

$$L^{-1} = \frac{H-1}{F}. \tag{C.8}$$

Writing the model in (C.6) on the format as in (C.7) gives

$$\begin{aligned} F &= \frac{1}{1-D}P \quad \text{and} \\ H &= (1-T)FP^{-1}TH_r \end{aligned} \tag{C.9}$$

where the spectrum, $\Phi_r(\omega)$, of the reference signal r is

$$\Phi_r(\omega) = |H_r|^2\Phi_v(\omega), \tag{C.10}$$

where $\Phi_v(\omega)$ is a constant since $v(t)$ is considered as white noise. Thus, given (C.8), we can compute L^{-1} in Figure C.1 as

$$L^{-1} = \frac{H-1}{F} = \frac{1-D}{P}\left((1-T)GP^{-1}TH_r - 1\right). \tag{C.11}$$

It follows from (C.11) that in order to be able to compute L^{-1} we need to know the system P and G. However, since G is an approximation of P and assuming that it is close, we can approximate L^{-1} as

$$L^{-1} = \frac{1-D}{P}\left((1-T)TH_r - 1\right). \tag{C.12}$$

With measurement noise ($\nu(t) \neq 0$)

In the case $\nu(t) \neq 0$ we get

$$\varepsilon(t) = \frac{D^{-1}L^{-1}}{1 - D + PL^{-1}} \left(y_d(t) - \nu(t) \right) - P^{-1} y_d(t) \big) \tag{C.13}$$

$$= \frac{D^{-1}L^{-1} - P^{-1}(1-D) - D^{-1}L^{-1}}{1 - D + PL^{-1}} y_d(t) - \frac{D^{-1}L^{-1}}{1 - D + PL^{-1}} \nu(t) \tag{C.14}$$

by calculations from Figure C.1. The filtered version of (C.13) is, hence, given by

$$\tilde{\varepsilon}(t) = \frac{-SGP^{-1}}{1 + \frac{D^{-1}}{1-D} PL^{-1}} y_d(t) + \frac{-SG\frac{1}{1-D}L^{-1}}{1 + \frac{1}{1-D} PL^{-1}} \nu(t).$$

With similar arguments as in the previous section and with a model given by

$$y(t) = Fu(t) + H_1 v(t) + H_2 e(t)$$

we identify F and H_1 as in (C.9) ($H_1 = H$) and

$$H_2 = -SG \frac{1}{1-D} L^{-1} H_\nu$$

where the spectrum $\Phi_\nu(\omega)$ of the noise $\nu(t)$ is given by

$$\Phi_\nu(\omega) = |H_\nu|^2 \Phi_e(\omega)$$

where $\Phi_e(\omega)$ is a constant corresponding to white noise. If we consider $\Phi_e(\omega) = \Phi_e(\omega) = 1$ then $H = H_1 + H_2$ and L^{-1} can be obtained as in (C.11) or as in the approximation (C.12).

Appendix D

Proof of Theorems 7.2 and 7.3.

First we consider the following lemma concerning the covariance estimate.

Lemma D.1. *Let*

$$\hat{r}_y^N(\tau) = \begin{cases} \frac{1}{N}\sum_{t=1+|\tau|}^{N} y(t)y(t+|\tau|), & |\tau| \le N-1 \\ 0, & |\tau| \ge N \end{cases} \tag{D.1}$$

and

$$r_y(\tau) = Ey(t)y(t-\tau) \tag{D.2}$$

then

$$\left|\hat{r}_y^N(\tau) - r_y(\tau)\right| \le \begin{cases} C\frac{1}{\sqrt{N}}\log^3 N \ w.p.\ 1\ , |\tau| \le N-1 \\ C\lambda^{|\tau|}, |\tau| \ge N \end{cases} \tag{D.3}$$

for some $C < \infty$ *and* $0 < \lambda < 1$.

Proof. We have

$$\hat{r}_y^N(\tau) - r_y(\tau) = \frac{1}{N}\sum_{t=\tau+1}^{N}(y(t)y(t-\tau) - r_y(\tau)) - \frac{\tau}{N}r_y(\tau) \tag{D.4}$$

where $y(t)y(t-\tau)$ is exponentially forgetting of order 2, then according to Lemma 2.14 and Lemma 2.15 in (Hjalmarsson 1993)

$$\begin{aligned}
&\left| \sum_{t=\tau+1}^{N} \left(y(t)y(t-\tau) - r_y(\tau) \right) \right| \leq C\sqrt{N}\log^3 N \text{ w.p. } 1 \\
&\Rightarrow \left| \hat{r}_y^N(\tau) - r_y(\tau) \right| \leq C\frac{1}{\sqrt{N}}\log^3 N + \frac{|\tau|}{N} C\lambda^{|\tau|} \\
&\leq C\frac{1}{\sqrt{N}}\log^3 N \text{ w.p. } 1
\end{aligned} \tag{D.5}$$

□

The asymptotic variance of $\hat{\phi}_p(\omega)$ is given by (Brillinger 1981)

$$\lim_{N\to\infty} E\left\{ [\hat{\phi}_p(\omega_k) - \phi(\omega_k)][\hat{\phi}_p(\omega_l) - \phi(\omega_l)] \right\} = \begin{cases} \phi^2(\omega_k) & \omega_k = \pm\omega_l \\ 0 & \omega_k \neq \pm\omega_l \end{cases}. \tag{D.6}$$

assuming that $y(t)$ is a stationary signal and that there is an $l \geq 0$ with

$$\sum_{v_1,\ldots,v_{k-1}=-\infty}^{\infty} \left(1 + |v_i|^l\right) |E\{y(t)y(t+v_1),\ldots,y(t+v_{k-1})\}| < \infty \tag{D.7}$$

for $i = 1,\ldots,k-1$ and $\forall k$ where $y(t)$ is a zero mean signal. In addition to the variance result we note that the distribution of the spectral estimate, (Brillinger 1981), is

$$\hat{\phi}_p(\omega) \sim \phi(\omega)\chi_2^2/2 \tag{D.8}$$

assuming the signal to be stationary (Brillinger 1981) and that $\forall k$

$$\sum_{u_1,\ldots,u_{k-1}=-\infty}^{\infty} |E\{y(t)y(t+u_1)\cdots y(t+u_{k-1})\}| < \infty. \tag{D.9}$$

where $y(t)$ is a zero mean signal. In (D.8) χ_2^2 denotes the chi-squared distribution with two degrees of freedom.

Remark: The condition in (D.7) implies that for, $l > 0$, in time, well separated values of the process are even less dependent than in (D.9). When both (D.9) and (D.7) are satisfied y is exponentially forgetting of all orders.

D.1 Convergence of $V_{QSD,N}(\theta)$

This section contains the proof of Theorem 7.2 which is also proven in (Chiu 1988). The quadratic cost function is given by

$$V_{QSD,N}(\theta) = \frac{1}{2N}\sum_{k=0}^{N-1}(\hat{\phi}(\omega_k^N) - \phi(\omega_k^N,\theta))^2\frac{1}{\phi^2(\omega_k^N)}, \tag{D.10}$$

where $\omega_k^N = i\frac{2\pi k}{N}$. The superscript N of ω_k^N is used to point out that the resolution if frequency is depending on the number of samples. Here we will show that

$$\sup_{\theta\in\Theta}|V_{QSD,N}(\theta) - V_{QSD}(\theta)| \to 0 \quad \text{w.p. 1 as } N\to\infty, \tag{D.11}$$

where

$$V_{QSD}(\theta) = \frac{1}{4\pi}\int_{-\pi}^{\pi}(\phi(\omega) - \phi(\omega,\theta))^2\frac{1}{\phi^2(\omega)}d\omega, \tag{D.12}$$

when Θ is a compact set.

The proof is based on the assumptions $M1, M2, M3, S1$ and $S2$ given in Section 7.4. The estimated spectrum, denoted $\hat{\phi}(\omega)$, is the periodogram or equivalently the correlogram. Hence, no windowing or averaging operations have been used to smooth the spectral estimate. The weighting $\frac{1}{\phi^2(\omega)}$ is assumed to be the true spectrum, although in reality this is a smoothed spectrum

Equation (D.10) can be rewritten as

$$\begin{aligned}
V_{QSD,N}(\theta) &= \frac{1}{2N}\sum_{k=0}^{N-1}(\hat{\phi}(\omega_k^N) - \phi(\omega_k^N,\theta))^2\frac{1}{\phi^2(\omega_k^N)} \\
&= \frac{1}{2N}\sum_{k=0}^{N-1}(\phi(\omega_k^N) - \phi(\omega_k^N,\theta))^2\frac{1}{\phi^2(\omega_k^N)} && \text{(D.13)} \\
&\quad - \frac{1}{N}\sum_{k=0}^{N-1}(\phi(\omega_k^N) - \phi(\omega_k^N,\theta))(\hat{\phi}(\omega_k^N) - \phi(\omega_k^N))\frac{1}{\phi^2(\omega_k^N)} && \text{(D.14)} \\
&\quad + \frac{1}{2N}\sum_{k=0}^{N-1}(\hat{\phi}(\omega_k^N) - \phi(\omega_k^N))^2\frac{1}{\phi^2(\omega_k^N)}. && \text{(D.15)}
\end{aligned}$$

We get

$$V_{QSD,N}(\theta) - V_{QSD}(\theta) =$$

$$\underbrace{\frac{1}{2N}\sum_{k=0}^{N-1}(\phi(\omega_k^N) - \phi(\omega_k^N,\theta))^2\frac{1}{\phi^2(\omega_k^N)} - \frac{1}{4\pi}\int_{-\pi}^{\pi}(\phi(\omega) - \phi(\omega,\theta))^2\frac{1}{\phi^2(\omega)}d\omega}_{=\Delta_N^1(\theta)}$$

$$\underbrace{-\frac{1}{N}\sum_{k=0}^{N-1}(\phi(\omega_k^N) - \phi(\omega_k^N,\theta))(\hat{\phi}(\omega_k^N) - \phi(\omega_k^N))\frac{1}{\phi^2(\omega_k^N)}}_{=\Delta_N^2(\theta)}$$

$$\underbrace{+\frac{1}{2N}\sum_{k=0}^{N-1}(\hat{\phi}(\omega_k^N) - \phi(\omega_k^N))\frac{1}{\phi^2(\omega_k^N)} - \frac{1}{2}}_{=\Delta_N^3}$$

It will now be shown that $\Delta_N^i \to 0$ w.p. 1 as $N \to \infty$ ($i = 1, 2$ and 3).

I) $\Delta_N^1(\theta)$

Define

$$f_N(\omega,\theta) = \left|\phi(\omega_k^N) - \phi(\omega_k^N,\theta)\right|^2\frac{1}{\phi^2(\omega)} \quad \left|\omega - \omega_k^N\right| < \frac{\pi}{N}$$

$$f(\omega,\theta) = \left|\phi(\omega) - \phi(\omega,\theta)\right|^2\frac{1}{\phi^2(\omega)}$$

then

$$\sup_{\omega,\theta\in\Theta}|f_N(\omega,\theta) - f(\omega,\theta)| \to 0 \text{ w.p. 1 as } N \to \infty$$

due to assumptions $M1$ and $S1$ in Section 7.4. Hence,

$$\begin{aligned}\left|\Delta_N^1(\theta)\right| &= \left|\frac{1}{4\pi}\int_{-\pi}^{\pi}(f_N(\omega,\theta) - f(\omega,\theta))\,d\omega\right| \\ &\le \frac{1}{4\pi}\int_{-\pi}^{\pi}|f_N(\omega,\theta) - f(\omega,\theta)|\,d\omega \\ &\le \varepsilon \;\forall\; \theta \in \Theta\end{aligned}$$

provided N is large enough. In conclusion

$$\sup_{\theta\in\Theta}\left|\Delta_N^1(\theta)\right| \to 0 \text{ w.p. 1 as } N \to \infty.$$

II) $\Delta^2(\theta)$

We have

$$\begin{aligned}\hat{\phi}(\omega_k^N) &= \frac{1}{N}\left|\sum_{t=1}^{N} y(t)e^{-i\omega_k^N t}\right|^2 \\ &= \sum_{\tau=-\infty}^{\infty} \hat{r}_y^N(\tau)e^{-i\frac{2\pi k}{N}\tau}\end{aligned}$$

where $\hat{r}_y^N(\tau)$ defined as in (D.1). Let

$$\beta(\omega,\theta) = \frac{\phi(\omega)-\phi(\omega,\theta)}{\phi^2(\omega)}.$$

With $y(t)$ exponentially forgetting in combination with Assumption $M3$ implies that

$$\phi(\omega)-\phi(\omega,\theta) = \sum_{k=-\infty}^{\infty} g_k(\theta)e^{-i\omega k} \tag{D.16}$$

with $|g_k(\theta)| \leq C\lambda^{|k|}$. Assumption $S2$ and (D.16) implies that

$$\beta(\omega,\theta) = \sum_{l=-\infty}^{\infty} p(l,\theta)e^{-i\omega l} \tag{D.17}$$

where $|p(l,\theta)| \leq C\lambda^{|\tau|}$. We write $\Delta_N^2(\theta)$ as

$$\begin{aligned}\Delta_N^2(\theta) &= \frac{1}{N}\sum_{k=0}^{N-1}\left(\hat{\phi}(\omega_k^N)-\phi(\omega_k^N)\right)\beta(\omega_k^N,\theta) \\ &= \frac{1}{N}\sum_{k=0}^{N-1}\sum_{\tau=-\infty}^{\infty}\left(\hat{r}_y^N(\tau)-r_y(\tau)\right)e^{-i\frac{2\pi k}{N}\tau}\beta(\omega_k^N,\theta) \\ &= \sum_{\tau=-\infty}^{\infty}\left(\hat{r}_y^N(\tau)-r_y(\tau)\right)\frac{1}{N}\sum_{k=0}^{N}\beta(\omega_k^N,\theta)e^{-i\frac{2\pi k}{N}\tau},\end{aligned}$$

where

$$\begin{aligned}\frac{1}{N}\sum_{k=0}^{N-1}\beta(\omega_k^N,\theta)e^{-i\frac{2\pi k}{N}\tau} &= \frac{1}{N}\sum_{k=0}^{N-1}\sum_{l=-\infty}^{\infty}p(l,\theta)e^{-i\frac{2\pi k}{N}l}e^{-i\frac{2\pi k}{N}\tau}\\ &= \sum_{l=-\infty}^{\infty}p(l,\theta)\frac{1}{N}\sum_{k=0}^{N-1}e^{-i\frac{2\pi k}{N}(l+\tau)}\\ &= \sum_{q=-\infty}^{\infty}p(-\tau+qN,\theta).\end{aligned}$$

Now we have

$$\begin{aligned}\sup_{\theta\in\Theta}\left|\Delta_N^2(\theta)\right| &= \sup_{\theta\in\Theta}\left|\sum_{\tau=-\infty}^{\infty}\left(\hat{r}_y^N(\tau)-r_y(\tau)\right)\sum_{q=-\infty}^{\infty}p(-\tau+qN,\theta)\right|\\ &\le \sum_{\tau=-\infty}^{\infty}\left|\hat{r}_y^N(\tau)-r_y(\tau)\right|C\sum_{q=-\infty}^{\infty}\lambda^{|-\tau|+qN}\\ &\le C\sum_{|\tau|>N-1}\left|\underbrace{\hat{r}_y^N(\tau)}_{=0}-r_y(\tau)\right|\\ &\quad + C\sum_{|\tau|\le N-1}\left|\hat{r}_y^N(\tau)-r_y(\tau)\right|\sum_{q=-\infty}^{\infty}\lambda^{|-\tau+qN|}\\ &\le C\sum_{|\tau|>N}\lambda^{|\tau|}+C\sum_{|\tau|\le N-1}\frac{\log^3 N}{\sqrt{N}}\sum_{q=-\infty}^{\infty}\lambda^{|-\tau+qN|}\\ &\le C\lambda^N+C\frac{\log^3 N}{\sqrt{N}}\sum_{l=0}^{\infty}\lambda^l\\ &\le C\lambda^N+C\frac{\log^3 N}{\sqrt{N}}\to 0 \text{ w.p. 1 as } N\to\infty. \qquad \text{(D.18)}\end{aligned}$$

where the first inequality is due to (D.17) and the third inequality is due to Lemma D.1.

III) Δ^3

It remains to show that (D.15) converges to

$$\frac{1}{2N}\sum_{k=0}^{N-1}\left(\hat{\phi}(\omega_k^N)-\phi(\omega_k^N)\right)^2-\frac{1}{\phi^2(\omega_k^N)}\to\frac{1}{2}\text{ w.p.1 as }N\to\infty. \quad \text{(D.19)}$$

By applying

$$\frac{1}{2}=\frac{1}{2N}\sum_{k=0}^{N-1}\frac{\phi^2(\omega_k^N)}{\phi^2(\omega_k^N)}$$

it can be shown that (D.19) holds if

$$\frac{1}{2N}\sum_{k=0}^{N-1}\left(\left(\hat{\phi}(\omega_k^N)-\phi(\omega_k^N)\right)^2-\phi^2(\omega_k^N)\right)\frac{1}{\phi^2(\omega_k^N)} \to 0 \text{ w.p. } 1 \text{ as } N\to\infty. \quad \text{(D.20)}$$

Rewriting the left side of (D.20) gives

$$\begin{aligned}&\frac{1}{2N}\sum_{k=0}^{N-1}\left(\left(\hat{\phi}(\omega_k^N)-\phi(\omega_k^N)\right)^2-\phi^2(\omega_k^N)\right)\frac{1}{\phi^2(\omega_k^N)}\\&=\frac{1}{2N}\sum_{k=0}^{N-1}\left(\hat{\phi}^2(\omega_k^N)+\phi^2(\omega_k^N)-2\hat{\phi}(\omega_k^N)\phi(\omega_k^N)-\phi^2(\omega_k^N)\right)\frac{1}{\phi^2(\omega_k^N)}\\&=\frac{1}{2N}\sum_{k=0}^{N-1}\left(\hat{\phi}(\omega_k^N)-\phi(\omega_k^N)\right)\frac{\hat{\phi}(\omega_k^N)}{\phi^2(\omega_k^N)} \quad \text{(D.21)}\end{aligned}$$

and the structure of the right most side of (D.21) is similar to the structure of (D.14), with

$$\beta(\omega_k^N)=\frac{\hat{\phi}(\omega_k^N)}{\phi^2(\omega_k^N)}. \quad \text{(D.22)}$$

Assuming that $\beta(\omega_k^N)$ given in (D.22) obeys the same properties as in (D.17) then (D.21) tends to zero as $N\to\infty$. It can be noted that Δ^3 is independent of θ and therefore of less interest than $\Delta^1(\theta)$ and $\Delta^2(\theta)$.

D.2 Convergence of $V_{SML,N}(\theta)$

The proof of Theorem 7.3 follows the outline in the previous section under the assumptions $M1, M2, M3, M4, M5, S1$ and $S2$ stated in Section 7.4. In the spectral based ML case we have

$$\begin{aligned} V_N(\theta) = V_{SML,N}(\theta) &= \frac{1}{N}\sum_{k=0}^{N-1}\frac{\hat{\phi}(\omega_k^N)}{\phi(\omega_k^N,\theta)} + \log\phi(\omega_k^N,\theta) \\ &= \frac{1}{N}\sum_{k=0}^{N-1}\frac{\hat{\phi}(\omega_k^N)}{\phi(\omega_k^N,\theta)} + \log\lambda(\theta) + \log\left|H(\omega_k^N,\theta)\right|^2 \\ &= \frac{1}{N}\sum_{k=0}^{N-1}\left\{\frac{\hat{\phi}(\omega_k^N)}{\phi(\omega_k^N,\theta)} + \log\lambda(\theta)\right\}, \end{aligned} \tag{D.23}$$

where the last equality follows since

$$\frac{1}{N}\sum_{k=0}^{N-1}\log\left|H(\omega_k^N,\theta)\right|^2 = 0,$$

assuming that $H(q,\theta)$ is stable and monic, see Section 3.3 for further details. We have

$$V_{SML}(\theta) = \frac{1}{2\pi}\int_{-\pi}^{\pi}\frac{\phi(\omega)}{\phi(\omega,\theta)}d\omega + \log\lambda(\theta).$$

Equation (D.23) can now be rewritten as

$$V_N(\theta) = \frac{1}{N}\sum_{k=0}^{N-1}\frac{\phi(\omega_k^N)}{\phi(\omega_k^N,\theta)} + \frac{1}{N}\sum_{k=0}^{N-1}\frac{\hat{\phi}(\omega_k^N)-\phi(\omega_k^N)}{\phi(\omega_k^N,\theta)} + \log\lambda(\theta)$$

and we get

$$\begin{aligned} V_N(\theta) - V(\theta) = &\underbrace{\frac{1}{N}\sum_{k=0}^{N-1}\frac{\phi(\omega_k^N)}{\phi(\omega_k^N,\theta)} - \frac{1}{2\pi}\int_{-\pi}^{\pi}\frac{\phi(\omega)}{\phi(\omega,\theta)}d\omega}_{=\Omega_N^1(\theta)} \\ &+ \underbrace{\frac{1}{N}\sum_{k=0}^{N-1}\frac{\hat{\phi}(\omega_k^N)-\phi(\omega_k^N)}{\phi(\omega_k^N,\theta)}}_{=\Omega_N^2(\theta)}. \end{aligned}$$

If we denote

$$f_N(\omega,\theta) = \frac{\phi(\omega_k^N)}{\phi(\omega_k^N,\theta)}, \quad |\omega - \omega_k^N| < \frac{\pi}{N}$$
$$f(\omega,\theta) = \frac{\phi(\omega)}{\phi(\omega,\theta)}.$$

Assuming $|\omega - \omega_k^N| < \frac{\pi}{N}$

$$\begin{aligned}
&|f_N(\omega,\theta) - f(\omega,\theta)| \\
&\qquad = \left| \frac{\phi(\omega,\theta)\phi(\omega_k^N) - \phi(\omega_k^N,\theta)\phi(\omega)}{\phi(\omega_k^N,\theta)\phi(\omega,\theta)} \right| \\
&\qquad = \left| \frac{(\phi(\omega,\theta) - \phi(\omega_k^N,\theta))\phi(\omega_k^N) - \phi(\omega_k^N,\theta)(\phi(\omega_k^N) - \phi(\omega))}{\phi(\omega_k^N,\theta)\phi(\omega,\theta)} \right| \\
&\qquad \leq C \left\{ \left|\phi(\omega,\theta) - \phi(\omega_k^N,\theta)\right| + \left|\phi(\omega_k^N) - \phi(\omega)\right| \right\},
\end{aligned}$$

where the inequality follows from $\phi(\omega,\theta) < M$, $\phi(\omega,\theta) > \delta$, and $\phi(\omega) > \delta$. Under the condition that ϕ is uniformly continuous and that $\phi(\omega,\theta)$ being equicontinuous this implies that

$$\sup_{\theta\in\Theta,\omega} |f_N(\omega,\theta) - f(\omega,\theta)| \to 0 \text{ w.p. } 1 \text{ as } N \to \infty.$$

Thus, as in the QSD case for $\Delta_N^2(\theta)$ in the previous section

$$\begin{aligned}
\Omega_N^1(\theta) &= \left| \frac{1}{2\pi} \int_{-\pi}^{\pi} (f_N(\omega,\theta) - f(\omega,\theta))\, d\omega \right| \\
&\leq \frac{1}{2\pi} \int_{-\pi}^{\pi} |f_N(\omega,\theta) - f(\omega,\theta)|\, d\omega \quad \leq \varepsilon \ \forall\ \theta \in \Theta,
\end{aligned}$$

provided N is large enough. In conclusion

$$\sup_{\theta\in\Theta} \left|\Omega_N^1(\theta)\right| \to 0 \text{ w.p.1 as } N \to \infty.$$

To prove that $\Omega_N^2(\theta)$ tends to zero as $N \to \infty$, we use assumption M5 and compare to results for $\Delta_N^2(\theta)$ in (D.18). With

$$\beta(\omega_k^N,\theta) = \frac{1}{\phi(\omega_k^N,\theta)},$$

the result in (D.18) is valid also for $\Omega_N^2(\theta)$ and thus

$$\sup_{\theta\in\Theta} \left|\Omega_N^2(\theta)\right| \to 0 \text{ w.p. } 1 \text{ as } N \to \infty.$$

Appendix E

Proof of Theorem 7.4

To show Theorem 7.4 we consider one element at a time in the covariance matrix. Note that the proof given here is similar to the proof in (Chiu 1988) although somewhat more clarifying. Based on the argument that $V'_{QSD,N}(\theta)$ being equal to in $V'_{SML,N}(\theta)$ when $\theta = \theta_0$ we will use $V'_{QSD,N}(\theta)$ as given in (7.17) below since it simplifies the calculations. First recall that we are analyzing $\lim_{N\to\infty} NE\{(\hat{\theta}_N - \theta_0)(\hat{\theta}_N - \theta_0)^T\}$ by studying

$$\lim_{N\to\infty} N[\overline{V}''(\theta_0)]^{-1} E\{V'_N(\theta_0)V'_N(\theta_0)^T\}[\overline{V}''(\theta_0)]^{-1}.$$

The second derivative $V''_{\theta_i\theta_j,N}(\theta)$ can be derived from (7.17) and we get

$$V''_{\theta_i\theta_j,N}(\theta) = \frac{1}{N}\sum_{k=0}^{N-1}\left(\frac{\phi''_{\theta_i\theta_j}(\omega_k,\theta)}{\phi^2(\omega_k)}\left(\hat{\phi}_N(\omega_k) - \phi(\omega_k,\theta)\right) + \frac{\phi'_{\theta_i}(\omega_k,\theta)(\phi'_{\theta_j}(\omega_k,\theta))^T}{\phi^2(\omega_k)}\right). \tag{E.1}$$

Computing the expected value and the limit as $N \to \infty$ and the result is

$$\begin{aligned}
\overline{V}''_{\theta_i\theta_j}(\theta) &= \lim_{N\to\infty} E\{V''_{\theta_i\theta_j,N}(\theta)\} \\
&= \lim_{N\to\infty} \left(\frac{1}{N} \sum_{k=0}^{N-1} \frac{\phi'_{\theta_i}(\omega_k,\theta)(\phi'_{\theta_j}(\omega_k,\theta))^T}{\phi^2(\omega_k)} + \right. \\
&\quad \left. \frac{1}{N} \sum_{k=0}^{N-1} \frac{\phi''_{\theta_i\theta_j}(\omega_k,\theta)}{\phi^2(\omega_k)} E\left(\hat{\phi}_N(\omega_k) - \phi(\omega_k,\theta)\right) \right) \\
&\quad \to \frac{1}{2\pi} \int_{-\pi}^{\pi} \frac{\phi'_{\theta_i}(\omega,\theta)(\phi'_{\theta_j}(\omega,\theta))^T}{\phi^2(\omega)} d\omega, \qquad \text{(E.2)}
\end{aligned}$$

where the second term (on the third line) vanishes since $\hat{\phi}_N(\omega)$ is an asymptotically unbiased estimate of $\phi(\omega)$, (Brillinger 1981). The result in (E.2) is an element a_{ij} of the matrix A introduced in Theorem 7.4, hence,

$$A = \frac{1}{2\pi} \int_{-\pi}^{\pi} \frac{\phi'_\theta(\omega,\theta)(\phi'_\theta(\omega,\theta))^T}{\phi^2(\omega)} d\omega \Big|_{\theta=\theta_0}. \qquad \text{(E.3)}$$

It is somewhat more complicated to show that

$$\lim_{N\to\infty} NE\{V'_{\theta_i,N}(\theta)V'_{\theta_j,N}(\theta)^T\} = 2A + D \qquad \text{(E.4)}$$

where A is given in $(E.3)$ and

$$D = \frac{1}{2\pi} \int_{-\pi}^{\pi} \int_{-\pi}^{\pi} \phi'_\theta(\omega,\theta)(\phi'_\theta(\omega,\theta))^T \phi_4(\omega,-\omega,\mu) \frac{1}{\phi^2(\omega)} \frac{1}{\phi^2(\mu)} d\omega d\mu \Big|_{\theta=\theta_0},$$

where $\phi_4(\omega,-\omega,\mu)$ denotes the fourth-order cumulant spectrum.

To show (E.4) we first study

$$\begin{aligned}
&\lim_{N\to\infty} NE\{V'_{\theta_i,N}(\theta)V_{\theta_j,N}(\theta)^T\} \\
&\quad= \lim_{N\to\infty} NE\left(\left[\frac{1}{N}\sum_{k=0}^{N-1}\phi'_{\theta_i}(\omega_k,\theta)(\hat{\phi}_N(\omega_k)-\phi(\omega_k,\theta))\frac{1}{\phi^2(\omega_k)}\right]\times\right. \\
&\qquad\left.\left[\frac{1}{N}\sum_{l=0}^{N-1}(\hat{\phi}_N(\omega_l)-\phi(\omega_l,\theta))\phi'_{\theta_j}(\omega_l,\theta)\frac{1}{\phi^2(\omega_l)}\right]^T\right) \\
&\quad= \lim_{N\to\infty}\frac{1}{N}\sum_{k=0}^{N-1}\sum_{l=0}^{N-1}\phi'_{\theta_i}(\omega_k,\theta)E\{(\hat{\phi}_N(\omega_k)-\phi(\omega_k,\theta))\times \\
&\qquad(\hat{\phi}_N(\omega_l)-\phi(\omega_l,\theta))\}\phi'_{\theta_j}(\omega_l,\theta)^T\frac{1}{\phi^2(\omega_k)}\frac{1}{\phi^2(\omega_l)}. \qquad \text{(E.5)}
\end{aligned}$$

Then we consider $\mathrm{cov}(\hat{\phi}(\omega_k),\hat{\phi}(\omega_l)) =$
$E\{(\hat{\phi}_N(\omega_k)-\phi(\omega_k,\theta))(\hat{\phi}_N(\omega_l)-\phi(\omega_l,\theta))\}\Big|_{\theta=\theta_0}$ before returning to (E.5).
Denote the discrete time Fourier (DFT) transform of a real signal $y(t)$ by $Y(\omega_k)$ where

$$Y(\omega_k)=\sum_{t=0}^{N-1}y(t)e^{-i\omega_k t}$$

and $\omega_k=\frac{2\pi k}{N}$. The estimate of the second order spectrum is given by

$$\hat{\phi}_N(\omega_k)=\frac{1}{2\pi N}Y(\omega_k)Y(-\omega_k). \qquad \text{(E.6)}$$

Now, assuming a zero mean process we have

$$\begin{aligned}
&\mathrm{cov}(\hat{\phi}(\omega_k),\hat{\phi}(\omega_l)) = \frac{1}{(2\pi N)^2}\mathrm{cov}(Y(\omega_k)Y(-\omega_k)Y(\omega_l)Y(-\omega_l)) = \\
&\frac{(2\pi)^3}{N}\phi_4(\omega_k,-\omega_k,\omega_l)+\frac{(2\pi)^2}{N^2}\left(\frac{\sin(N(\omega_k+\omega_l)/2)}{\sin((\omega_k+\omega_l)/2)}\right)^2\phi^2(\omega_k) \\
&+\frac{(2\pi)^2}{N^2}\left(\frac{\sin(N(\omega_k-\omega_l)/2)}{\sin((\omega_k-\omega_l)/2)}\right)^2\phi^2(\omega_k) \\
&+\frac{\alpha_1}{N^2}\frac{\sin(N\omega_k/2)}{\sin(\omega_k/2)}\phi_3(-\omega_k,\omega_l) \\
&+\frac{\alpha_2}{N^2}\frac{\sin(N(\omega_k+\omega_l)/2)}{\sin((\omega_k+\omega_l)/2)}\phi(\omega_k)+\frac{\alpha_3}{N^2}, \qquad \text{(E.7)}
\end{aligned}$$

where α_i are real positive constants and

$$\phi(\omega_k) = \frac{1}{2\pi} \sum_{\tau=-\infty}^{\infty} c(\tau) e^{-i\omega_k \tau}$$

$$\phi_3(\omega_k, \omega_l) = \frac{1}{2\pi} \sum_{\tau_1=-\infty}^{\infty} \sum_{\tau_2=-\infty}^{\infty} c(\tau_1, \tau_2) e^{-i\omega_1 \tau_1} e^{-i\omega_2 \tau_2}$$

$$\phi_4(\omega_k, -\omega_k, \omega_l) = \frac{1}{(2\pi)^3} \sum_{\tau_1=-\infty}^{\infty} \sum_{\tau_2=-\infty}^{\infty} \sum_{\tau_3=-\infty}^{\infty} c(\tau_1, \tau_2, \tau_3) e^{-i \sum_{j=1}^{3} \omega_j \tau_j}.$$

Note that $\omega_k = \frac{2\pi k}{N}$ and

$$\frac{\sin\left(N(\frac{2\pi k}{N} - \frac{2\pi l}{N})/2\right)}{\sin\left((\frac{2\pi k}{N} - \frac{2\pi l}{N})/2\right)} = \frac{\sin\left(\pi(k-l)\right)}{\sin\left(\frac{\pi}{N}(k-l)\right)} = \begin{cases} 0, & (k \neq l) \\ N, & (k = l) \end{cases} . \qquad \text{(E.8)}$$

The result in (E.8) and the fact that the summation in (E.5) is over two dimensions, gives that the terms with a factor $\frac{1}{N^2}$ will tend to zero as $N \to \infty$. Hence,(E.5) can be rewritten as

$$\lim_{N\to\infty} \frac{1}{N^2} \sum_{k=0}^{N-1} \sum_{l=0}^{N-1} \phi'_{\theta_i}(\omega_k, \theta) \phi_4(\omega_k, -\omega_k, \omega_l) \phi'_{\theta_j}(\omega_l, \theta) \frac{1}{\phi^2(\omega_k)} \frac{1}{\phi^2(\omega_l)} +$$

$$\lim_{N\to\infty} \frac{1}{N} \sum_{k=0}^{N-1} \phi'_{\theta_i}(\omega_k, \theta) \phi'_{\theta_j}(\omega_k, \theta) \frac{1}{\phi^2(\omega_k)}. \qquad \text{(E.9)}$$

Assumption M1 gives that (E.9) converges to

$$\int_{-\pi}^{\pi} \int_{-\pi}^{\pi} \phi'_{\theta_i}(\omega, \theta) \phi_4(\omega, -\omega, \mu) \phi'_{\theta_j}(\mu, \theta) \frac{1}{\phi^2(\omega)} \frac{1}{\phi^2(\mu)} d\omega d\mu +$$

$$2 \int_{-\pi}^{\pi} \phi'_{\theta_i}(\omega, \theta) \phi'_{\theta_j}(\omega, \theta) \frac{1}{\phi^2(\omega)} d\omega.$$

which are the components of D and A, respectively.

Bibliography

Amann, N. and D.H. Owens (1994). Non-minimum phase plants in iterative learning control. In 'Second International Conference on Intelligent Systems Engineering'. Technical University of Hamburg, Germany. pp. 107–112.

Åström, K. (1980). 'Maximum likelihood and prediction error methods'. *Automatica* **16**, 551–574.

Åström, K. (1993). Matching criteria for control and identification. In 'Proc. European Control Conference (ECC)'. Groningen, The Netherlands. pp. 248–251.

Åström, K. and B. Wittenmark (1984). *Computer Controlled Systems*. Prentice-Hall. Englewood Cliffs, New Jersey.

Bendat, J. (1990). *Nonlinear System Analysis and Identification from Random Data*. John Wiley and Sons.

Billings, S. (1980). 'Identification of nonlinear systems - a survey'. *IEEE Proceedings* **127**(6), 272–285.

Bohlin, T. (1991). *Interactive System Identification: Prospects and Pitfalls*. Springer-Verlag.

Bohlin, T. (1994). 'A case study of grey box identification'. *Automatica* **30**, 307–318.

Brewer, J. (1978). 'Kronecker products and matrix calculus in system theory'. *IEEE Transactions on Circuits and Systems* **9**, 772–781.

Brillinger, D. (1981). *Time Series: Analysis and Theory*. Holden-Day.

Califano, C., S. Monaco and D. Normand-Cyrot (1998). 'On the discrete-time normal form'. *IEEE Transactions on Automatic Control* **43**, 1654–1658.

Chen, D. and B. Paden (1996). 'Stable inversion of nonlinear non-minimum phase systems'. *International Journal of Control* **64**(1), 81–97.

Chen, F. and H.K. Khalil (1995). 'Adaptive control of a class of nonlinear discrete-time systems using neural networks'. *IEEE Transactions on Automatic Control* **40**(5), 791–801.

Chen, H. (1995). 'Modeling and identification of parallel nonlinear systems - structural classification and parameter estimation methods'. *Proceedings of the IEEE* **83**(1), 39–66.

Chen, S. and S.A. Billings (1989). 'Modelling and analysis of nonlinear time-series'. *International Journal of Control* **50**(6), 2151–2171.

Chiu, S. (1988). 'Weighted least squares estimators on the frequency domain for the parameters of a time series'. *The Annals of Statistics* **16**(3), 1315–1326.

Choi, C. and G.M. Jeong (2001). 'Perfect tracking for maximum phase nonlinear systems by iterative learning control'. *International Journal of Systems Science*.

De Bruyne, F., B.D.O. Anderson, M. Gevers and N. Linard (1996). 'Iterative controller optimization for nonlinear systems'. *Proceedings of the 36th IEEE Conference on Decision and Control, USA*.

De Bruyne, F., B.D.O. Andersson, M. Gevers and N. Linard (1999). 'Gradient expressions for a closed-loop identification scheme with a tailor-made parametrization'. *Automatica* **35**(11), 1867–71.

Dennis, J. and R.B. Schnabel (1996). *Numerical Methods for Unconstrained Optimization and Nonlinear Equations*. SIAM.

Devasia, S., D. Chen and B. Paden (1996). 'Nonlinear inversion-based output tracking'. *IEEE Transactions on Automatic Control* **41**(7), 930–942.

Doh, T.-Y., J-H. Moon and M.J. Chung (1999). 'An iterative learning control for uncertain systems using structured singular values'. *Transactions of the American Society of Mechanical Engineers* **121**, 660–666.

Doyle, F., B.A. Ogunnaike and R.K. Pearson (1995). 'Nonlinear model-based control using second-order volterra models'. *Automatica* **31**(5), 697–714.

Fliess, M. (1986). 'A note on the invertibility of nonlinear input-output diofferential systems'. *Systems and Control Letters* **8**, 147–151.

Forssell, U. and H. Hjalmarsson (1999). Maximum likelihood estimation of models with unstable dynamics and nonminimum phase noise zeros. In '14th IFAC World Congress'. Beijing, P.R. China.

Forssell, U. and L. Ljung (1999). 'Closed-loop identification revisited'. *Automatica* **35**, 1215–1241.

Gevers, M. (1993). Towards a joint design of identification and control?. In H. L. Trentelman and J. C. Willems (Eds.). 'Essays on Control: Perspectives in the Theory and its Applications'. Birkhäuser.

Gevers, M., L. Ljung L and P. Van den Hof (2001). 'Asymptotic variance expressions for closed-loop identification'. *AUTOMATICA* **37**(5), 781–786.

Ghosh, J. and B. Paden (1999*a*). Iterative learning control for nonlinear non-minimum phase plants with input disturbances. In 'Proceedings of the American Control Conference'. San Diego, California, USA. pp. 2584–2589.

Ghosh, J. and B. Paden (1999*b*). Pseudo-inverse based iterative learning control for nonlinear plants with disturbances. In 'Proceedings of the 38th IEEE Conference on Decision and Control'. Phoenix, Arizona, USA. pp. 5206–5212.

Goodwin, G., J.H. Braslavsky and M.M. Seron (1999). Non-stationary stochastic embedding for transfer function estimation. In 'Proc. 14th IFAC World Congress, Beijing, China'.

Goodwin, G., M. Gevers and B. Ninness (1992). 'Quantifying the error in estimated transfer functions with application to model order selection'. *IEEE Trans. Automatic Control* **37**, 913–928.

Goodwin, G., M. Gevers and D.Q. Mayne (1991). Bias and variance distribution in transfer function estimates. In 'Proc. of IFAC/IFORS Symposium on Identification and Parameter Estimation'.

Goodwin, G., S.F. Graebe and M.E. Salgado (2001). *Control System Design*. Prentice Hall.

Grenander, U. and G. Szegö (1984). *Toeplitz forms and their applications*. second edition edn. Chelsea publishing company, New York.

Gunnarsson, S. and M. Norrlöf (2001). 'On the design of ilc algorithms using optimization'. *Automatica*.

Hannan, E. (1973). 'The asymptotic theory of linear time-series models'. *Journal of Applied Probability* **10**, 130–145.

Henriksson, B., O. Markusson and H. Hjalmarsson (2001). Control relevant identification of nonlinear systems using linear models. In 'American Control Conference (ACC)'. Arlington, USA. pp. 1178–1183.

Hirschorn, R. (1979*a*). 'Invertibility of multivariable nonlinear control systems'. *IEEE Transactions on Automatic Control* **AC-24**(6), 855–865.

Hirschorn, R. (1979*b*). 'Invertibility of nonlinear control systems'. *SIAM Journal of Control and Optimization* **17**(2), 289–297.

Hjalmarsson, H. (1993). Aspects on Incomplete Modeling in System Identification. PhD thesis. Linköping University.

Hjalmarsson, H. and L. Ljung (1992). 'Estimating model variance in the case of undermodeling'. *IEEE Trans. Automatic Control* **37**, 1004–1008.

Hjalmarsson, H., M. Gevers and F. De Bruyne (1996). 'For model based control design criteria, closed loop identification gives better performance'. *Automatica* **32**, 1659–1673.

Hjalmarsson, H., M. Gevers, S. Gunnarsson and O. Lequin (1998). 'Iterative Feedback Tuning: theory and applications'. *IEEE Control Systems Magazine* **18**(4), 26–41.

Hjalmarsson, H., S. Gunnarsson and M. Gevers (1995). Optimality and sub-optimality of iterative identification and control design schemes. In 'Proc. American Control Conference'. Seattle, Washington. pp. 2559–2563.

Horowitz, I. (1992). *Quantitative Feedback Design Theory (QFT)*. QFT Publications.

Hung, G. and L. Stark (1977). 'The kernel identification method (1910-1977) - review of theory, calculation, application and interpretation'. *Mathematical Biosciences* (37), 135–190.

Isidori, A. (1995). *Nonlinear Control Systems, Third edition*. Springer-Verlag.

Jazwinski, A. (1970). *Stochastic Processes and Filtering Theory*. Academic Press.

Jeong, G. and C.H. Choi (2001). Iterative learning control with advanced output data for nonminimum phase systems. In 'Proceedings of the American Control Conference (ACC)'. pp. 890–895.

Juditsky, A., H. Hjalmarsson, A. Benveniste, B. Delyon, L. Ljung, J. Sjöberg and Q. Zhang (1995). 'Nonlinear black-box modeling in system identification: Mathematical foundations'. *Automatica* **31**, 1725–1750.

Kay, S. (1993). *Fundamentals of Statistical Signal Processing, Estimation Theory*. Prentice-Hall.

Khalil, H. (1996). *Nonlinear Systems*. Prentice Hall.

Kollàr, I. (1994). 'Frequency domain system identification'. *The Mathworks Inc. Natick MA*.

Kosut, R. (1999). Iterative adaptive (unfalsified) control. In 'Proceedings of the 7th Mediterranen Conference on Control and Automation'. Haifa, Israel. pp. 344–364.

Kotta, U. (1990). 'Right inverse of a discrete time non-linear system'. *International journal of control* **51**(1), 1–9.

Kotta, U. (1995). *Inversion Method in the Discrete-time Nonlinear Control Systems, Synthesis Problems, (Lecture Notes in Control and Information Sciences)*. Springer-Verlag.

Lee, W., B.D.O. Anderson, R.L. Kosut and I.M.Y Mareels (1993). 'A new approach to adaptive robust control'. *Int. Journal of Adaptive Control and Signal Processing* **7**, 183–211.

Leontaritis, I. and S.A. Billings (1985*a*). 'Input-output parametric models for nonlinear systems. part i: deterministic nonlinear systems'. *International journal of control* **41**(2), 303–328.

Leontaritis, I. and S.A. Billings (1985*b*). 'Input-output parametric models for nonlinear systems. part ii: stochastic nonlinear systems'. *International journal of control* **41**(2), 329–344.

Lii, K. (1996). 'Nonlinear systems and higher-order statistics with applications'. *Signal Processing* pp. 165–177.

Ljung, L. (1999). *System Identification, Theory for the user, Second Edition*. Prentice-Hall.

Ljung, L. and T. Söderström (1983). *Theory and Practice of Recursive Identification*. MIT Press. Cambridge, Massachusetts.

Lu, J. and R.E. Skelton (2001). 'Integrating closed-loop identification and control using control energy sensitivity'. *International Journal of Control* **74**(14), 1412–1424.

Luenberger, D. (1969). *Optimization by Vector Space Methods*. Wiley.

Markusson, O. and H. Hjalmarsson (1998). Parameter estimation in partitioned nonlinear stochastic models. In 'Proc. European Signal Processing Conference'. Vol. 2. Rhodes, Greece. pp. 1021–1024.

Markusson, O. and H. Hjalmarsson (2000*a*). Inversion of nonlinear stochastic models for parameter estimation. In 'IEEE Conference on Decision and Control'. Sydney, Australia. pp. 1591–1596.

Markusson, O. and H. Hjalmarsson (2000*b*). Spectral based parameter estimation in nonlinear stochastic models. In 'Symposium on System Identification'. IFAC and AACC. Santa Barbara, USA.

Markusson, O. and H. Hjalmarsson (2001*a*). Higher order cumulant based parameter estimation in nonlinear time series models. In 'American Control Conference (ACC)'. Arlington, USA. pp. 4888–4889.

Markusson, O. and H. Hjalmarsson (2001*b*). 'Inversion of nonlinear stochastic models for the purpose of parameter estimation'. *International Journal of Control*. Accepted for publication.

Markusson, O. and H. Hjalmarsson (2001*c*). Spectral matching for parameter estimation in nonlinear input-output models. In 'European Control Conference (ECC)'. Porto, Portugal. pp. 3665–3670.

Markusson, O. and T. Bohlin (1997). Identification of a nonlinear eeg generating model. In 'Proc. IEEE Workshop on Nonlinear Signal and Image Processing'. Michigan,USA.

Markusson, O., H. Hjalmarsson and M. Norrlöf (2001). Iterative learning control of nonlinear non-minimum phase systems and its application to system and model inversion. In 'IEEE Conference on Decision and Control (CDC)'. Orlando, USA.

Markusson, O., H. Hjalmarsson and M. Norrlöf (2002). A general framework for iterative learning control. In 'IFAC World Congress on Automatic Control'. Barcelona, Spain (Submitted).

Mendel, J. (1991). 'Tutorial on higher-order statistics (spectra) in signal processing ans system theory: Theoretical results and some applications'. *Proceedings of the IEEE* **79**(3), 278–305.

Milanese, M. and A. Vicino (1991). 'Estimation theory for nonlinear models and set membership uncertainty'. *Automatica* **27**(2), 403–408.

Monaco, S. and D. Normand-Cyrot (1987). Minimum-phase nonlinear discrete-time systems and feedback stabilization. In 'In Proc. IEEE Conference on Decision and Control'. pp. 979–985.

Moore, K. (1993). *Iterative learning control for Deterministic Systems, Advances in Industrial Control*. Springer-Verlag.

Moore, K. (1999). *Applied and Computational Controls, Signal Processing, and Circuits*. Vol. 1. Springer-Verlag. chapter 4.

Morari, M. and E. Zafiriou (1989*a*). *Robust Process Control*. Prentice-Hall,Englewood Cliffs, NJ.

Morari, M. and E. Zafiriou (1989*b*). *Robust Process Control*. Prentice-Hall. Englewood Cliffs, NJ.

Nijsse, G., M. Verhagen and N.J. Doelman (2001). A new subspace based approach to iterative learning control. In 'Proceedings of the European Control Conference (ECC)'. pp. 3375–3380.

Nikias, C. and A.P. Petropulu (1993). *Higher-order spectra analysis.* Prentice-Hall,Eaglewood Cliffs, NJ.

Ninness, B. and G. Goodwin (1995). 'Estimation of model quality'. *Automatica* **31**, 32–74.

Nordsjö, A. (1998). Studies of identification of time-invariant and time-varying nonlinear systems. PhD thesis. The Royal Institute of Technology.

Norrlöf, M. (2000). Iterative Learning Control Analysis, Design and Experiments. PhD thesis. Linköping University.

Oppenheim, A. and R.W. Schafer (1989). *Discrete-Time Signal Processing.* Prentice-Hall.

Owens, D. and G. Munde (2000). 'Error convergence in an adaptive iterative learning controller'. *International Journal of Control* **73**, 851–857.

Perdon, A., G. Conte and S Longhi (1992). 'Invertibility and inversion of linear periodic systems'. *Automatica* **28**(3), 645–648.

Pillai, S. and T.I. Shim (1993). *Spectrum Estimation and System Identification.* Springer-Verlag.

Pintelon, R. and G. Schoukens, J.and Vandersteen (1997). 'Frequency domain system identification using arbitrary signals'. *IEEE Transactions on Automatic Control* **42**(12), 1717–1720.

Pintelon, R. and J. Schoukens (1999). 'Time series analysis in the frequency domain'. *IEEE Transactions on Signal Processing* **47**(1), 206–210.

Pintelon, R., P. Guillaume, Y. Rolain, J. Schoukens and H. Van hamme (1994). 'Parametric identification of transfer functions in the frequency domain - a survey'. *IEEE Transactions on Automatic Control* **39**(11), 2245–2260.

Roh, C. L., M.N. Lee and M.J. Chung (1996). 'ILC for non-minimum phase systems'. *International Journal of Systems Science* **27**(4), 419–424.

Rugh, W. (1996). *Linear system theory*. Prentice-Hall.

Saab, S. (1999). 'Robustness and convergence rate of a discrete-time learning control algorithm for a class of nonlinear systems'. *International Journal of Robust and Nonlinear Control* **9**, 559–571.

Safonov, M. and T-C Tsao (1997). 'The unfalsified control concept and learning'. *IEEE Trans. on Automatic Control*.

Savaresi, S. and G.O. Guardabassi (1998). 'Approximate I/O feedback linearization of discrete-time non-linear systems via virtual input direct design'. *Automatica* **34**, 715–722.

Schetzen, M. (1980). *The Volterra and Wiener theroies of nonlinear systems*. John Wiley and Sons, N.Y.

Schoukens, J., G. Vandersteen, R. Pintelon and P. Guillaume (1999). 'Frequency domain identification of linear systems using arbitrary excitations and a nonparametric noise model'. *IEEE Transactions on Automatic Control* **44**(2), 343–347.

Schrama, R. and P.M.J. Van den Hof (1993). Iterative identification and control design: A three step procedure with robustness analysis. In 'Proc. European Control Conference (ECC)'. Groningen. pp. 237–241.

Shalvi, O. and E. Weinstein (1994). 'Maximum likelihood and lower bounds in system identification with non-gaussian inputs.'. *IEEE Transactions on information theory* **40**(2), 328–339.

Sjöberg, J., Q Zhang, L Ljung, A Benveniste, B Delyon, P-Y Glorennec, H Hjalmarsson and A Juditsky (1995). 'Nonlinear black-box modeling in system identification: a unified overview'. *Automatica* **31**, 1691–1724.

Skogestad, S. and I. Postlethwaite (1996). *Multivariable Feedback Control, Analysis and Design*. John Wiley and Sons.

Söderström, T. (1994). *Discrete-Time Stochastic Systems, Estimation & Control*. Prentice Hall.

Söderström, T. and P. Stoica (1989). *System Identification*. Prentice Hall.

Sogo, T., K. Kinoshita and N. Adachi (2000). Iterative learning control using adjoint systems for nonlinear non-minimum phase systems. In 'IEEE Conference on Decision and Control'. pp. 3445–3446.

Stoica, P. and R. Moses (1997). *Introduction to Spectral Analysis*. Prentice-Hall.

Tong, H. (1990). *Non-linear Time Series*. Oxford Science Publications.

Tugnait, J. (1987). 'Identification of linear stochastic systems via second- and fourth-order cumulant matching'. *IEEE Transactions on Information Theory* **33**(3), 393–407.

Tugnait, J. and C. Tontiruttananon (1998). 'Identification of linear systems via spectral analysis given time-domain data: Consistency, reduced order approximation, and performance analysis'. *IEEE Transactions on Automatic Control* **43**(10), 1354–1373.

Van den Hof, P. (1997). Closed loop issues in system identification. In '11th IFAC Symposium on System Identification'. Vol. 4. Fukuoka, Japan. pp. 1651–1664.

Vidyasagar, M. (1993). *Nonlinear Systems Analysis*. Prentice-Hall.

Wang, D. (1998). 'Convergence and robustness of discrete time nonlinear systems with iterative learning control'. *Automatica* **34**(11), 1445–1448.

Wang, S. and I. Horowitz (1985). Create - a new adaptive technique. In 'In Prooceedings of 19:th Annual Conference on Information Sciences and Systems'.

Whittle, P. (1951). Hypothesis testing in time series analysis. PhD thesis. Uppsala University.

Wiener, N. (1958). *Nonlinear problems in random theory*. Technology Press and Wiley.

Zhang, Z., R.R. Bitmead and M.Gevers (1995). 'Iterative weighted least-squares identification and weighted lqg control design'. *Automatica* **31**(11), 1577–1594.